

10

CAE Analysis Results

CAE techniques were used in the ULSAB-AVC concept design program to evaluate structural concepts and to optimize the structure.

10.1 BACKGROUND

Computer Aided Engineering (CAE) techniques were used in the ULSAB-AVC concept design program as a tool to evaluate the structural concepts and to optimize the structure. The CAE team was an integral part of the engineering team and the general approach followed the steps outlined below.

- Finite Element (FE) models of the concept structures were constructed from CAD data
- The structural performance of the design concept was evaluated for both crash and stiffness load cases
- Iterations of the design were undertaken and evaluated. These could include, for example, use of tailor welded blanks, use of different steels, or design changes.
- Decisions were made on the design direction based on the CAE results
- Further optimization was then undertaken for mass reduction while maintaining a high level of structural performance

The performance of the ULSAB-AVC concepts was predicted for body structure performance (static and dynamic stiffness) and crashworthiness as described in the following sections.

10.1.1. Body Structure Performance

The following load cases were analyzed to predict the structural performances of the ULSAB-AVC C-Class and PNGV-Class vehicle concept structures:

- Static Torsional Rigidity
- Static Bending Rigidity
- Normal Modes

The body-in-white structural performance targets for ULSAB-AVC are summarized in the following Table 10.1.1-1.

Table 10.1.1-1 Structural performance targets

Target	C-Class	PNGV-Class
Static Bending Rigidity (N/mm)	11,000	12,000
Static Torsion Rigidity (Nm/deg)	12,000	13,000
First Bending Mode (Hz)	48	48
First Torsion Mode (Hz)	35	40

10.1.2. Crashworthiness

The following impact events were analyzed to predict the crashworthiness of the structure:

- US-NCAP - 100% frontal crash at 35 mph (56 km/h) into rigid barrier
- Euro-NCAP front crash - 40% overlap offset frontal crash at 64 km/h into deformable barrier
- US-SINCAP – US side impact barrier impact at 38.5 mph (61.6 km/h)
- Side Pole Impact – side impact into rigid pole at 20 mph (32 km/h)
- Rear Impact – moving barrier crash at 35 mph (56 km/h)
- Roof crush / Rollover
- Low speed impact – 100% front crash at 15 km/h into rigid barrier

A description of the crash events and particular considerations for each event are presented in Tables 10.1.2.1 through 10.1.2-7.

Table 10.1.2-1 US-NCAP description

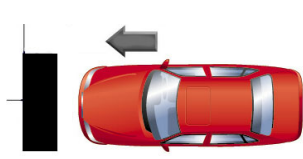
Crash Event	Criteria for Crashworthiness Assessment
US-NCAP 35 mph (56 km/h) full face rigid barrier, zero degree impact 	Overall dynamic deformation Structure energy management Vehicle deceleration pulse A-pillar deformation Steering column displacement
Considerations	
US-NCAP test is demanding on occupant restraint system Results from US-NCAP tests are used to establish US-NCAP Star Rating US-NCAP Star Ratings are published to enable consumers to make judgements on vehicle safety	

Table 10.1.2-2 Euro-NCAP description


Crash Event	Criteria for Crashworthiness Assessment
<p>Euro-NCAP 64 km/h, 40% overlap, offset deformable barrier, zero degree impact</p> 	<p>Structure energy management Passenger cell integrity A-pillar displacement Footwell intrusion Steering column displacement</p>
Considerations	
<p>Euro-NCAP frontal impact test is demanding on vehicle structure Results from Euro-NCAP tests are used to establish Euro-NCAP Star Rating Euro-NCAP Star Ratings are published to enable consumers to make judgements on vehicle safety</p>	

Table 10.1.2-3 SINCAP description

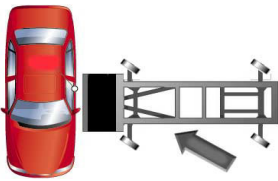
Crash Event	Criteria for Crashworthiness Assessment
<p>US-SINCAP Side Impact - 38.5 mph (61.6 km/h) impact by 1370 kg trolley moving at 63 degrees to longitudinal axis of the vehicle</p> 	<p>Structure energy management Intrusion velocity Intrusion profile</p>
Considerations	
<p>Results from US-SINCAP tests are used to establish US-SINCAP Star Rating US-SINCAP Star Ratings are published to enable consumers to make judgements on vehicle safety</p>	

Table 10.1.2-4 Side Pole Impact description

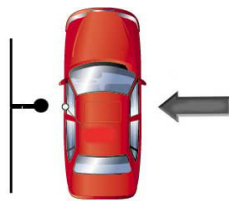
Crash Event	Criteria for Crashworthiness Assessment
<p>Side Pole Impact - 32 km/h impact with dia.254 mm rigid pole aligned with the occupant head Centre of Gravity. Pole extends from 100mm above ground to above vehicle roofline.</p> 	<p>Structure energy management Pole intrusion velocity Overall intrusion</p>
Considerations	
<p>Side Pole test is demanding on vehicle structure Side Pole test is an optional test used for establishing the Euro-NCAP Star Rating</p>	

Table 10.1.2-5 Rear Impact description

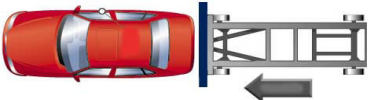
Crash Event	Criteria for Crashworthiness Assessment
<p>Rear Impact - 35 mph (56 km/h) rigid moving barrier 4000lb (1814 kg) impact with rear of vehicle in brakes-off condition</p> 	<p>Deformation in region of fuel tank</p> <p>Structure energy management</p> <p>R-point movement</p>
Considerations	
Rear Impact test is used to assess fuel system integrity	

Table 10.1.2-6 Roof Crush/Rollover description

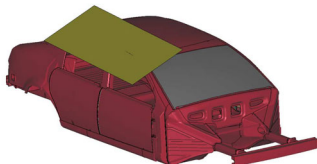
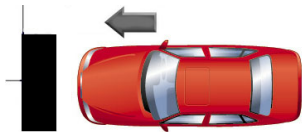
Crash Event	Criteria for Crashworthiness Assessment
<p>Roof Crush / Rollover - An inclined rigid loading device is forced against the A-pillar/roof side structure, quasi-statically. The force-displacement characteristic is recorded.</p> 	<p>Stability of structure</p> <p>Peak force recorded in 127 mm of displacement</p>
Considerations	
Roof crush test measures the ability of upper structure to support the vehicle in a rollover situation	

Table 10.1.2-7 Low Speed Impact description

Crash Event	Criteria for Crashworthiness Assessment
<p>15 km/h impact into full-face rigid barrier at zero degrees</p> 	<p>Contain damage in bumper system components</p>
Considerations	
Repairability of the vehicle is important for cost of ownership and insurance	

10.2. Static and Dynamic Stiffness

Based on CAD surface data the FE-Models (Figures 10.2-1 and 10.2-2) for the body-in-white were created. The symmetry of the structure enabled a half model to be considered for the static and dynamic stiffness analyses. Appropriate boundary conditions were applied at the $y = 0$ symmetry plane for the symmetric (bending) and anti-symmetric (torsion) load cases. The stiffness model comprised triangle and quadrilateral shell elements. Welded connections were modeled with rigid elements for both spotwelded and laser welded parts. The CAE models for the static and dynamic analyses comprised the following:

- Welded body structure
- Bonded windshield and rear-quarter glass (C-Class)
- Bonded windshield and back light (PNGV-Class)

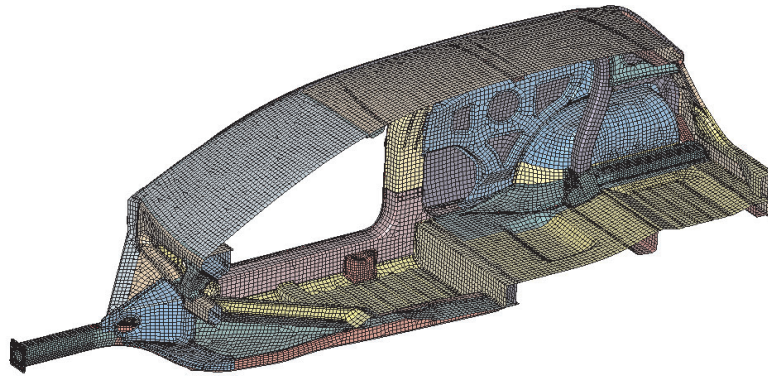


Figure 10.2-1 C-Class Finite Element model

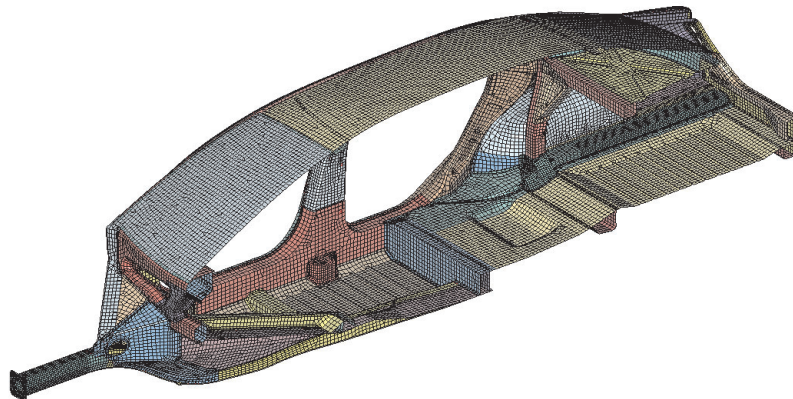


Figure 10.2-2 PNGV-Class Finite Element model

Sizes for the C-Class and PNGV-Class stiffness models are summarized in Table 10.2-1.

Table 10.2-1 ULSAB-AVC CAE model sizes

Stiffness Model Size	C-Class	PNGV-Class
Number of Nodes	61000	66100
Number of Elements	59000	64000

10.2.1. Torsional Stiffness

A load of 1000 N was applied on the front longitudinal member at the front subframe mount location while the body structure was constrained at the rear spring attachment in the lateral and vertical directions. Anti-symmetric boundary conditions were applied at the plane of symmetry.

The deformed shapes for the static torsion load case are shown in Figures 10.2.1-1 and 10.2.1-2. Figures 10.2.1-3 and 10.2.1-4 show the static torsion angle of twist along the length of the vehicle (x-axis) for C-Class and PNGV-Class respectively. Strain energy contour plots (Figures 10.2.1-5 and 10.2.1-6) show the strain energy density distribution in the structures for this load case.

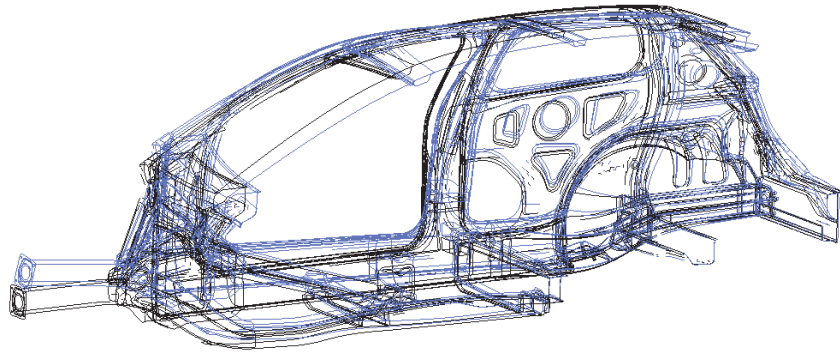


Figure 10.2.1-1 C-Class static torsion deformed shape

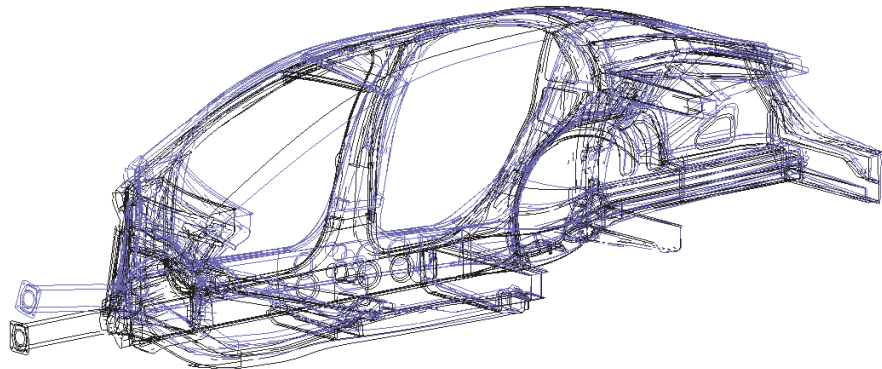


Figure 10.2.1-2 PNV-Class static torsion deformed shape

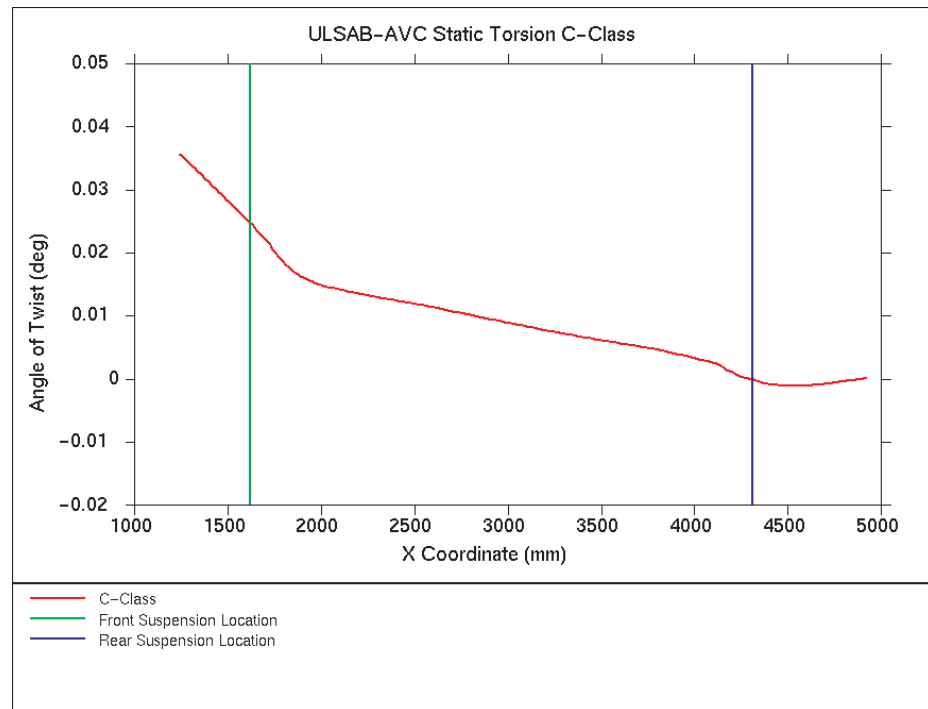


Figure 10.2.1-3 C-Class static torsion angle of twist

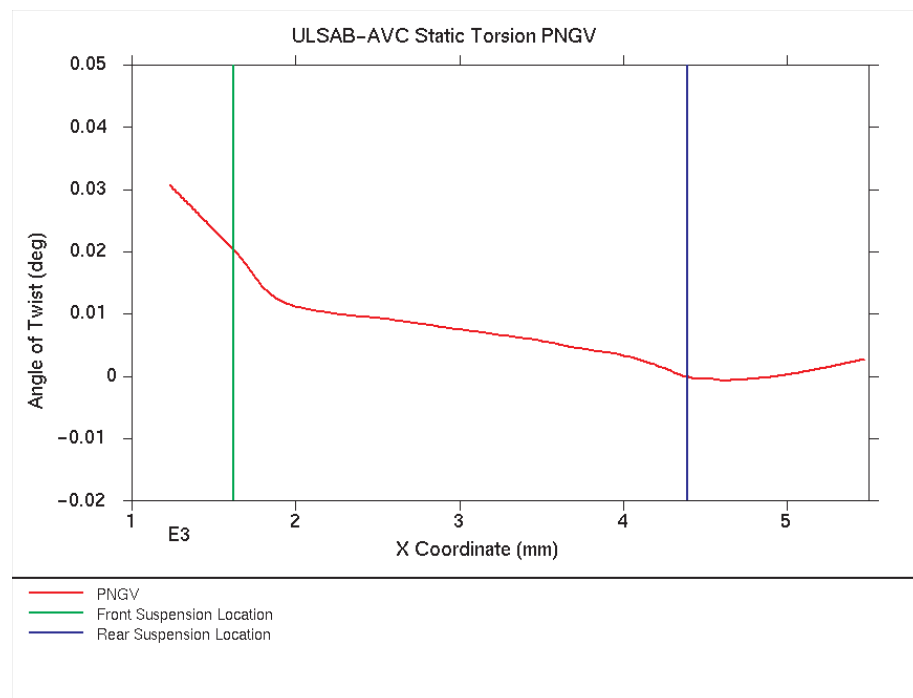


Figure 10.2.1-4 PNGV-Class static torsion angle of twist

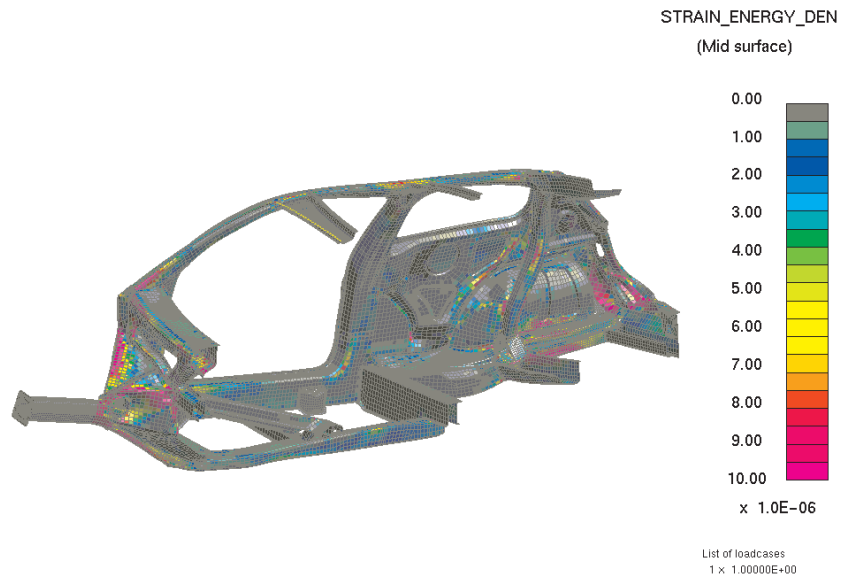


Figure 10.2.1-5 C-Class static torsion strain energy density contours

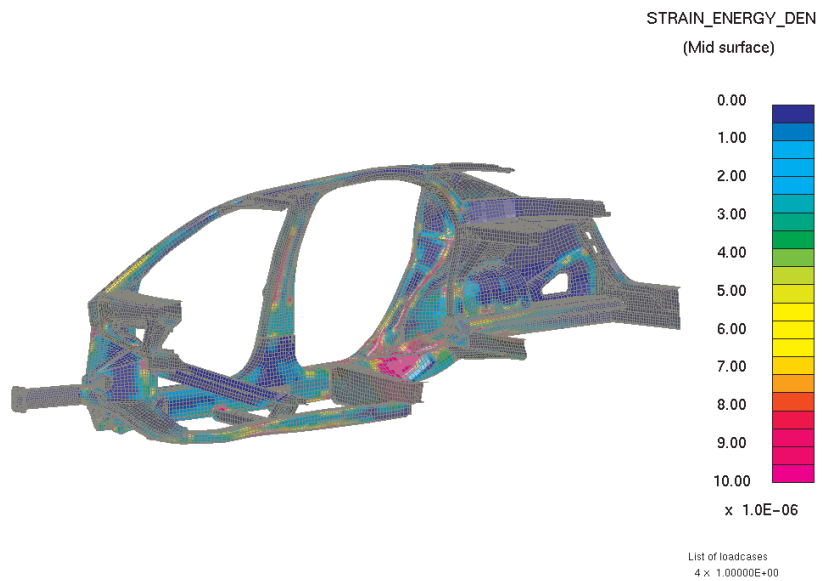


Figure 10.2.1-6 PNGV-Class static torsion strain energy density contours

10.2.2. Bending Stiffness

The loads were applied to the center of the front seats and to the center of the two outer rear seats. The measurements were taken under a load of $F_b \text{ max} = 1000 \text{ N}$. The body was supported at the front subframe mount location on the front longitudinal member in the vertical direction and at the rear spring attachment in both the vertical and longitudinal directions. Symmetric boundary conditions were applied at the plane of symmetry.

The deformed shapes for the static bending load case are shown in Figures 10.2.2-1 and 10.2.2-2. Figures 10.2.2-3 and 10.2.2-4 show the vertical displacement along the length of the vehicle (x-axis) for C-Class and PNGV-Class respectively. Strain energy contour plots (Figures 10.2.2-5 and 10.2.2-6) show the strain energy distribution in the structures for this load case.

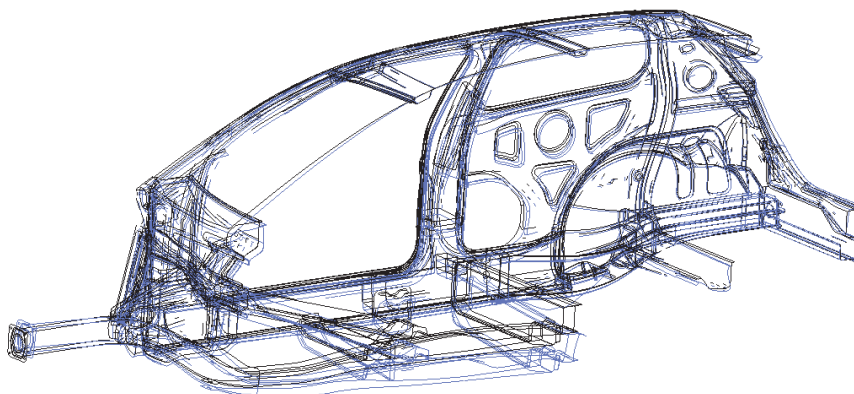


Figure 10.2.2-1 C-Class static bending deformed shape

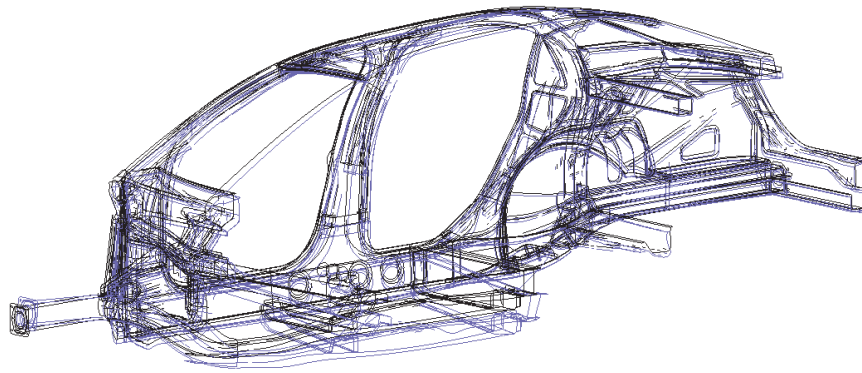


Figure 10.2.2-2 PNGV-Class static bending deformed shape

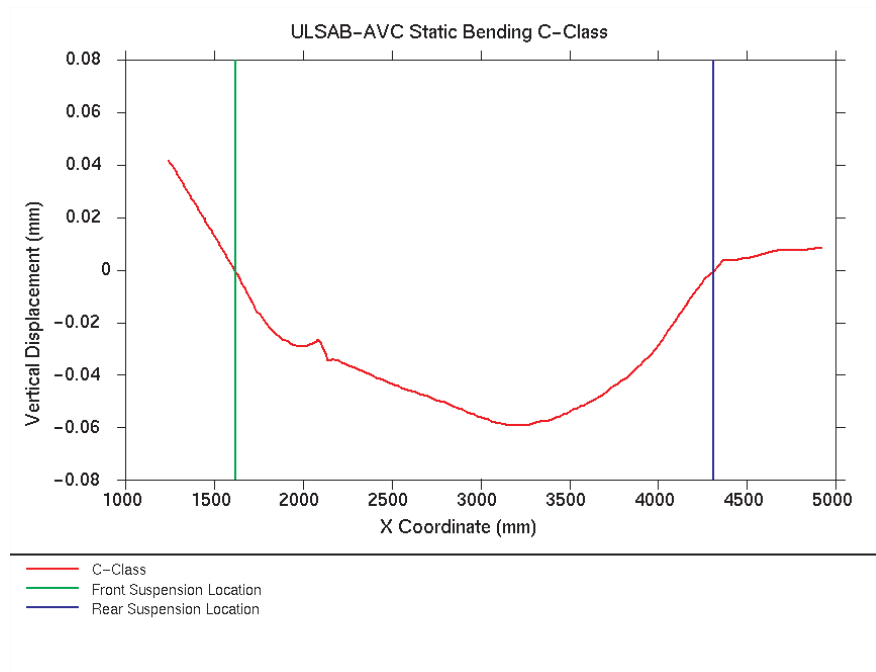


Figure 10.2.2-3 C-Class vertical displacement graph

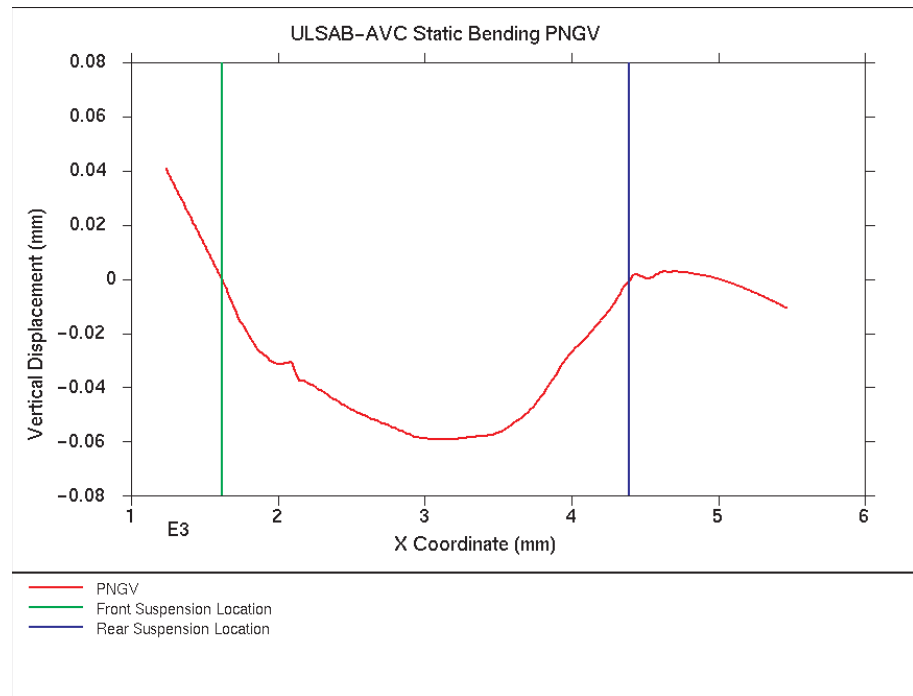


Figure 10.2.2-4 PNGV-Class vertical displacement graph

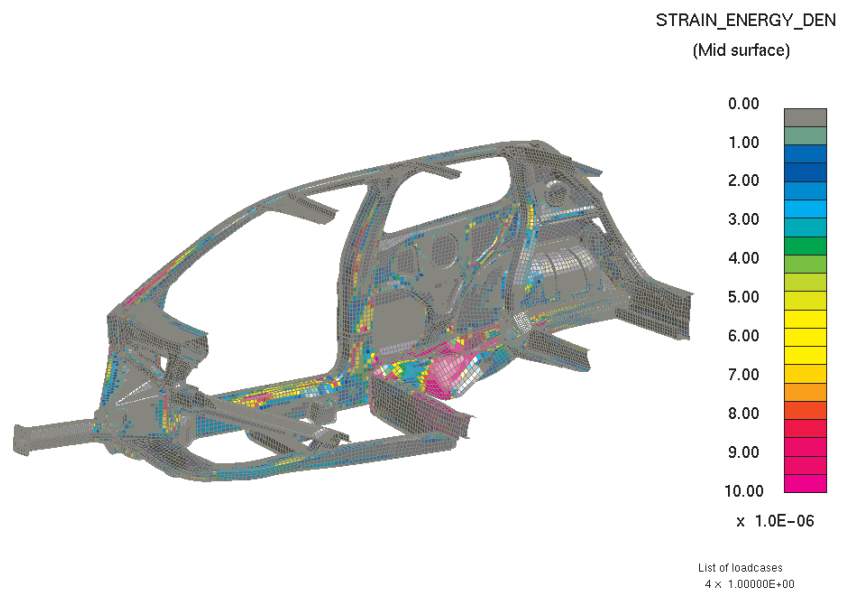


Figure 10.2.2-5 C-Class strain energy contours

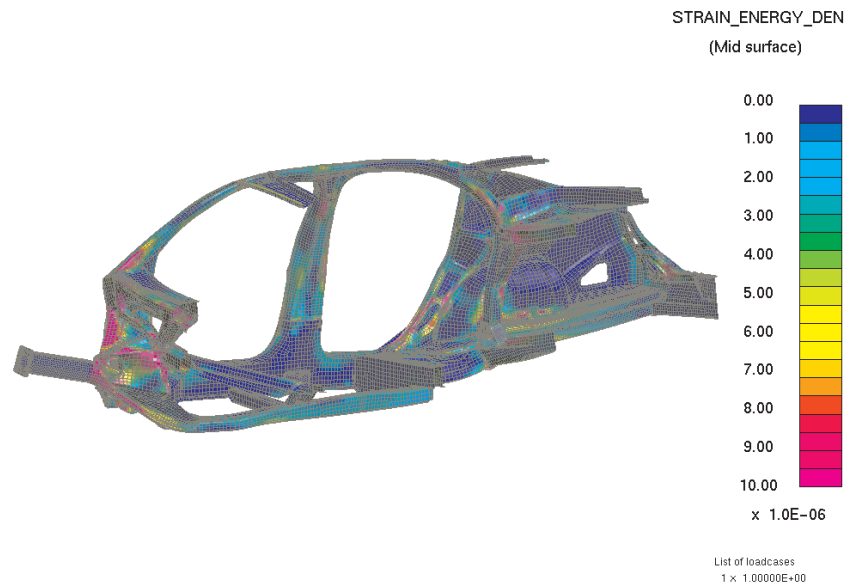


Figure 10.2.2-6 PNGV-Class strain energy contours

10.2.3. Normal Modes

The results of the normal modes analysis bending and torision are shown in Tables 10.2.3-1 and 10.2.3-2 and the deformed shapes presented in Figures 10.2.3-1 through 10.2.3-4.

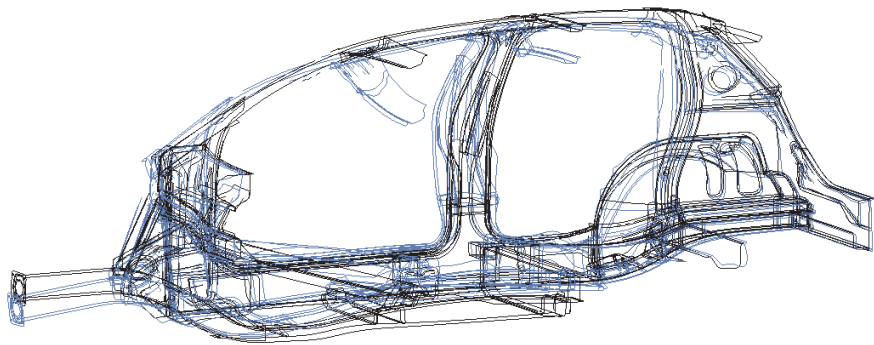


Figure 10.2.3-1 C-Class first bending frequency

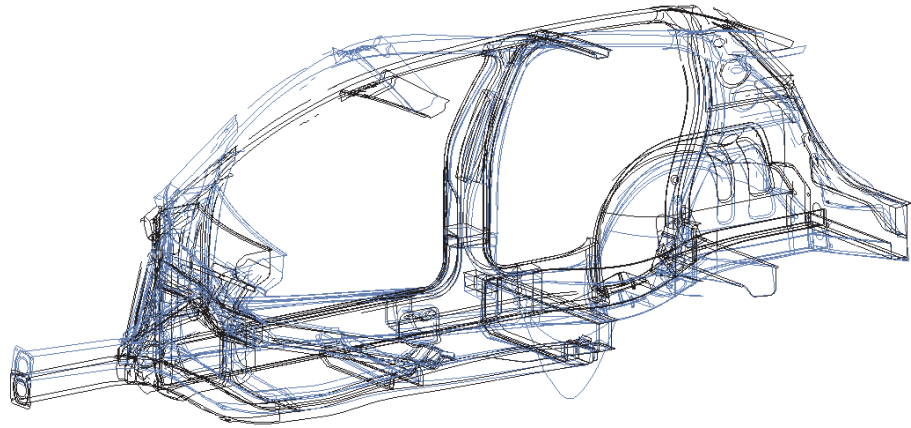


Figure 10.2.3-2 C-Class first torsion frequency

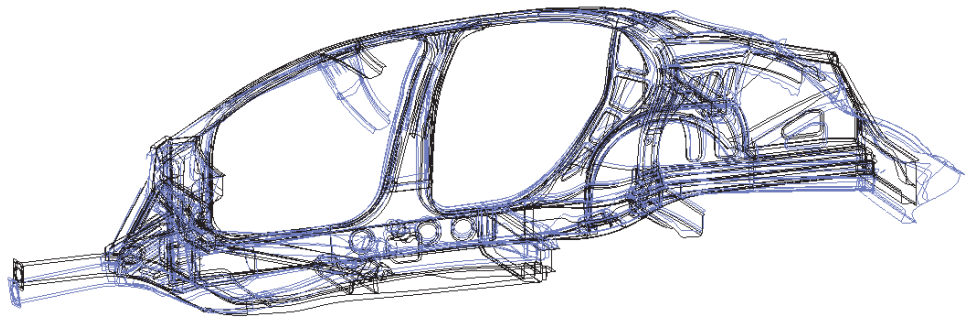


Figure 10.2.3-3 PNGV-Class first bending frequency

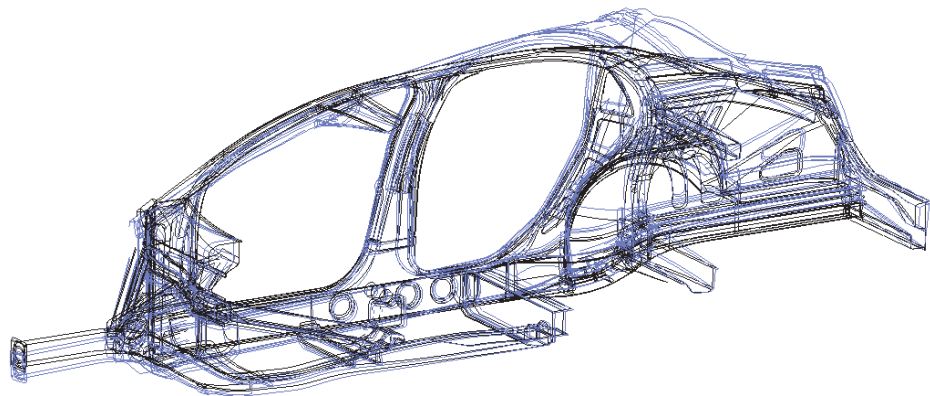


Figure 10.2.3-4 PNGV-Class first torsion frequency

Table 10.2.3-1 C-Class normal mode results

C-Class	Target	Result
Static Bending Rigidity* (N/mm)	11,000	17,050
Static Torsion Rigidity* (Nm/deg)	12,000	14,350
First Bending Mode* (Hz)	48	58.2
First Torsion Mode* (Hz)	35	49
Front End Lateral* (Hz)	> 55	> 70

* without bumper

Table 10.2.3-2 PNGV-Class normal mode results

PNGV-Class	Target	Result
Static Bending Rigidity (N/mm)	12,000	17,150
Static Torsion Rigidity (Nm/deg)	13,000	17,400
First Bending Mode (Hz)	48	66.5
First Torsion Mode (Hz)	40	44.1
First End Lateral (Hz)	> 55	> 70

*without bumper

10.2.4. Stress Analysis

An analysis to simulate typical peak road load inputs to the structure was undertaken to provide information on the potential high-risk areas of the body structure which could be susceptible to durability concerns. A '3G' bump load was applied to the suspension locations and the resulting stresses are presented in figures 10.2.4-1 and 10.2.4-2 for the C-Class and PNGV-Class vehicles respectively.

The stress distributions could be used in a subsequent project to identify areas of the structure, which should be assessed with regards to their durability.

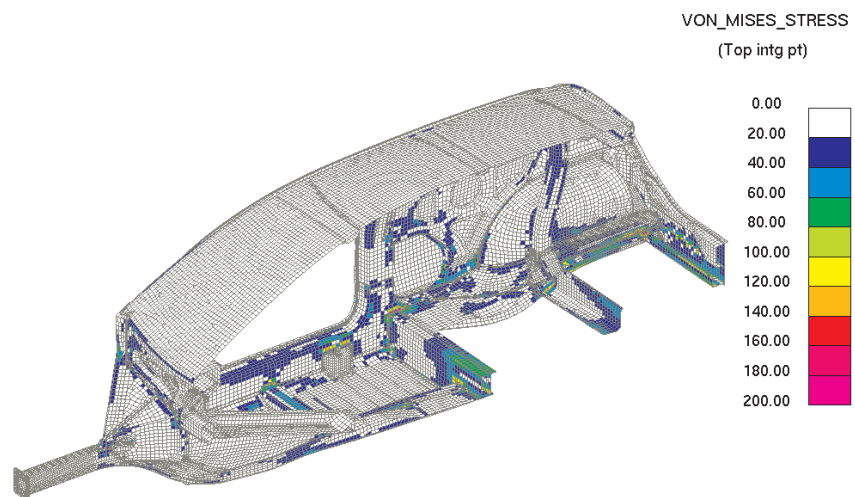


Figure 10.2.4-1 C-Class 3G bump load stress contours

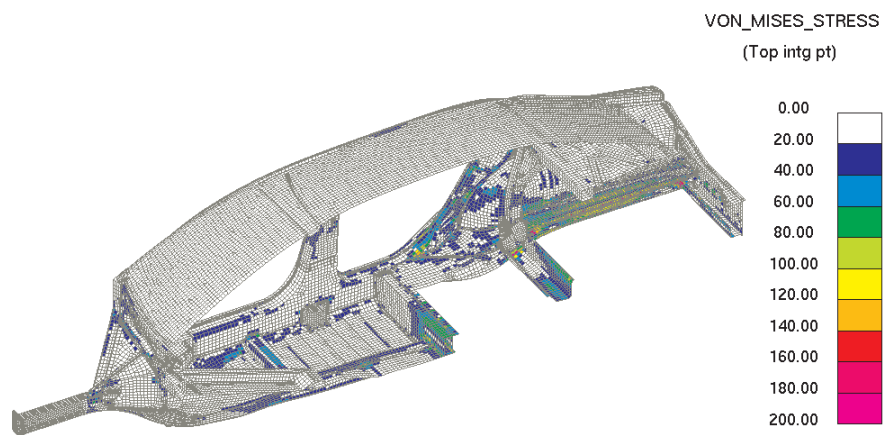


Figure 10.2.4-2 PNGV-Class 3G bump load stress contours

10.3. Crash Analysis

One common crash model was generated for each of the C-Class and PNGV-Class vehicles to conduct the following load cases:

- US-NCAP - 100% frontal crash at 35 mph into rigid barrier
- Euro-NCAP front crash - 40% overlap offset frontal crash at 64 km/h into deformable barrier
- US-SINCAP – US side impact barrier impact at 38.5 mph
- Side Pole Impact – side impact into rigid pole at 20 mph
- Rear Impact - moving barrier crash at 35 mph
- Low speed impact – 100% front crash at 15 km/h into rigid barrier

All crash-relevant car components were modeled, such as:

- Wheels and tires
- Engine and transmission
- Chassis system with subframe
- Steering column
- Fuel tank
- Bumper system including crashbox
- Radiator with fan
- Doors, front and rear without glass
- Fixed glass

Figures 10.3-1 and 10.3-2 show the C-Class and PNGV-Class crash FE-models. Model sizes for the PNGV-CLASS and C-Class stiffness models are summarized in Table 10.3-1.

Table 10.3-1 Crash model sizes

Crash Model Size	C-Class	PNGV-Class
Number of Nodes	182500	201500
Number of Elements	178000	196000

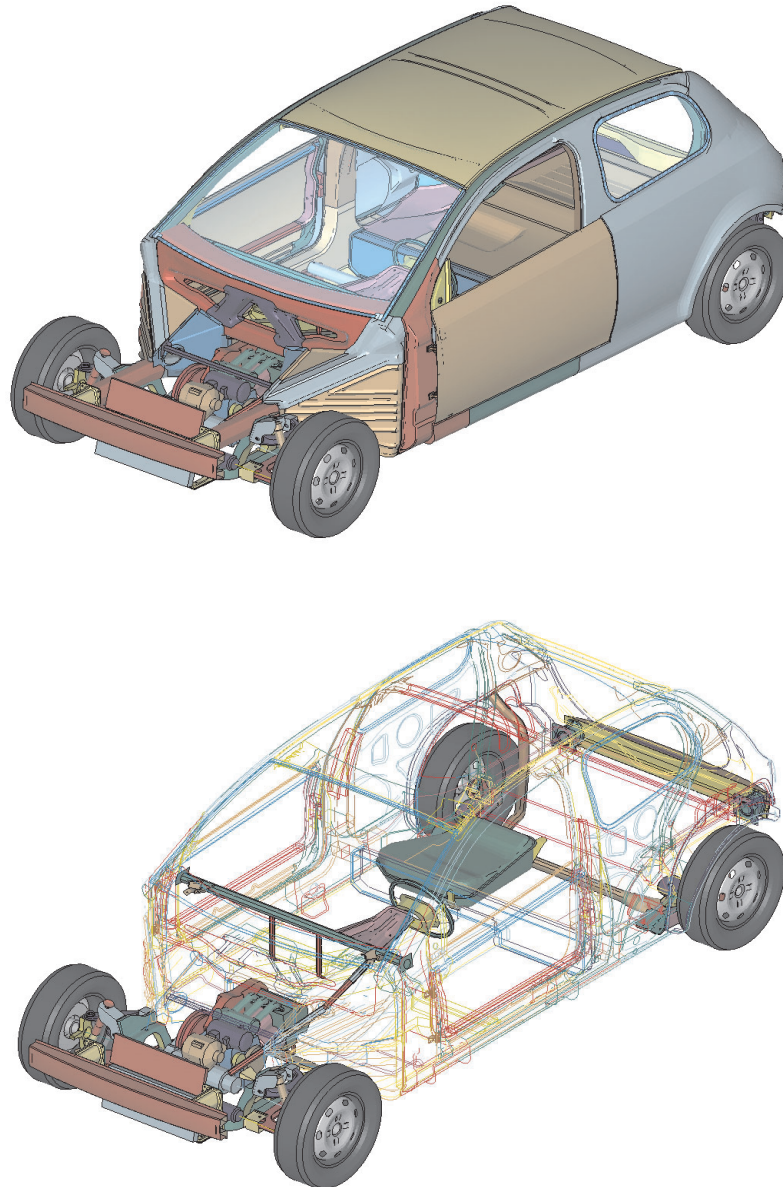


Figure 10.3-1 C-Class finite element crash model complete

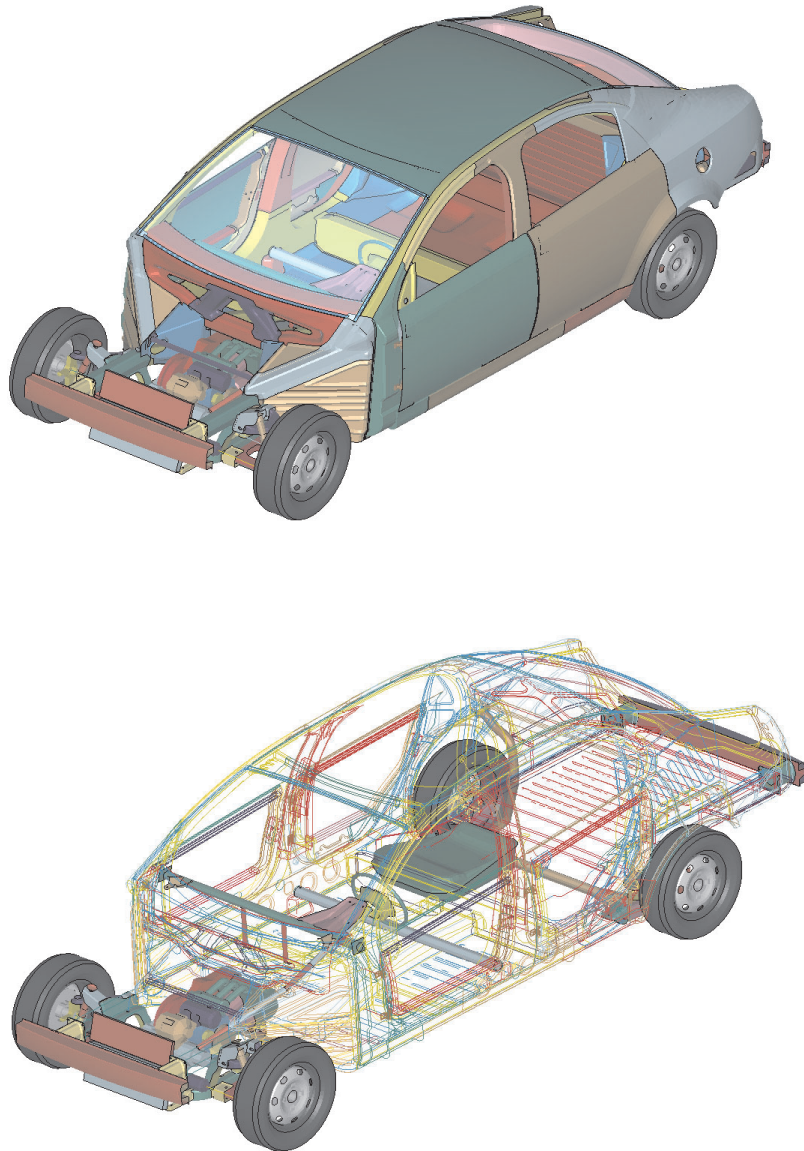


Figure 10.3-2 PNV-Class finite element crash model complete

The vehicle crash mass was defined to be base curb weight plus two 50th percentile male dummies with 113 kg of luggage. The crash mass for the C-Class and PNGV-Class vehicles is shown in Table 10.3-2.

Table 10.3-2 Crash Mass

	C-Class Diesel	C-Class Gasoline	PNGV-Class Diesel	PNGV-Class Gasoline
Curb Mass	1023	980	1102	1059
Luggage	113	113	113	113
Occupants 2x	149	149	149	149
Optional Equipment	49	49	49	49
Total Crash Mass	1334	1291	1413	1370
	1309 (+25)	1266 (+25)	1388 (+25)	1345 (+25)

For each of the crash events, a vehicle variant was chosen for the analysis as shown in Table 10.3-3. These variants were selected to show the most severe case or the range of results possible. In the US-NCAP event, for example, the acceleration level is an important parameter and the C-Class gasoline (lightest variant) was chosen to show the most severe acceleration results. For the PNGV-Class, the heaviest variant (diesel) was selected to show the least severe acceleration results, but the most severe intrusion. In the Euro-NCAP event, the heaviest variant for each class (diesel) was selected to show the most severe levels of footwell intrusion.

Table 10.3-3 Vehicle variations

Event	C-Class	PNGV-Class
US-NCAP	Gasoline	Diesel
Euro NCAP	Diesel	Diesel
US SINCAP	Diesel	Diesel
Side Pole	Diesel	Diesel
Rear Impact	Diesel	Diesel
Low Speed Impact	--	Diesel

For the roof crush analysis, the full model with reduced contents was used (see Figures 10.3-3 and 10.3-4). The models included the following:

- Fixed glass
- Doors, front and rear without glass

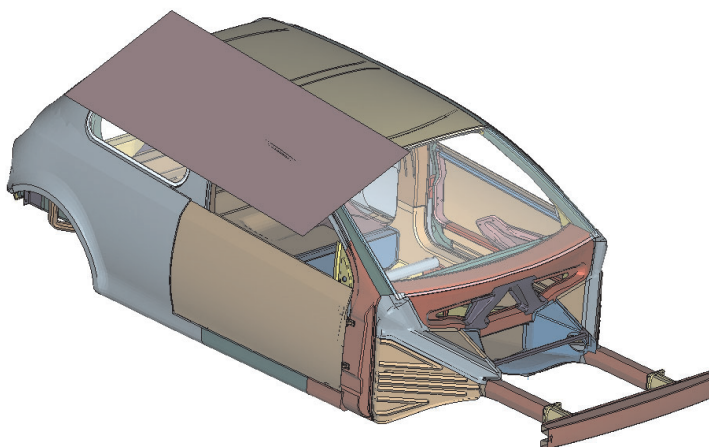


Figure 10.3-3 C-Class roof crush finite element model

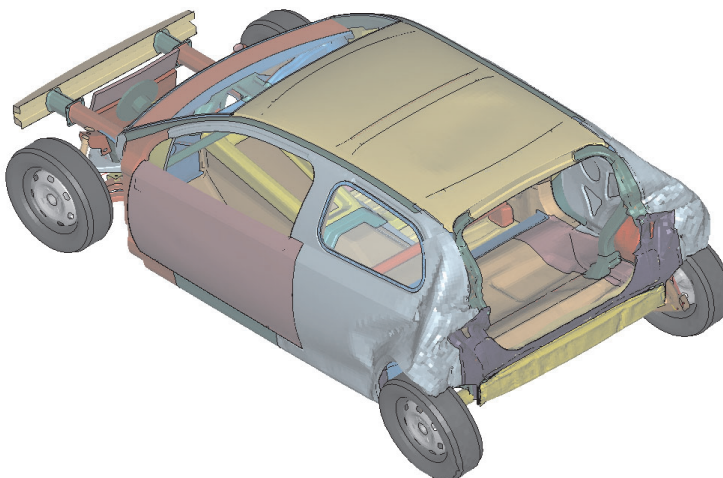


Figure 10.3-4 PNGV-Class roof crush finite element model

The steel material properties used for the CAE models were obtained from the ULSAB-AVC Consortium materials database. The steel material properties included the dynamic strain rate characteristic of the steel.

10.3.1. US-NCAP Front Crash

The frontal impact test of the New Car Assessment Program (NCAP) undertaken by the National Highway and Traffic Safety Association (NHTSA) is a full frontal barrier test at a vehicle speed of 35 mph (Figure 10.1.2-1).

The focus of design in the ULSAB-AVC program was on progressive crush of the main front longitudinal members; distribution of the load into the tunnel, sill, and A-pillar; A-pillar stability; stability of the door ring; footwell intrusion; and passenger compartment residual space. The objective was to make use of the available crush space in an efficient manner and minimize deformation of the occupant compartment.

The analysis including occupants and a fully developed interior concept was not part of the ULSAB-AVC concept phase scope of work. Therefore, no occupant injury assessment could be made. However, the concept structure was compared to the structural performance of similar vehicles to assess the potential of the concept to achieve the highest Star Rating for the US-NCAP test. The Star Rating assessment is presented later in this report.

The US-NCAP Frontal Crash undeformed (time = 0) and deformed shape (at time = 100 ms) for C-Class and PNGV-Class vehicles are shown in Figures 10.3.1-1 through 10.3.1-4. The residual intrusion in the footwell area is shown in Figure 10.3.1-5 for the C-Class and Figure 10.3.1-6 for the PNGV-Class vehicle. Low footwell intrusion is important in minimizing lower-leg injuries to the occupants.

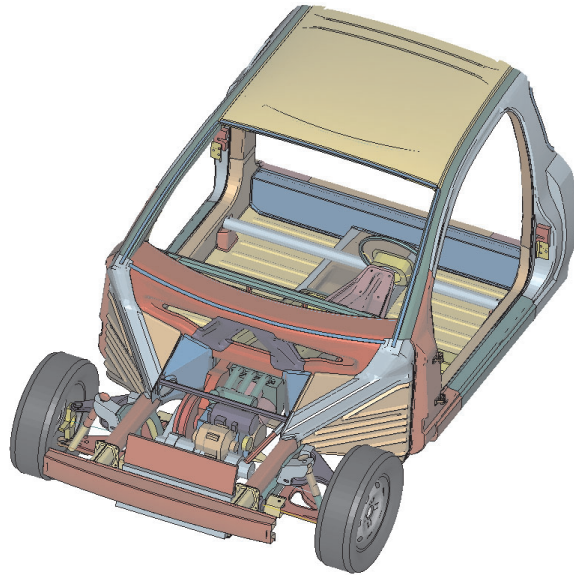


Figure 10.3.1-1 C-Class US-NCAP undeformed shape

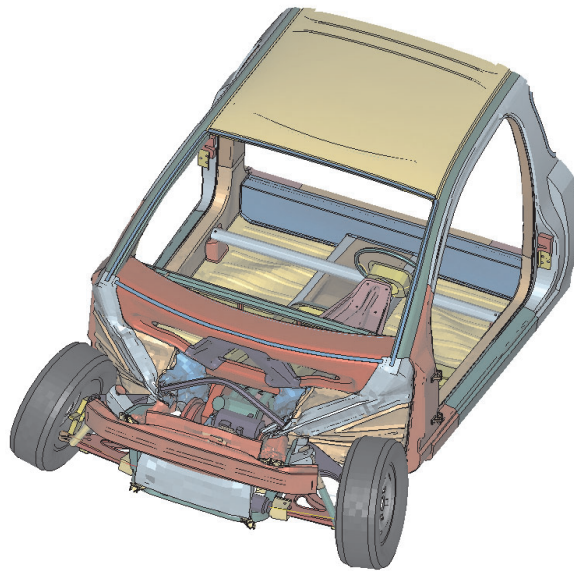


Figure 10.3.1-2 C-Class US-NCAP deformed shape

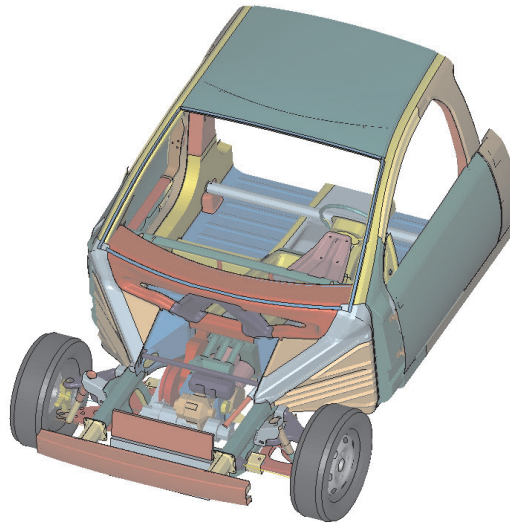


Figure 10.3.1-3 PNGV-Class US-NCAP undeformed shape

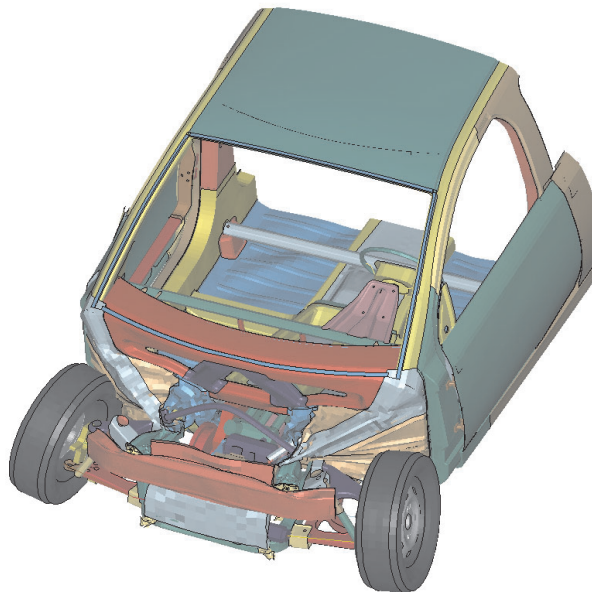


Figure 10.3.1-4 PNGV-Class US-NCAP deformed shape

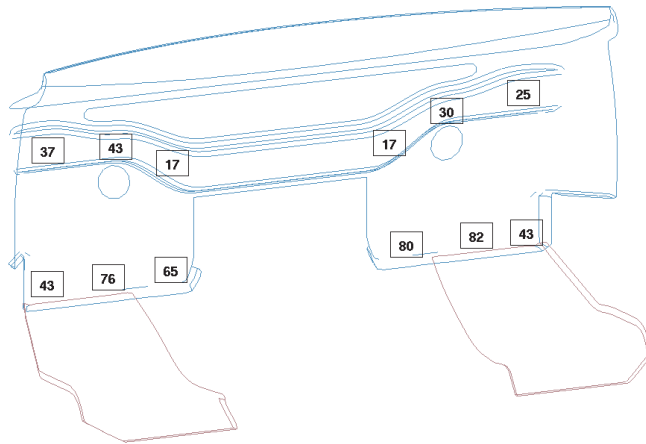


Figure 10.3.1-5 C-Class US-NCAP residual footwell intrusion

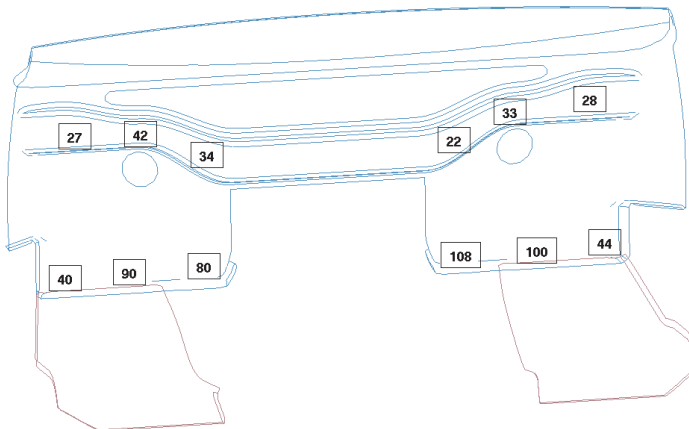


Figure 10.3.1-6 PNGV-Class US-NCAP residual footwell intrusion

The internal energy absorption diagram in Figure 10.3.1-7 gives an overview of the energy absorbed in the parts subframe, bumper, bumper box, front rails and pyramid (transition structure from longitudinals to the A-pillar/tunnel/rocker, excluding front rails) transition at the time of maximum deformation of the structure. The PNGV-Class vehicle is the heavier variant, therefore, the absorbed energy is proportionately higher.

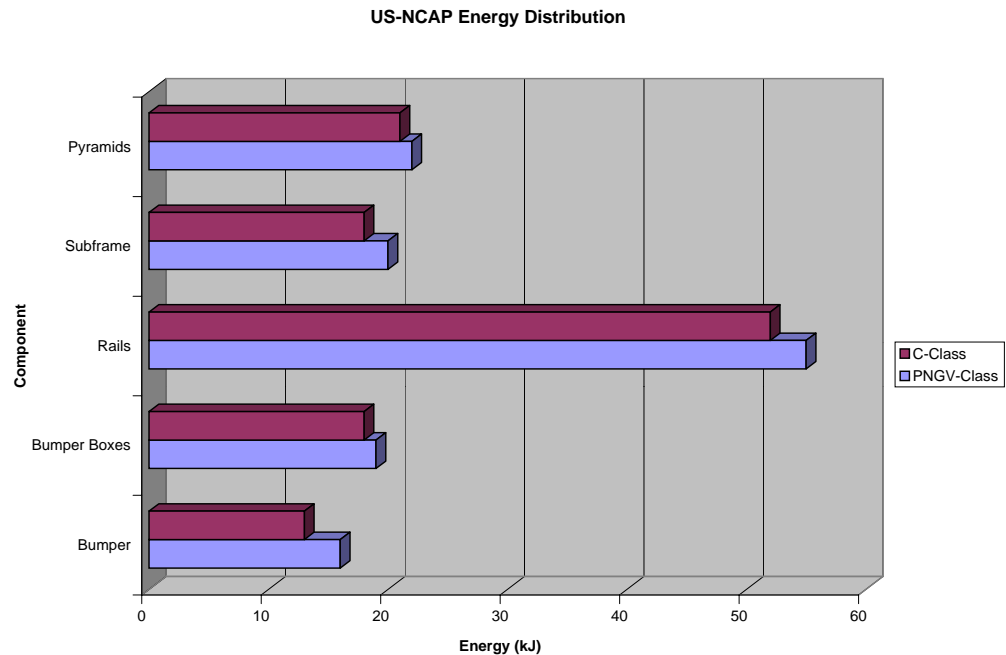


Figure 10.3.1-7 Energy distribution in the structure

Figure 10.3.1-8 shows the common front end structure of the C-Class and PNGV-Class vehicles. Figures 10.3.1-9 and 10.3.1-10 show the typical section forces for the most important front end structure components for C-Class and PNGV-Class respectively. The front longitudinal members are the main load paths at the front of the structure. The load distribution into the rest of the structure shows the rocker supporting a similar level of force to the total force supported by the A-pillar and tunnel combined.

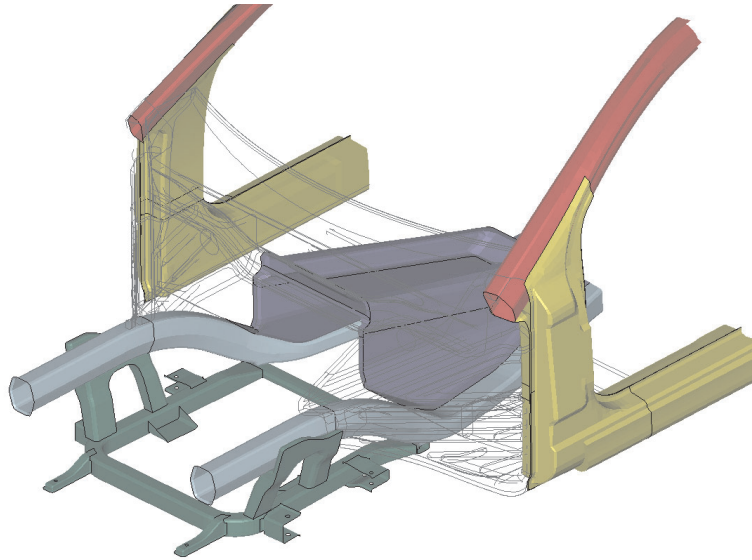


Figure 10.3.1-8 Common front end structure for ULSAB-AVC

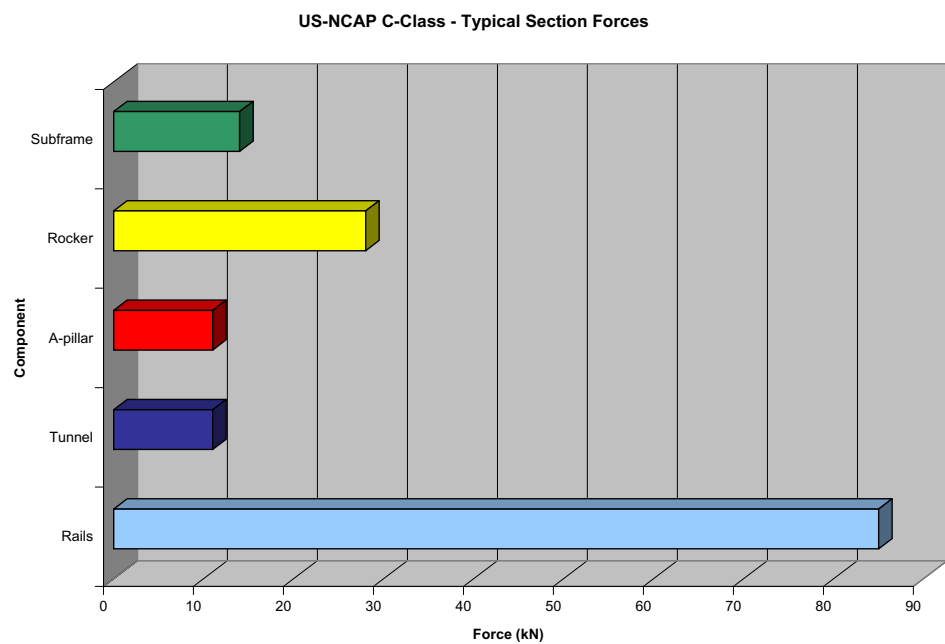


Figure 10.3.1-9 C-Class typical section forces

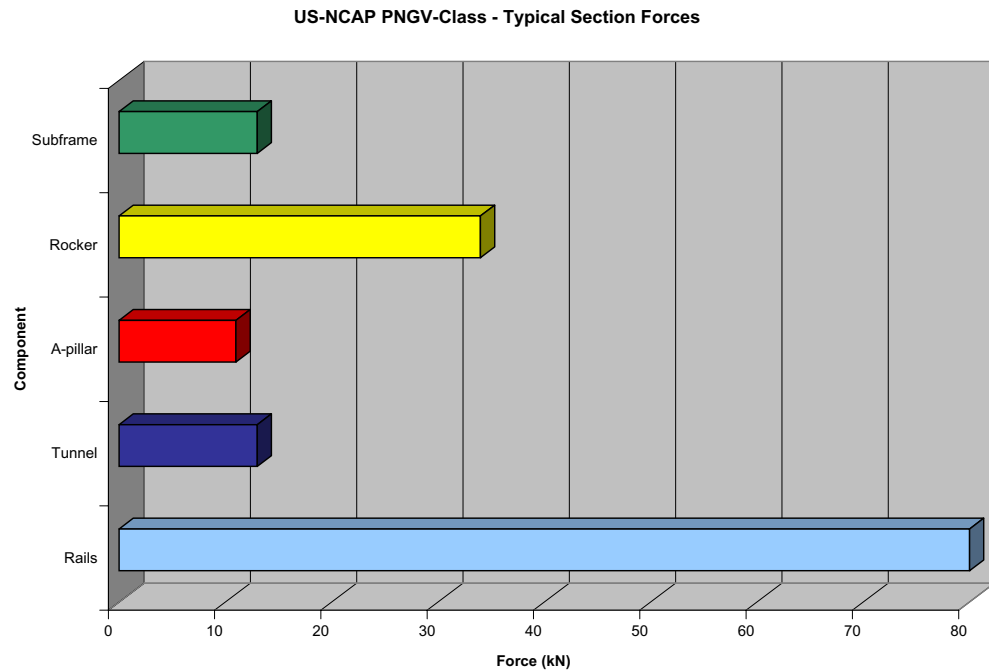


Figure 10.3.1-10 PNGV-Class typical section forces

The B-pillar longitudinal displacement, velocity and acceleration curves for the C-Class and PNGV-Class vehicles are shown in Figures 10.3.1-11 to 10.3.1-16. The acceleration results have been filtered using an SAE C-60 filter. These results are the average values from the left and right hand sides of the vehicle. Table 10.3.1-1 summarizes the targets and results of each of the vehicles for this crash event.

The target for dynamic crush has not been achieved. However, this target was more of a guideline than an absolute target and the ULSAB-AVC concept is an efficient structure, which achieves a high level of crashworthiness and is comparable in dynamic crush with other vehicles. This is described in more detail in section 10.4 Star Rating Assessment.

Table 10.3.1-1 US-NCAP results summary

US-NCAP	C-Class	PNGV-Class	Target
Dynamic Crush (mm)	610	645	650
Time to zero velocity (msec)	66	70	n/a
Steering Column Rearward Movement (mm)	10	10	< 80

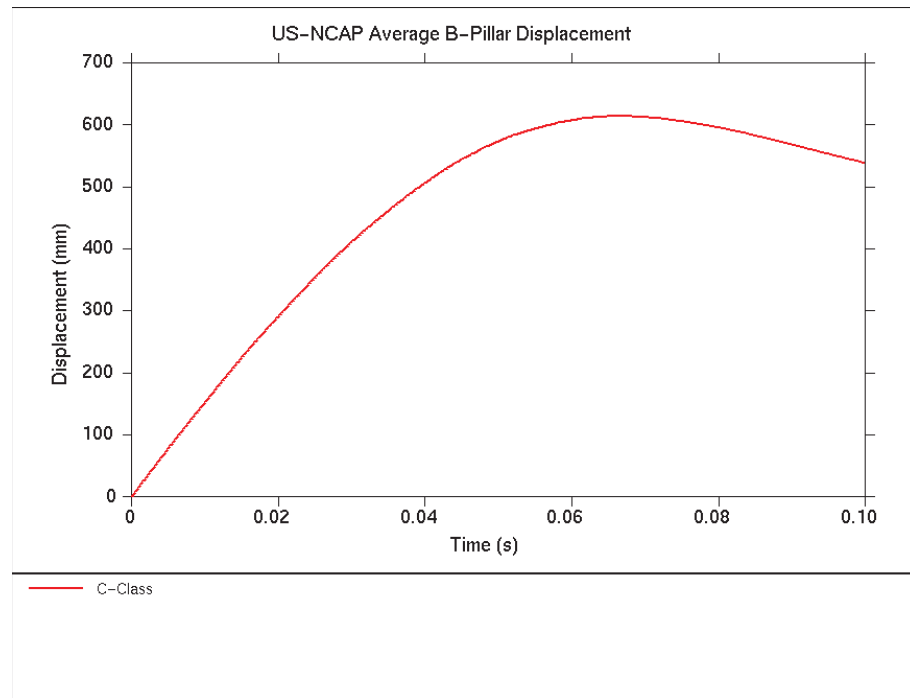


Figure 10.3.1-11 C-Class US-NCAP longitudinal B-Pillar displacement

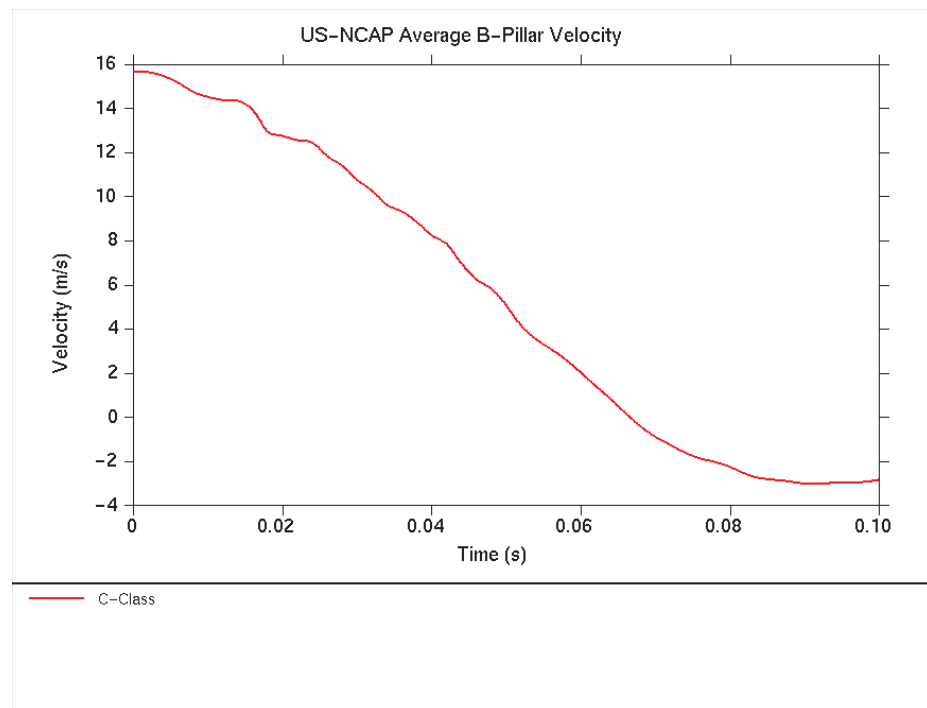


Figure 10.3.1-12 C-Class US-NCAP longitudinal B-Pillar velocity

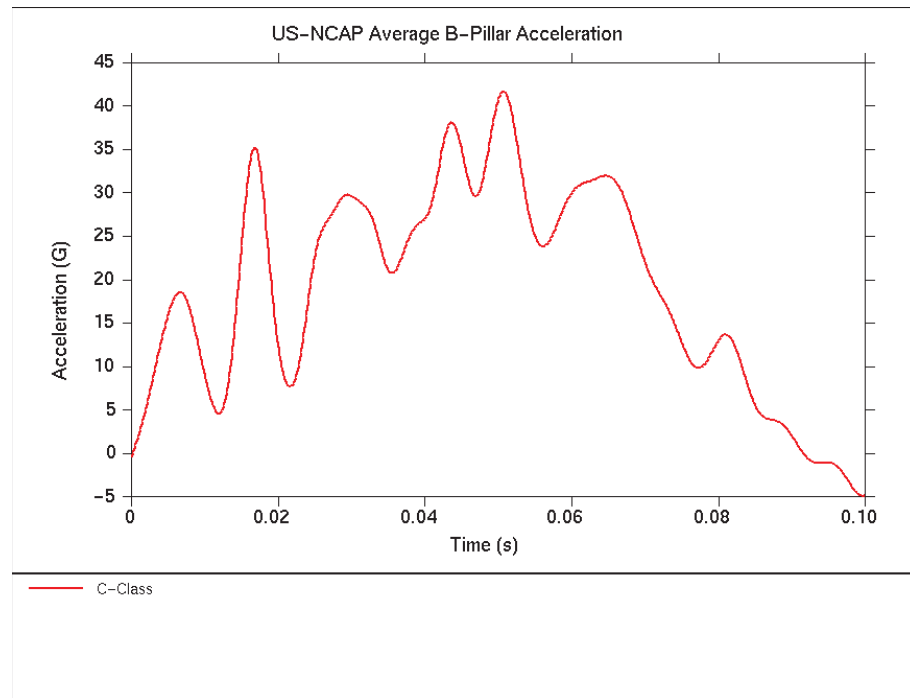


Figure 10.3.1-13 C-Class US-NCAP longitudinal B-Pillar acceleration

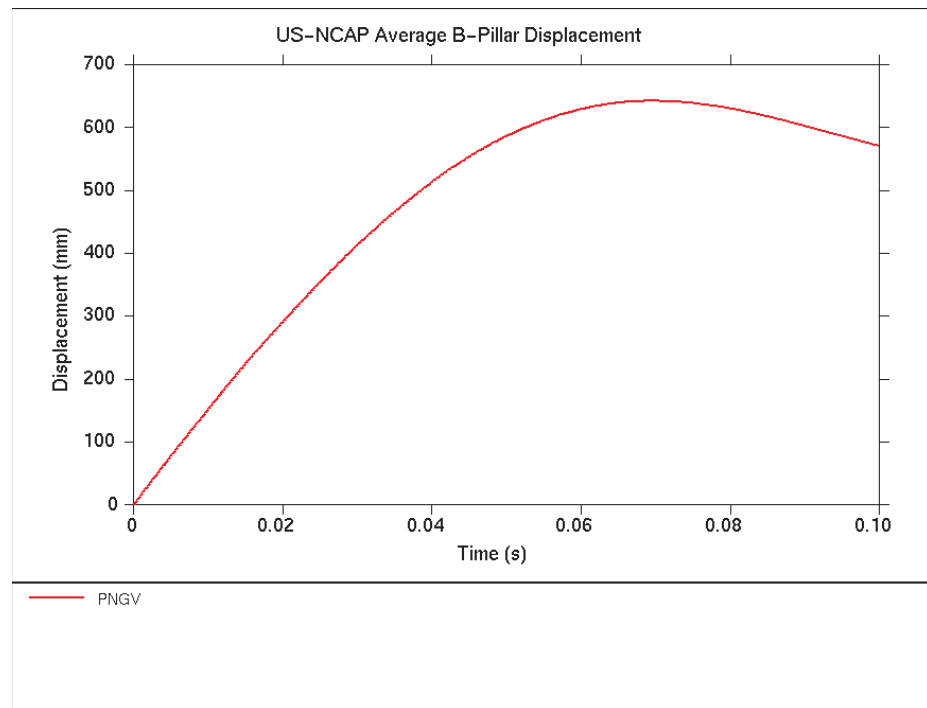


Figure 10.3.1-14 PNGV-Class US-NCAP longitudinal B-Pillar displacement

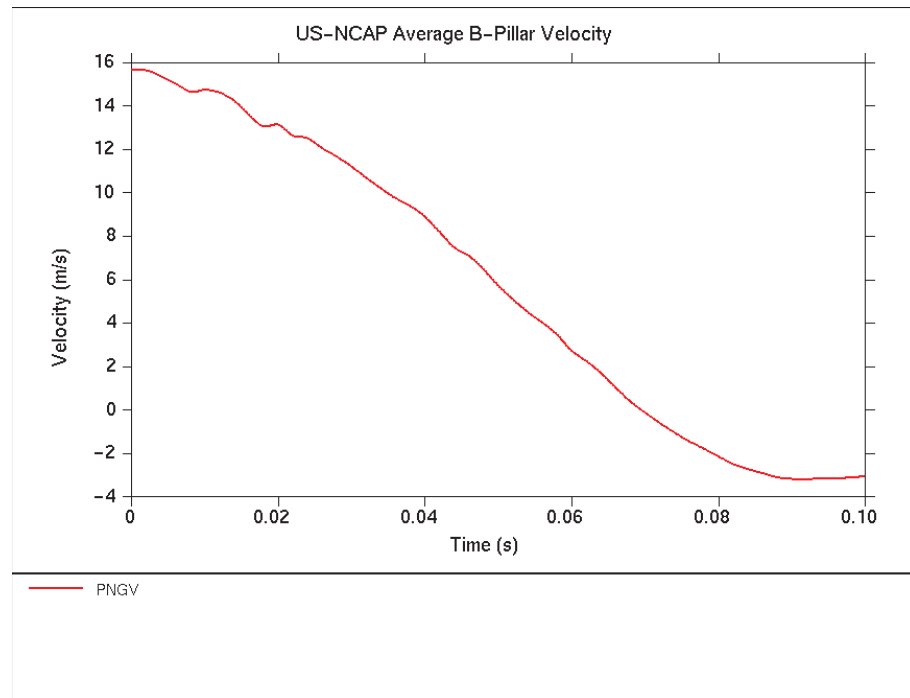


Figure 10.3.1-15 PNGV-Class US-NCAP longitudinal B-Pillar velocity

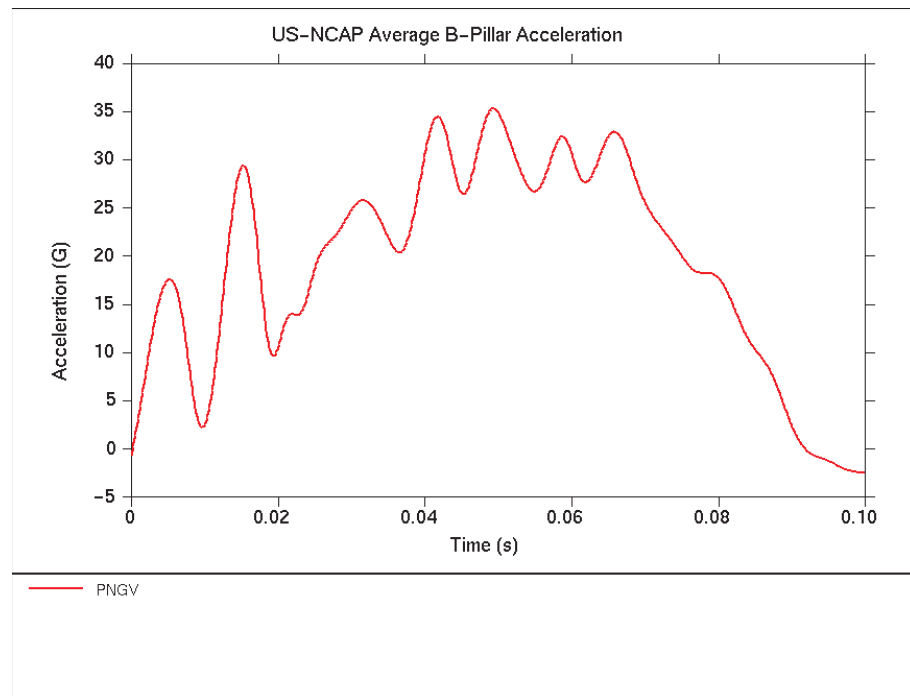


Figure 10.3.1-16 PNGV-Class US-NCAP longitudinal B-Pillar acceleration

The following table shows the NCAP crash events:

Table 10.3.1-2 US-NCAP crash events

Time (msec)		US-NCAP Timing of Major Events
C-Class	PNGV-Class	
6	6	Bumper crush box starts to crush
16	16	Initial crush of longitudinal
18	18	Radiator/Cooling pack contacts barrier
22	22	Tires contact barrier
32	32	Engine contacts barrier
34	34	Rear subframe mount detaches from body
40	40	Rear of tires contact body
44	44	Engine bay brace buckles, longitudinal crush ends
66	70	Maximum dynamic deformation reached

This analysis illustrates good progressive crush of the main longitudinal members. The engine and subframe detach from the body structure at the rear mounts to allow full use of the available crush space and to minimize footwell intrusion.

Because the analysis did not include dummies, injury assessment could not be made. Occupant injury is greatly affected by the structural crash behavior and steering column movement as well as by the knee bar design. Evaluation of passenger compartment intrusion can be made by looking at intrusion in the footwell area (Figures 10.3.1-5 and 10.3.1-6). The low levels of footwell intrusion and steering column movement predicted are good results from an occupant injury perspective.

10.3.2 Euro NCAP 40% Offset Frontal Crash

The European New Car Assessment Program (Euro NCAP) specifies an offset frontal impact at 64 km/h into a deformable barrier with a vehicle overlap of 40%. The deformable barrier conforms to that specified in ECE R-94 "Frontal Collision Protection". The configuration is shown in Figures 10.3.2-1 and 10.3.2-2.

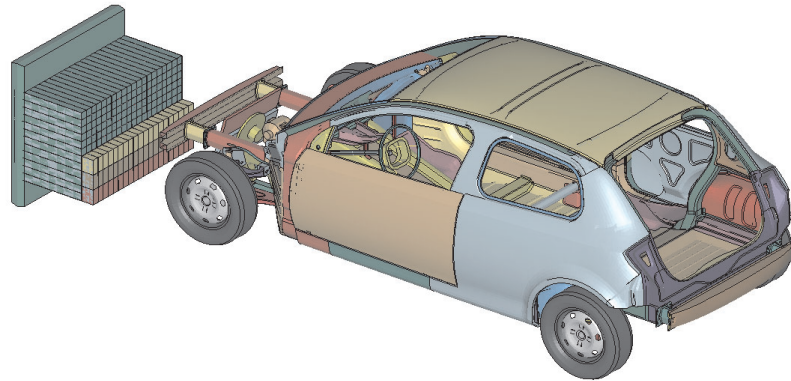


Figure 10.3.2-1 Euro-NCAP C-Class Front Impact Configuration

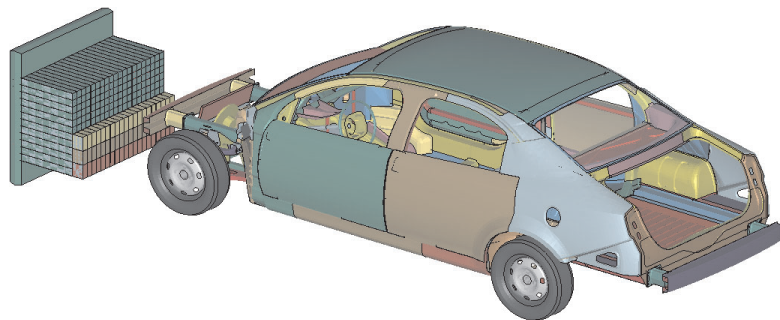


Figure 10.3.2-2 Euro-NCAP PNGV-Class Front Impact Configuration

The Euro-NCAP Frontal Crash undeformed (time = 0) and deformed shape (at time = 150 ms) for C-Class and PNGV-Class vehicles are shown in Figures 10.3.2-3 to 10.3.2-6. The residual deformation in the footwell area is shown in Fig. 10.3.2-7 for the C-Class and Figure 10.3.2-8 for the PNGV-Class vehicle. Low footwell intrusion is important in minimizing lower-leg injuries to the occupants.

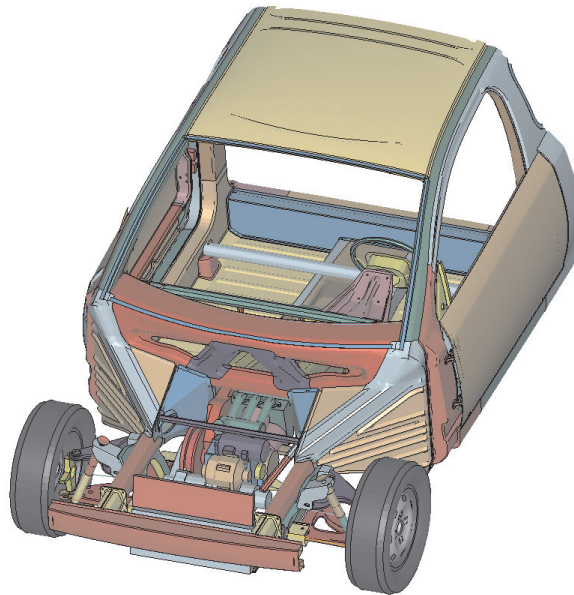


Figure 10.3.2-3 C-Class Euro-NCAP undeformed shape

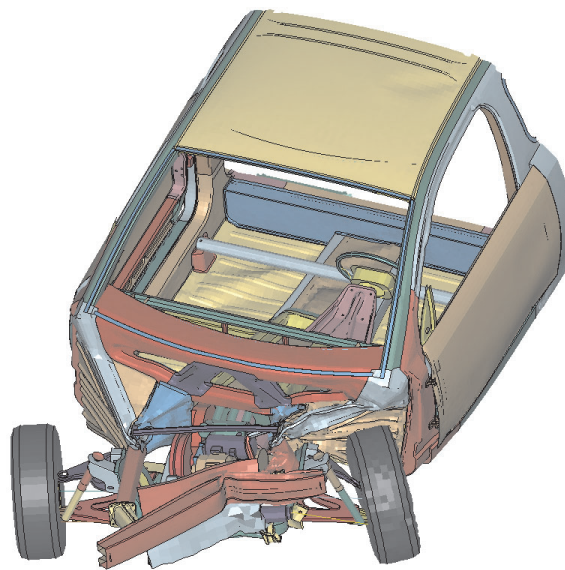


Figure 10.3.2-4 C-Class Euro-NCAP deformed shape

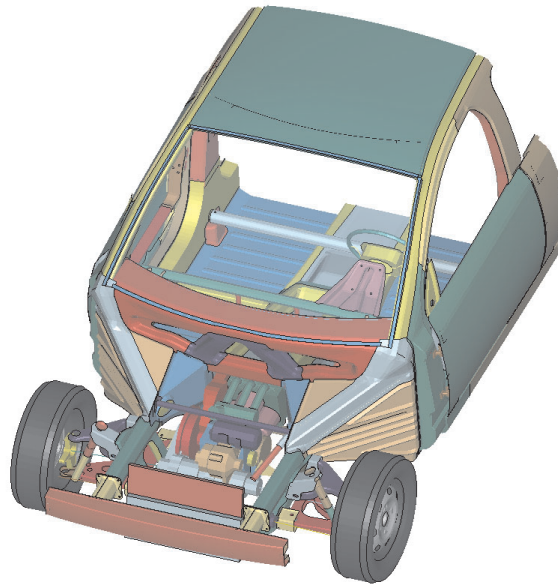


Figure 10.3.2-5 PNGV-Class Euro NCAP undeformed shape

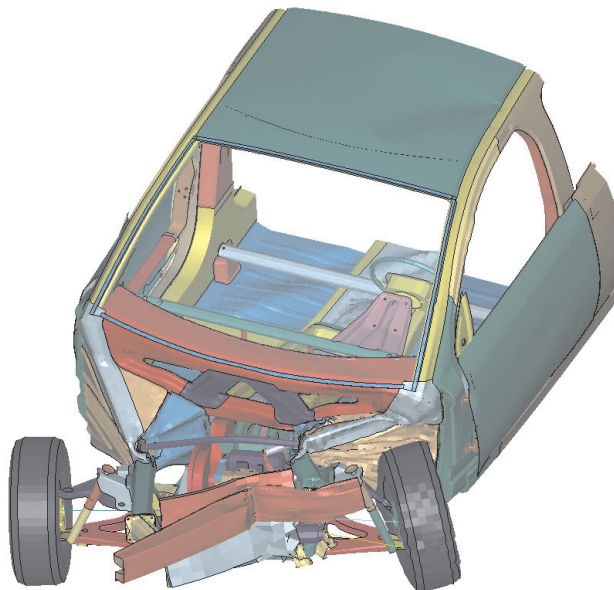


Figure 10.3.2-6 PNGV-Class Euro NCAP deformed shape

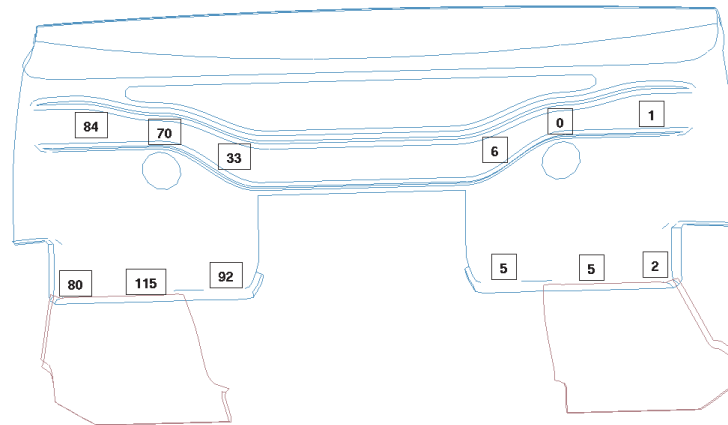


Figure 10.3.2-7 C-Class Euro-NCAP residual footwell intrusion

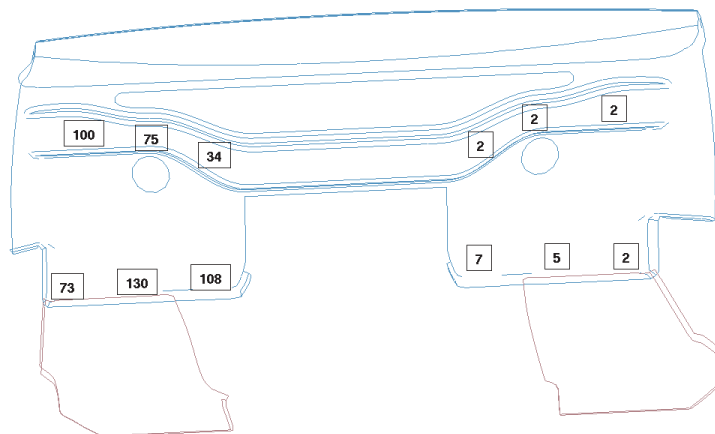


Figure 10.3.2-8 PNGV-Class Euro-NCAP residual footwell intrusion

The internal energy absorption diagram in Figure 10.3.2-9 gives an overview of the energy absorbed in the deformable barrier and the parts subframe, bumper, bumper box, front rail and pyramid (transition structure from longitudinals to the A-pillar/tunnel/rocker, excluding the front rails) at the time of maximum deformation of the structure. The PNGV-Class vehicle is the heavier variant, therefore in general, the absorbed energy is proportionately higher.

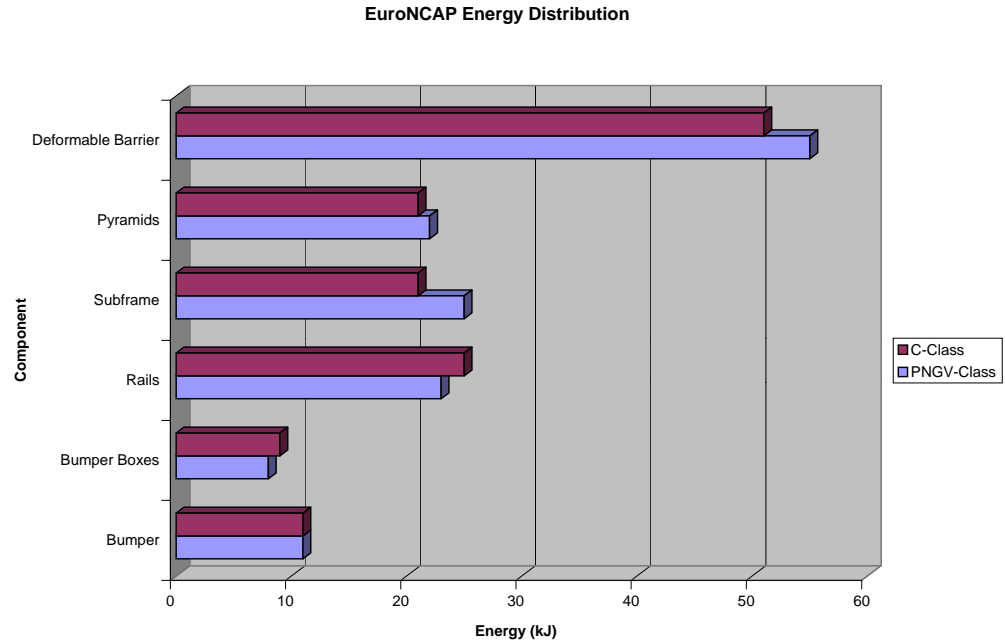


Figure 10.3.2-9 Euro NCAP energy distribution in the structures

The diagrams in Figures 10.3.2-10 and 10.3.2-11 show the typical section forces for the most important front structure components. The locations of the typical sections are shown in Figure 10.3.1-8. The front longitudinal members are the main load paths at the front of the structure. The load distribution into the rest of the structure shows the rocker supports a significant proportion of the total force. This is primarily when the load path is formed from the barrier through the wheel and into the rocker.

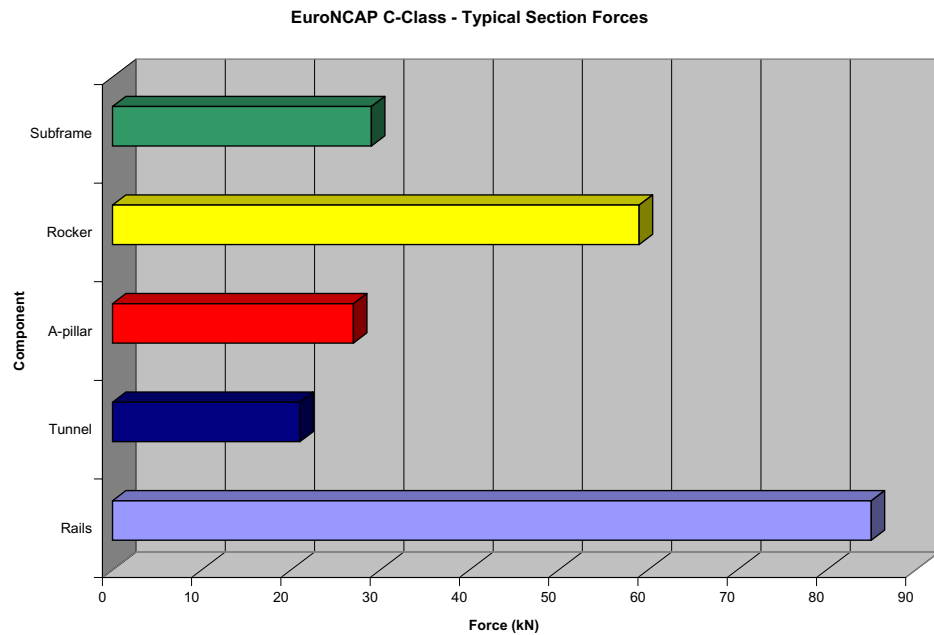


Figure 10.3.2-10 C-Class Euro-NCAP typical section forces

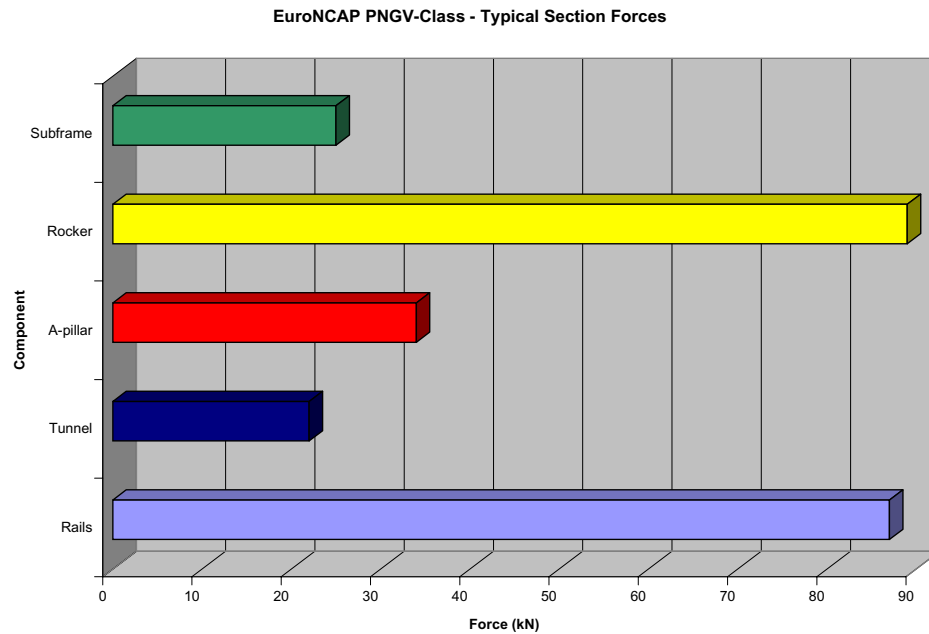


Figure 10.3.2-11 PNGV-Class Euro-NCAP typical section forces

The vehicle deformation, velocity and acceleration curves for the C-Class and PNGV-Class vehicles are shown in Figures 10.3.2-12 to 10.3.2-17. The velocity and acceleration results are the average values from the left and right hand sides of the vehicle. The acceleration results have been filtered with an SAE C-60 filter. Table 10.3.2-3 summarizes the results of each of the vehicles for this crash event.

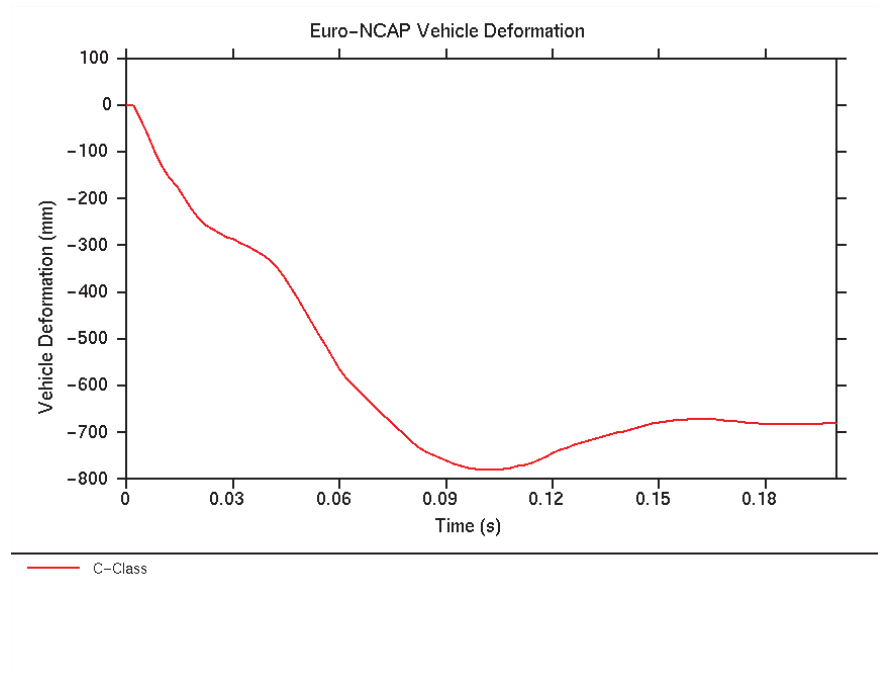


Figure 10.3.2-12 C-Class Euro-NCAP vehicle deformation

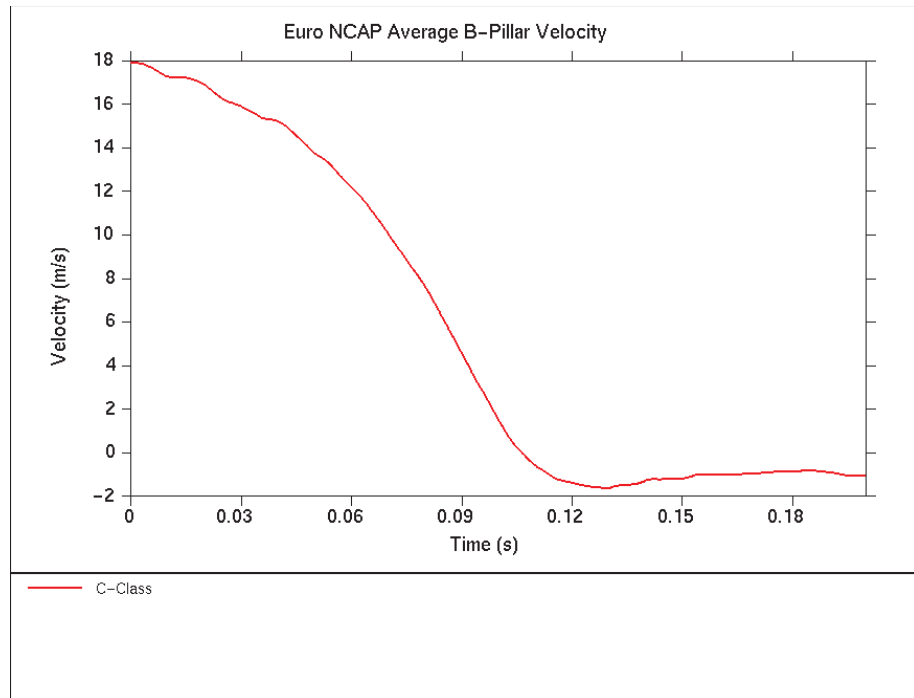


Figure 10.3.2-13 C-Class Euro-NCAP average longitudinal B-Pillar velocity

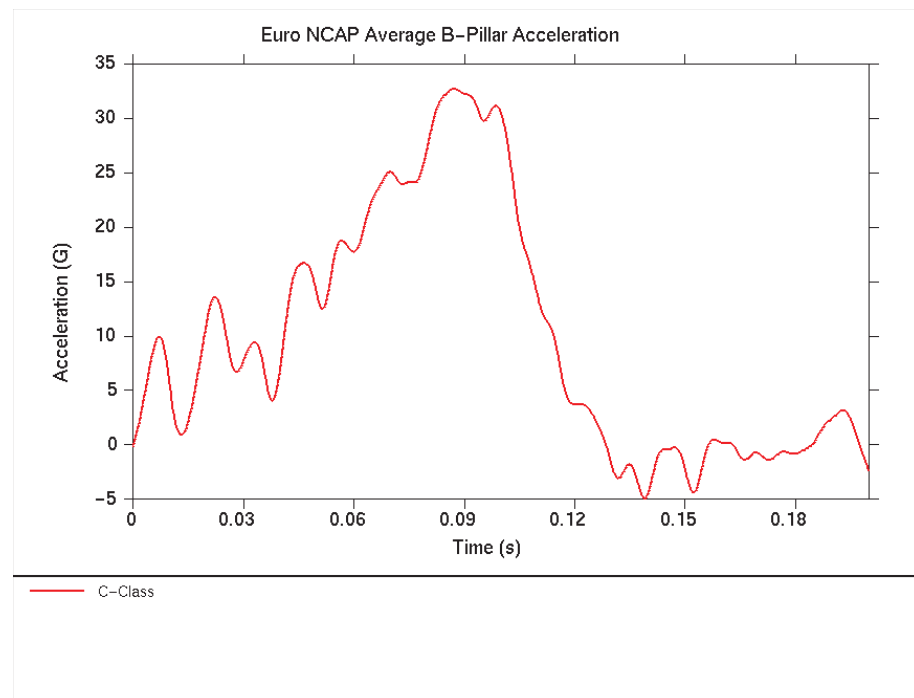


Figure 10.3.2-14 C-Class Euro-NCAP average longitudinal B-Pillar acceleration

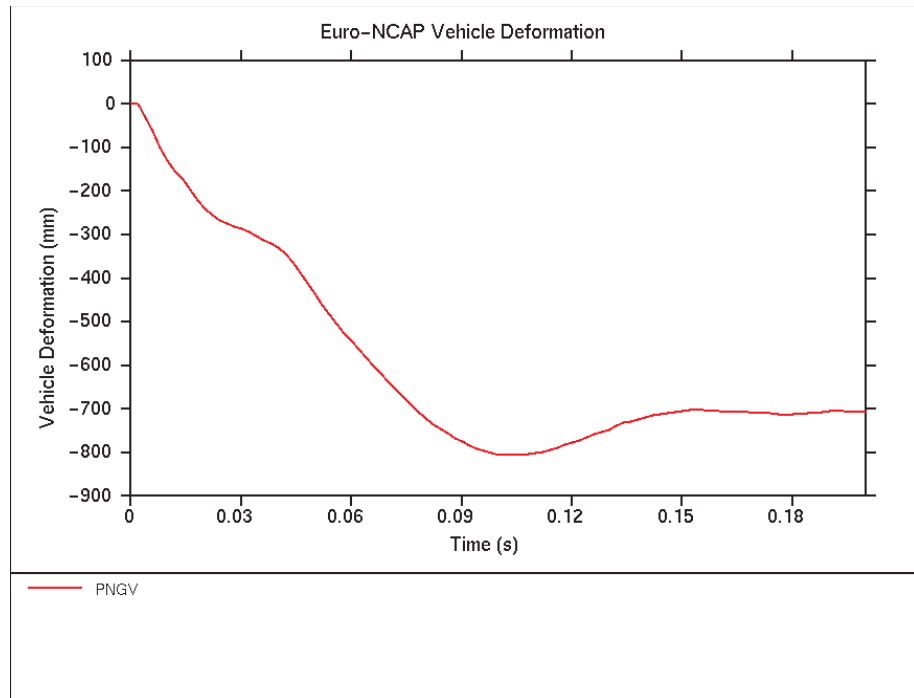


Figure 10.3.2-15 PNGV-Class Euro-NCAP vehicle deformation

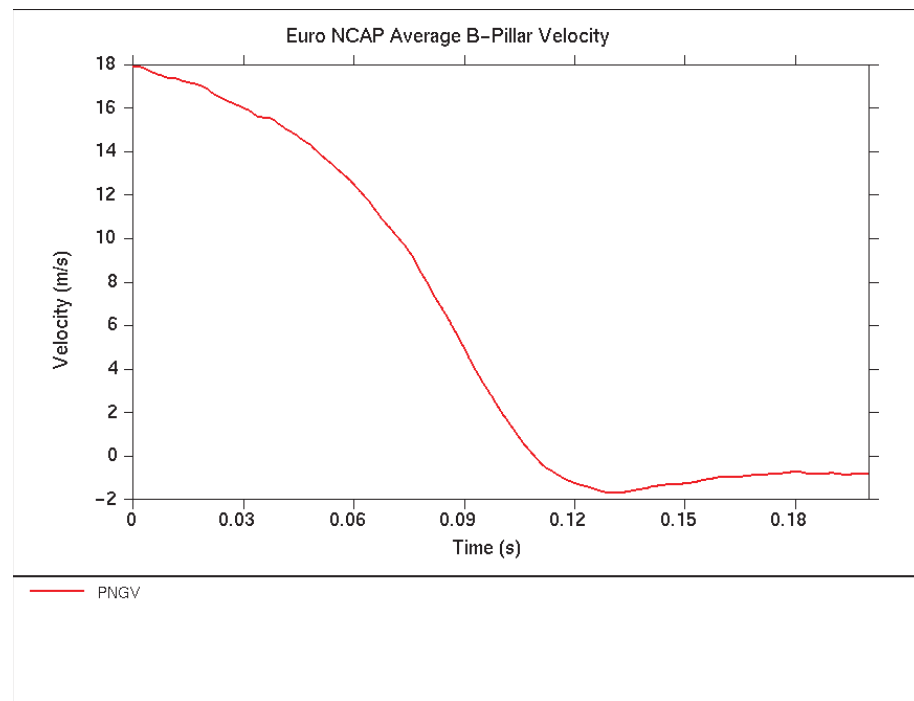


Figure 10.3.2-16 PNGV-Class Euro-NCAP average longitudinal B-Pillar velocity

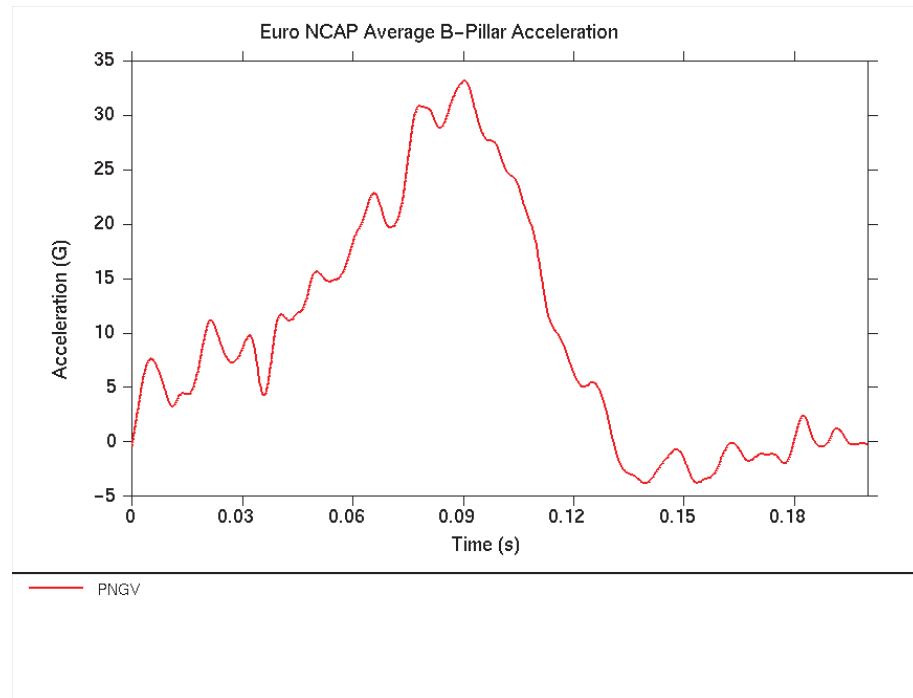


Figure 10.3.2-17 PNGV-Class Euro-NCAP average longitudinal B-Pillar acceleration

Table 10.3.2-1 shows the Euro-NCAP crash events:

Table 10.3.2-1 – Euro-NCAP crash events

Time (msec)		Euro NCAP Timing of Major Events
C-Class	PNGV-Class	
12	12	Bumper crush box starts to crush
18	18	Tires contact barrier
36	38	Subframe deforms at lower suspension wishbone
38	36	Rear of front tire contacts body
44	44	Bumper bottoms out deformable barrier
46	46	Longitudinal begins to crush
74	74	Engine bottoms out deformable barrier
102	104	Maximum dynamic deformation reached

The results are summarized in Table 10.3.2-2.

Table 10.3.2-2 Euro-NCAP results summary

Euro-NCAP	C-Class	PNGV-Class	Targets
Residual Footwell Intrusion (mm)	115	130	< 150
Steering Column Rearward Movement (mm)	25	20	< 80
A-pillar Displacement (mm)	10	10	< 50

The structures demonstrated good performance with a stable occupant compartment and minimal levels of footwell intrusion. The steering column movement and A-pillar stability were also good results for this severe test which are desirable attributes for occupant protection.

10.3.3 Rear Impact

The rear impact analysis considered for ULSAB-AVC is based on the United States Federal Rear Moving Barrier Test FMVSS-301, but conducted at an increased speed of 35 mph. The test specifically addresses fuel system integrity during a rear impact. The test configuration is shown in figures 10.3.3-1 and 10.3.3-2. The rear crash barrier is a rigid barrier mounted on a trolley with a mass of 1830 kg, and impacts the stationary vehicle at zero degrees with 100% overlap.

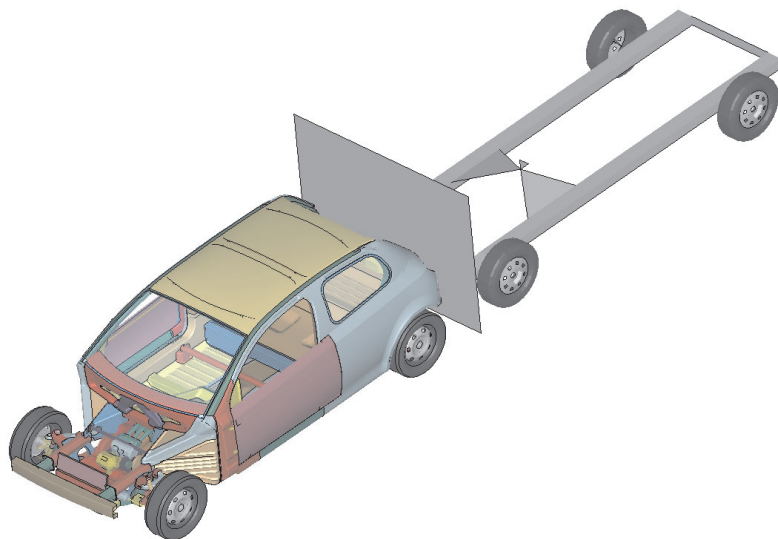


Figure 10.3.3-1 C-Class Rear impact configuration

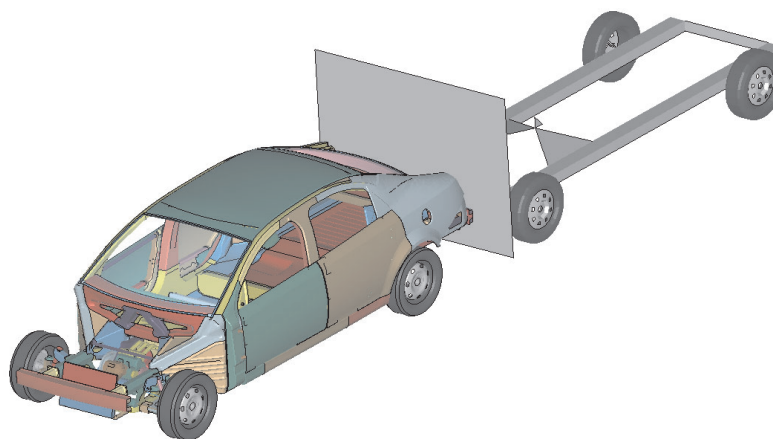


Figure 10.3.3-2 PNGV-Class Rear impact configuration

Integrity of the fuel system is evaluated by assessing the damage sustained by the fuel tank and fuel filler pipe. The additional goal of passenger compartment integrity is evaluated from the final deformation of the vehicle, and measuring the movement of the structure at the rear occupant R-point (seating reference point).

Deformed shape results for the C-Class and PNGV-Class vehicles are shown in Figures 10.3.3-3 through 10.3.3-10. The following Table 10.3.3-1 summarizes the structural deformation at the rear occupant for each vehicle.

Table 10.3.3-1 Structural deformation for rear occupant

Rear Impact	C-Class	PNGV-Class	Target
Rear Occupant R-Point Movement	20	5	< 50

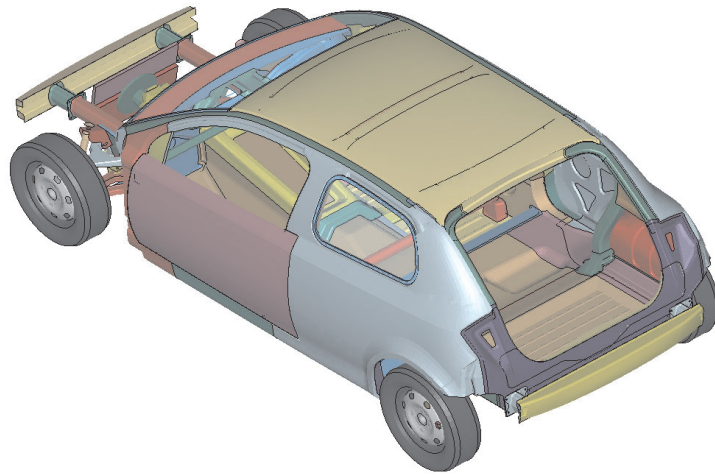


Figure 10.3.3-3 C-Class rear impact undeformed shape

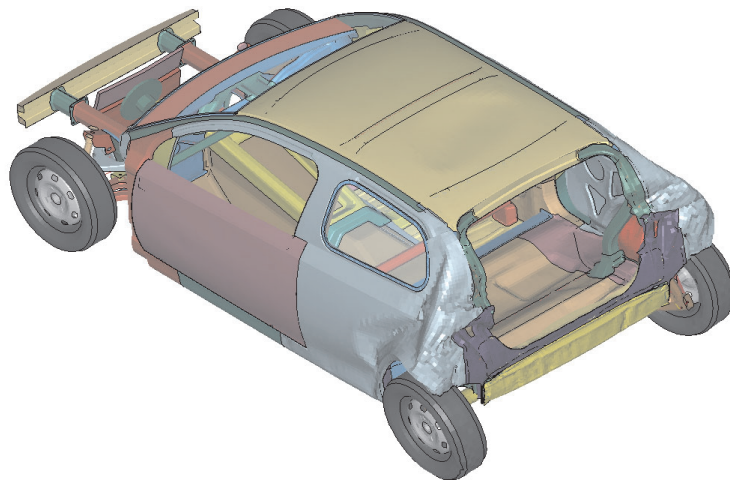


Figure 10.3.3-4 C-Class rear impact deformed shape

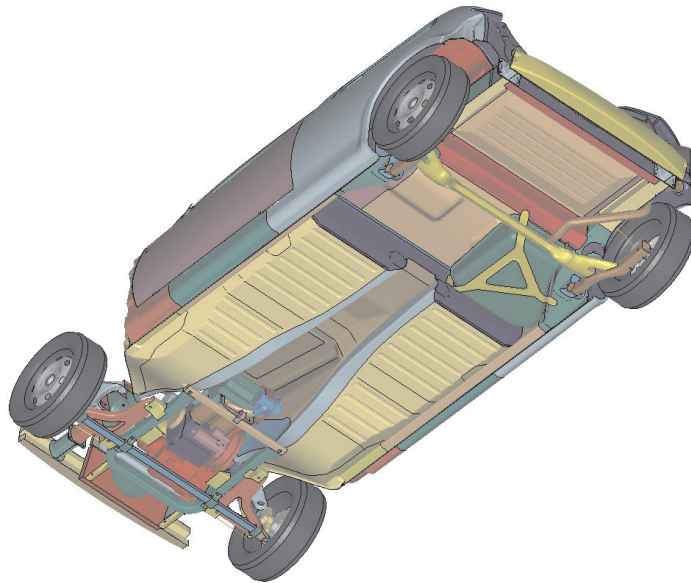


Figure 10.3.3-5 C-Class rear impact undeformed shape

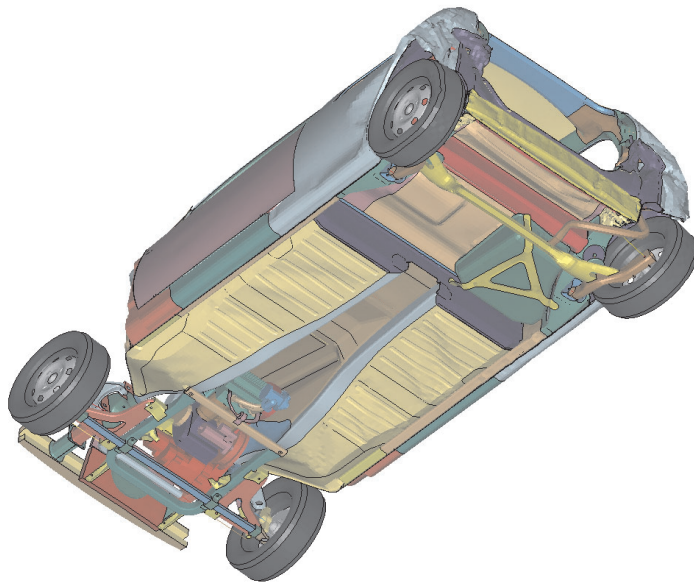


Figure 10.3.3-6 C-Class rear impact deformed shape

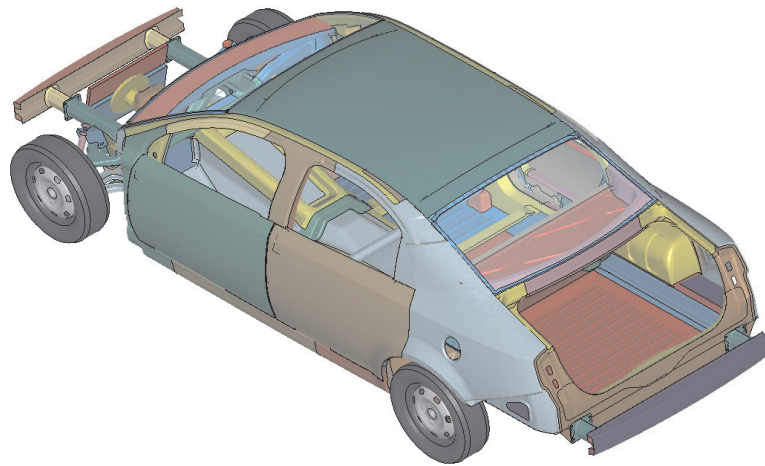


Figure 10.3.3-7 PNGV-Class rear impact undeformed shape

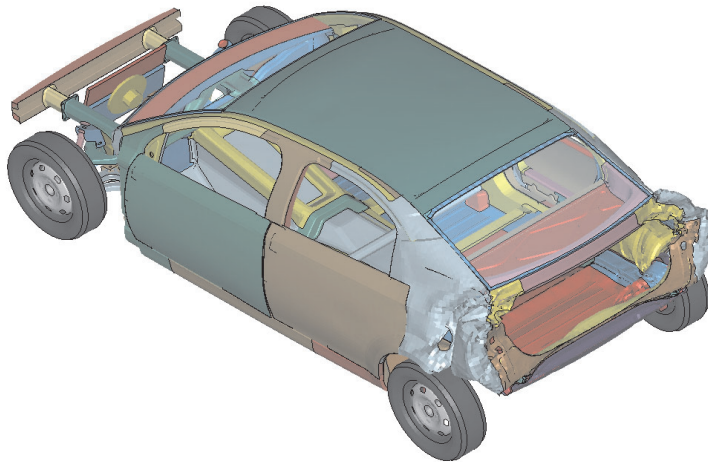


Figure 10.3.3-8 PNGV-Class rear impact deformed shape

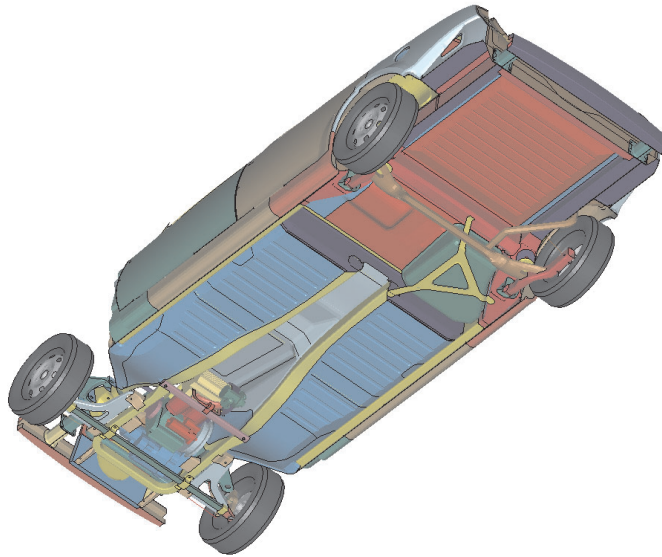


Figure 10.3.3-9 PNGV-Class rear impact undeformed shape

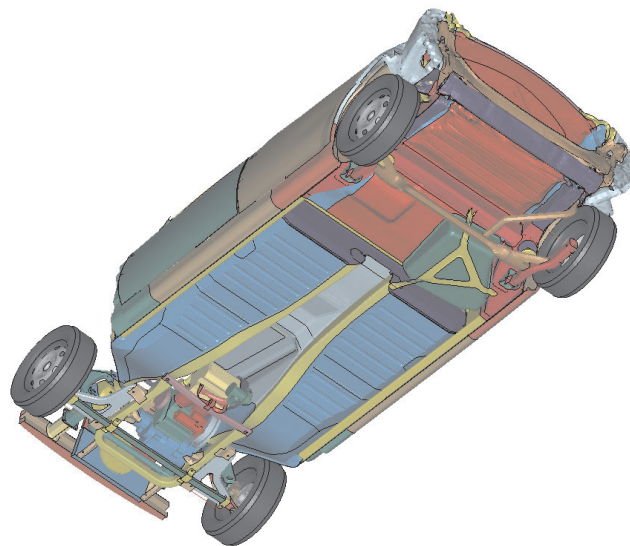


Figure 10.3.3-10 PNGV-Class rear impact deformed shape

The internal energy absorption diagrams for the C-Class and PNGV-Class vehicles are presented separately due to the difference in the structures at the rear. For the C-Class vehicle, the internal energy absorption diagram in Figure 10.3.3-11 gives an overview of the energy absorbed (at the time of maximum deformation) in the following parts – Floor Rear TWB2, Rear Rail TWB2, Crush Box Bumper, Floor Rear, Wheelhouse Inner TWB3, Bodyside Outer TWB2. For the PNGV, Figure 10.3.3-12 presents the internal energy absorbed by the following parts (at the time of maximum deformation) – Rear Rail TWB2, Floor Rear TWB2, Crush Box Bumper, Rear Rail Outer Floor Extension, Bodyside Outer TWB5 and Floor Rear.

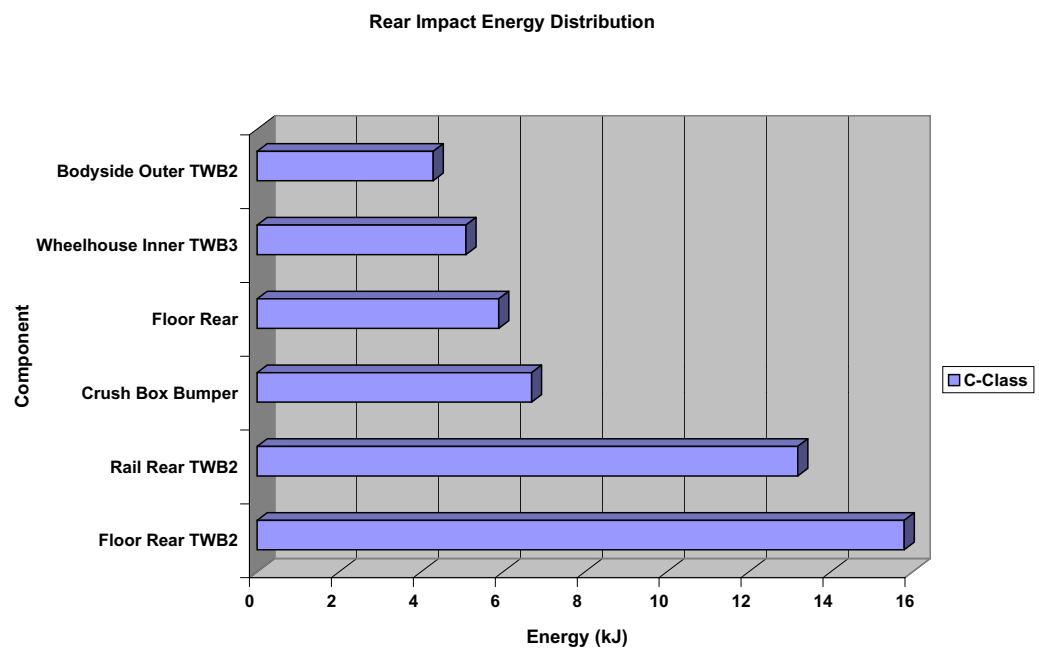


Figure 10.3.3-11 C-Class rear impact energy distribution

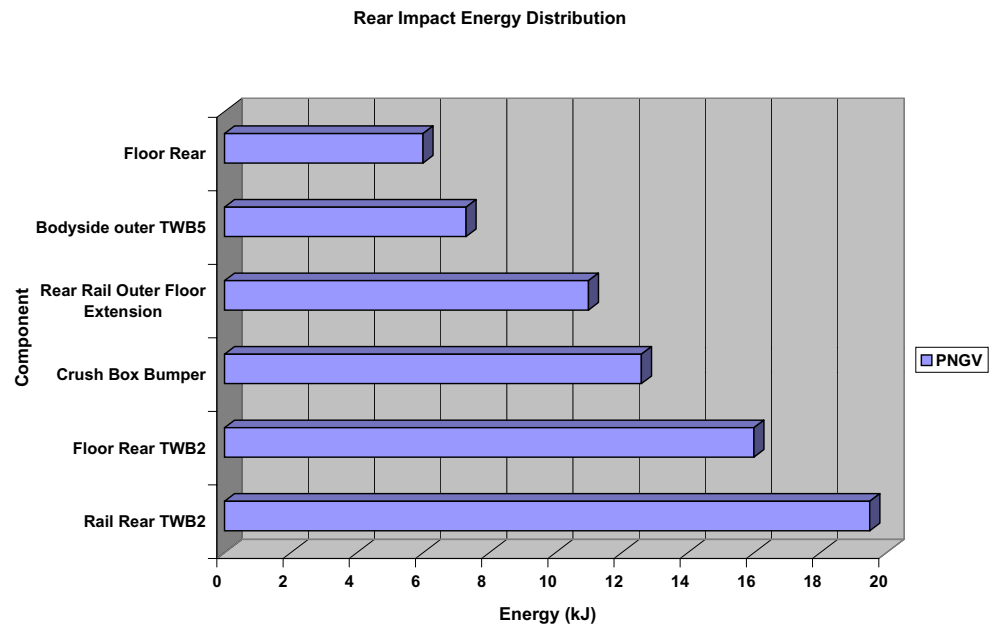


Figure 10.3.3-12 PNV-Class rear impact energy distribution

The typical section forces are measured in the Rocker, Rear Rail and Roof Side Rail for the C-Class. These locations are shown in Figure 10.3.3-13 for the C-Class vehicle. Figure 10.3.3-14 shows that the rocker plays a significant role in the C-Class vehicle due to the load path created by the barrier-wheel-rocker interaction.

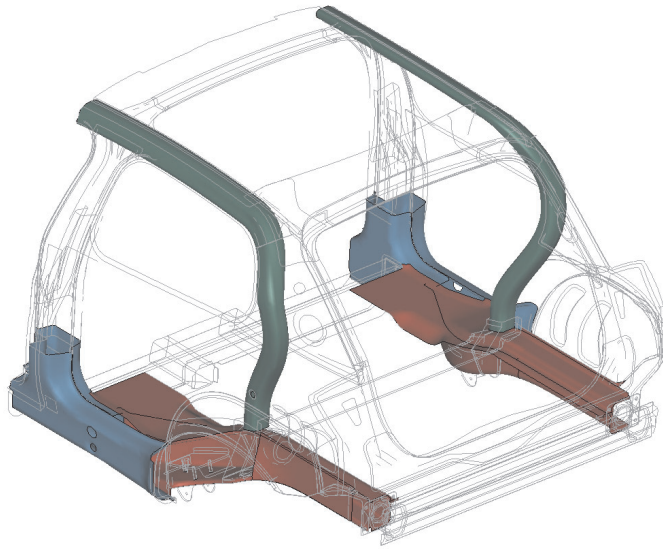


Figure 10.3.3-13 C-Class rear impact typical section locations

Rear Impact - Typical Section Forces - C-Class

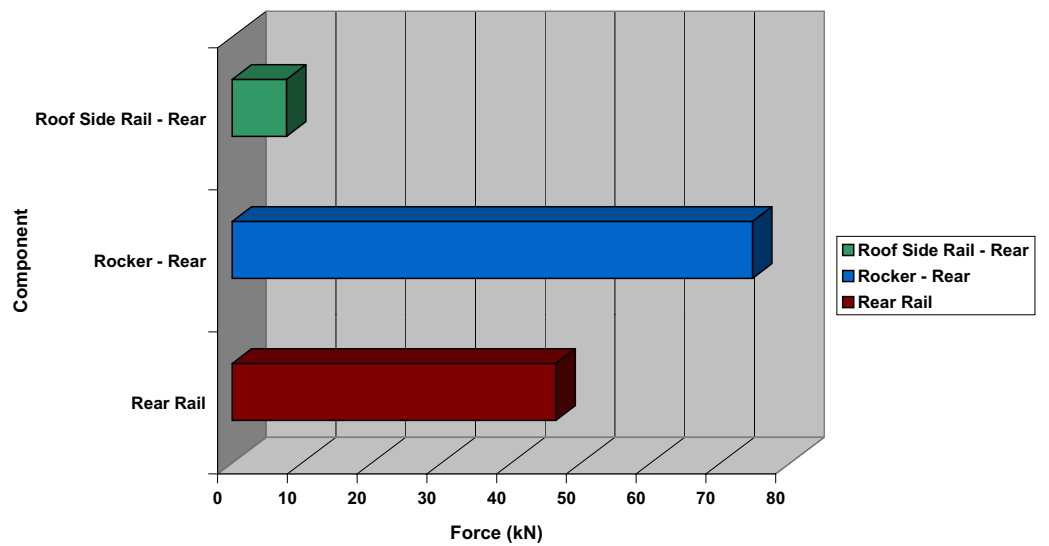


Figure 10.3.3-14 C-Class rear impact typical section forces

The typical section forces are also measured in the Rocker, Rear Rail and Roof Side Rail for the PNGV-Class. These locations are shown in Figure 10.3.3-15 for the PNGV-Class vehicle. Figure 10.3.3-16 shows that the rocker plays a significant role in the PNGV-Class vehicle due to the load path created by the barrier-wheel-rocker interaction.

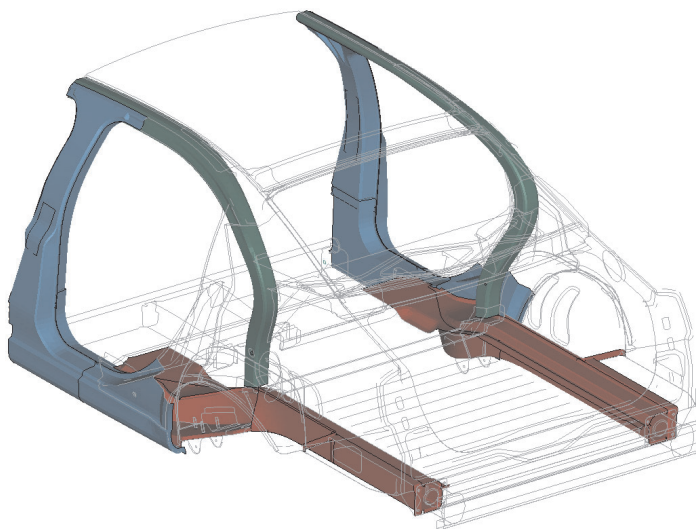


Figure 10.3.3-15 PNGV-Class rear impact typical section locations

Rear Impact - Typical Section Forces - PNGV-Class

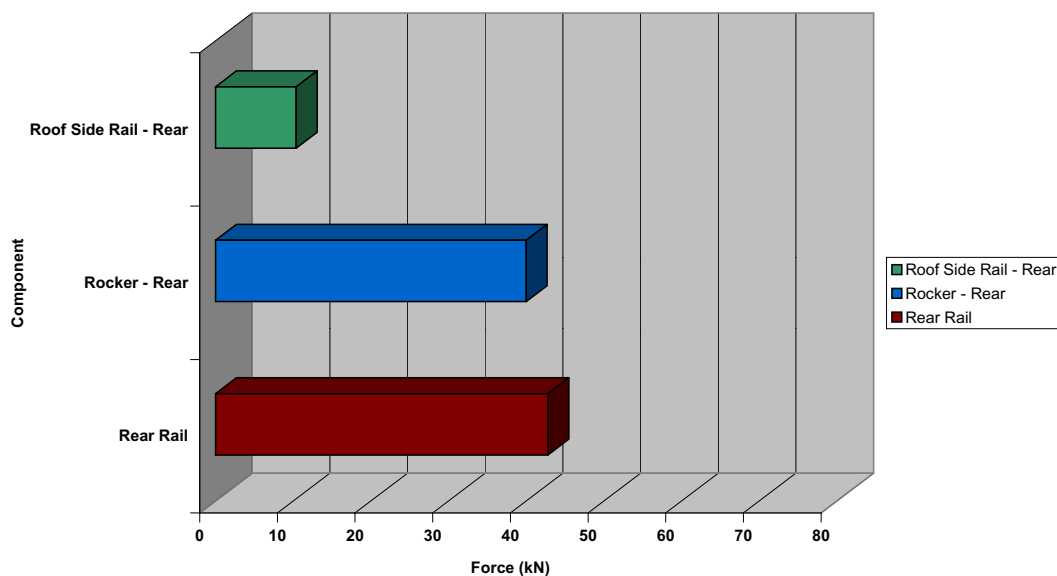


Figure 10.3.3-16 PNGV-Class rear impact typical section forces

The vehicle deformation, B-pillar velocity and acceleration curves for the C-Class and PNGV-Class vehicles are shown in Figures 10.3.3-17 through 10.3.3-22. These results are the average values from the left and right hand sides of the vehicle.

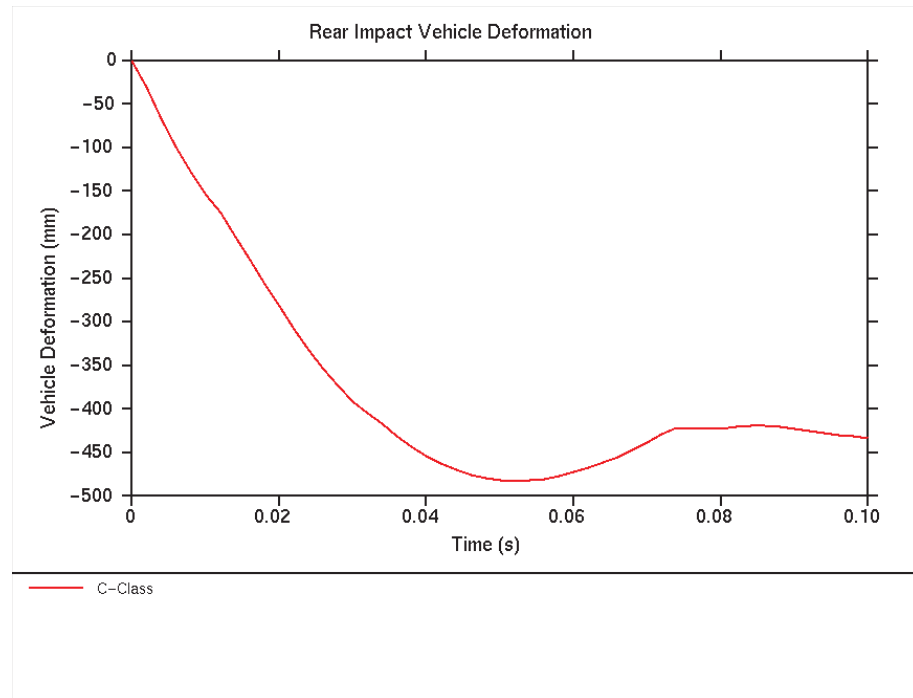


Figure 10.3.3-17 C-Class rear impact vehicle deformation

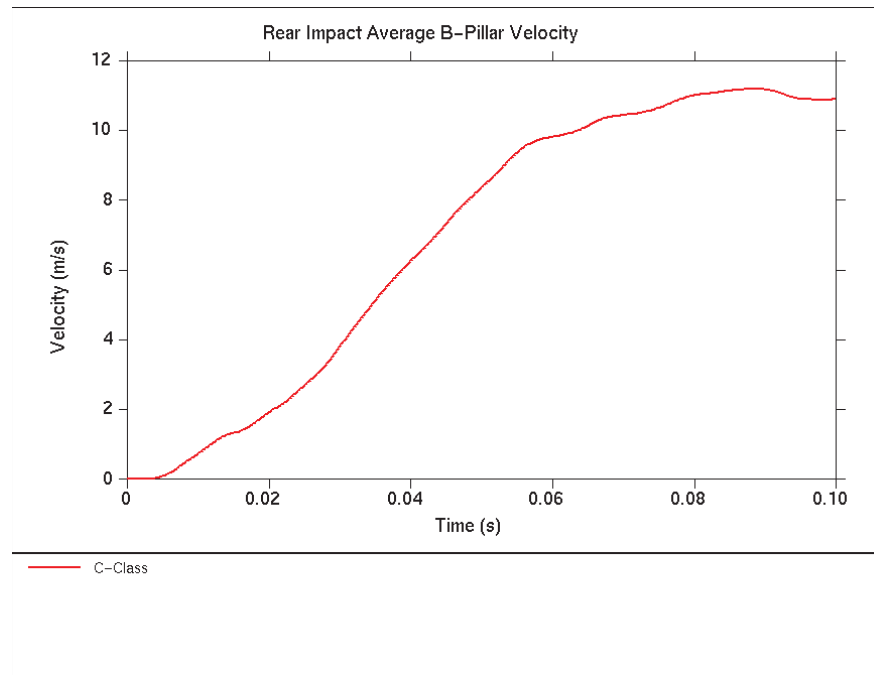


Figure 10.3.3-18 C-Class rear impact average longitudinal B-Pillar velocity

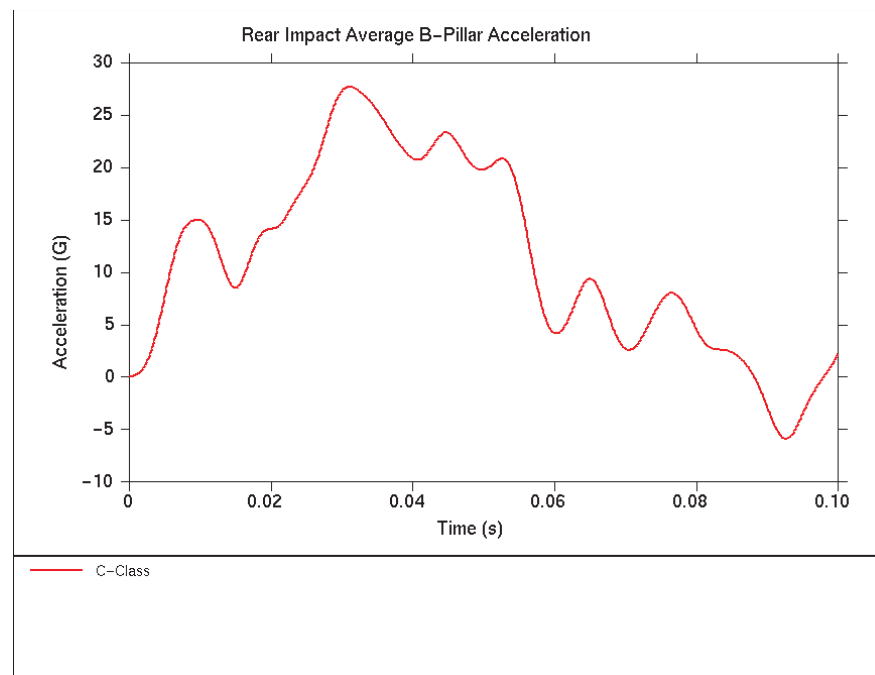


Figure 10.3.3-19 C-Class rear impact average longitudinal B-Pillar acceleration

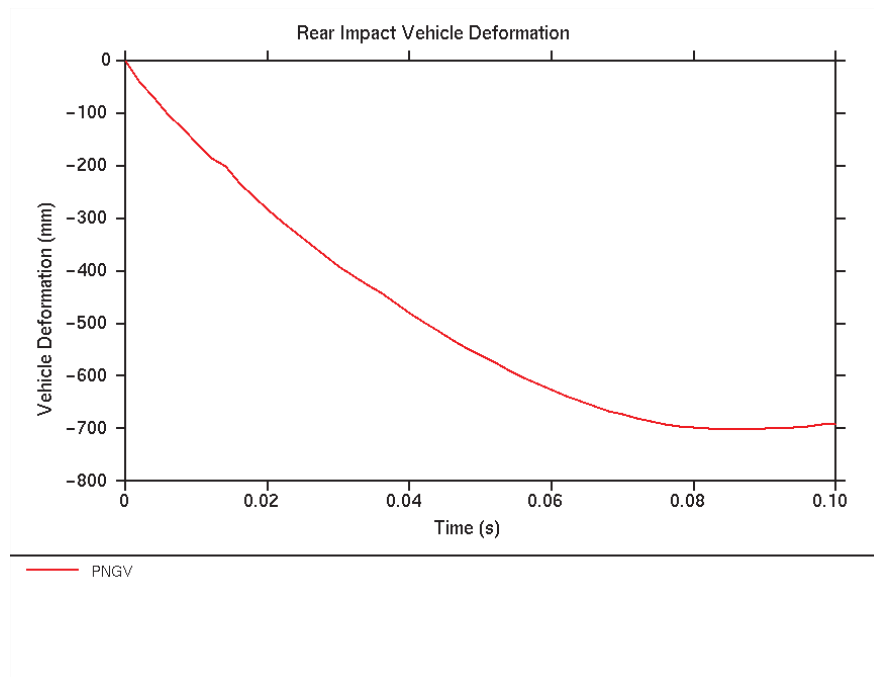


Figure 10.3.3-20 PNGV-Class rear impact vehicle deformation

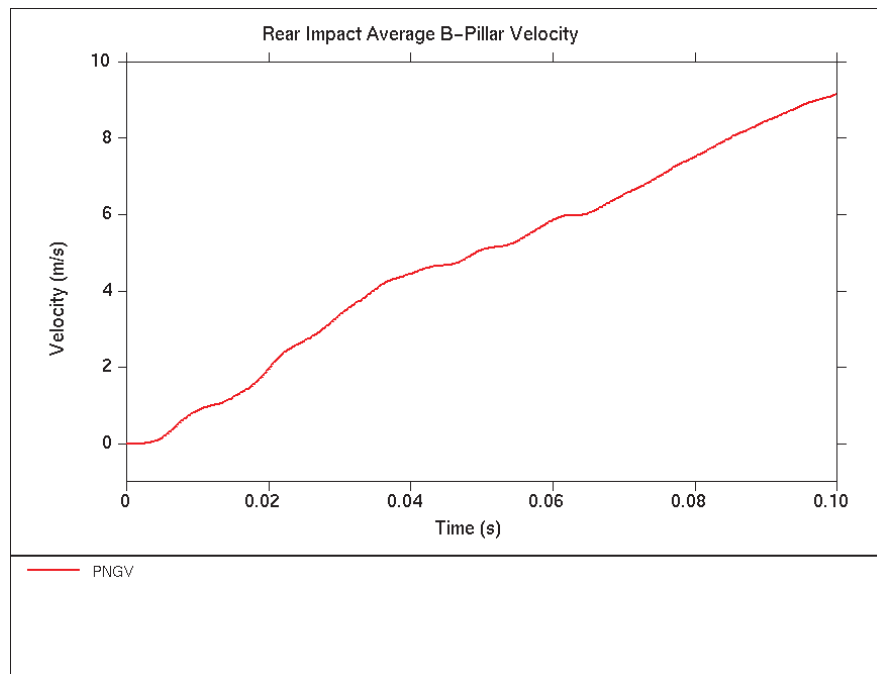


Figure 10.3.3-21 PNGV-Class rear impact average longitudinal B-Pillar velocity

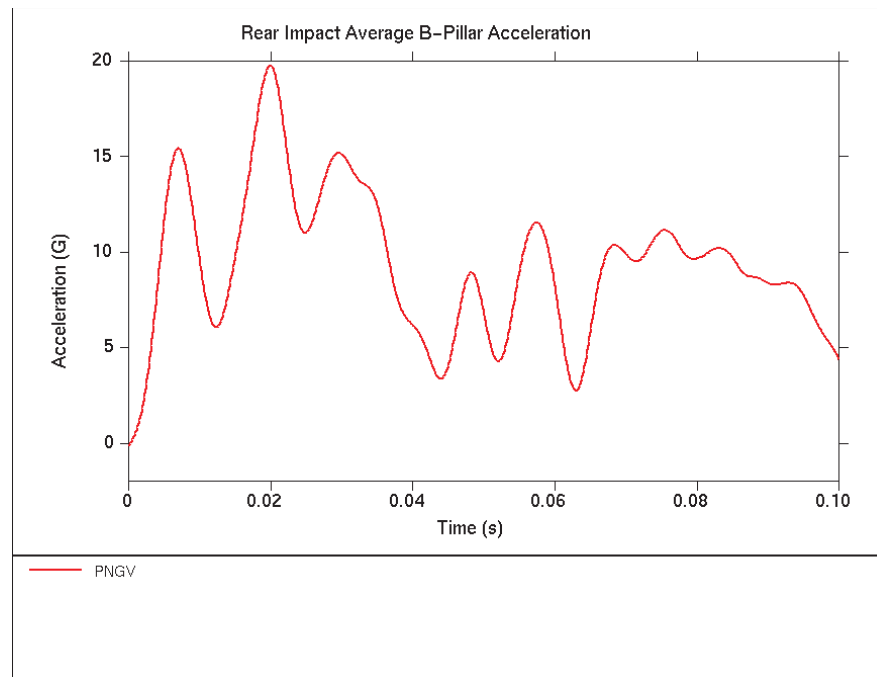


Figure 10.3.3-22 PNGV-Class rear impact average longitudinal B-Pillar acceleration

The following table explains the rear crash events after impact:

Table 10.3.3-2 Rear crash events summary

Time (msec)		Rear Impact Timing of Major Events
C-Class	PNGV-Class	
10	10	Bumper crush box stops crushing
12	14	Initial crush of longitudinal
22	-	Rear tires contact moving barrier
28	-	Fuel filler pipe is deformed slightly
-	30	Rear section of longitudinal bends down
40	-	Rear tires contact front of wheelhouse
52	86	Maximum dynamic deformation reached

This analysis shows minimal deformation of the fuel filler pipe in the case of the C-Class vehicle, and no fuel tank deformation in either vehicle. Therefore, the structural integrity of the fuel system is predicted to be maintained and no fuel leakage is expected.

10.3.4. US-SINCAP Analysis

The side impact test of the New Car Assessment Program (NCAP) undertaken by the US National Highway and Traffic Safety Association (NHTSA) specifies an impact on a stationary vehicle by a 1370 kg moving barrier at 38.5 mph (Figures 10.3.4-1 and 10.3.4-2). The moving barrier has angled wheels to provide the impact velocity of 38.5 mph at an angle of 63 degrees to the longitudinal axis of the vehicle. Performance of vehicles for this test is published as Star Ratings which are based on the occupant injury measurements recorded during the event.

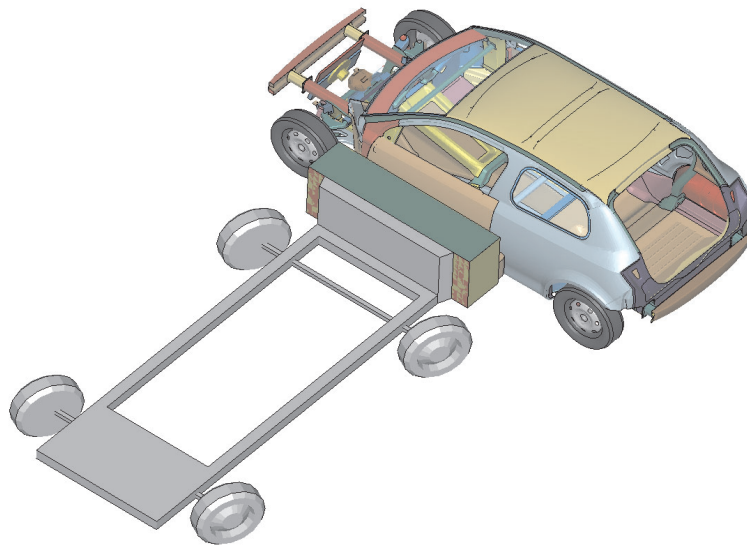


Figure 10.3.4-1 C-Class US-SINCAP Impact configuration

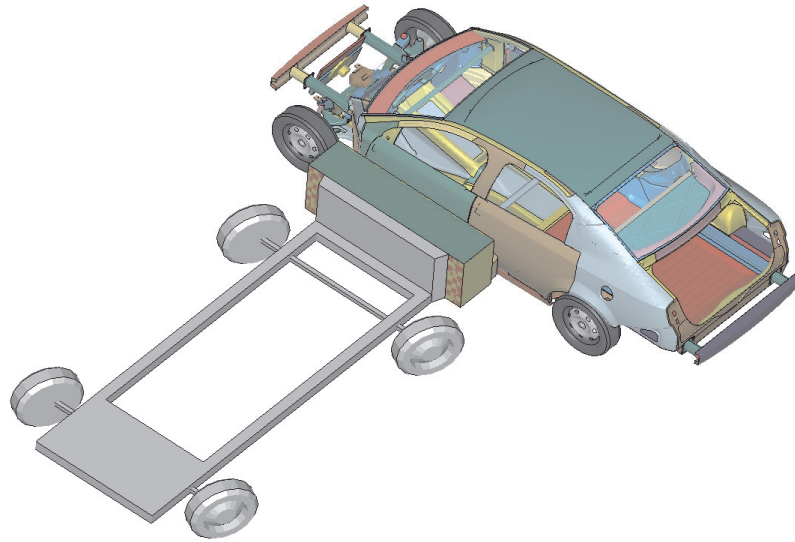


Figure 10.3.4-2 PNGV-Class US-SINCAP Impact configuration

Because the scope of analysis did not include side impact dummies, injury assessment could not be made. Occupant injury performance is greatly affected by seats, interior trim (which was not developed as part of the ULSAB-AVC concept study), restraint system design (e.g. seatbelts, and side airbags) as well as by the structural behavior. Structural performance and integrity can be assessed by considering the B-pillar intrusion velocity, overall shape of the deformation, buckling of the B-pillar, rotation of the rocker rails, crush of the front body hinge pillar, folding of the door beams and door belts, and cross-car underbody parts.

The side impact undeformed (time = 0 msec) and deformed shapes (time = 80 ms) for the C-Class and PNGV-Class vehicles are shown in Figures 10.3.4-3 to 14.

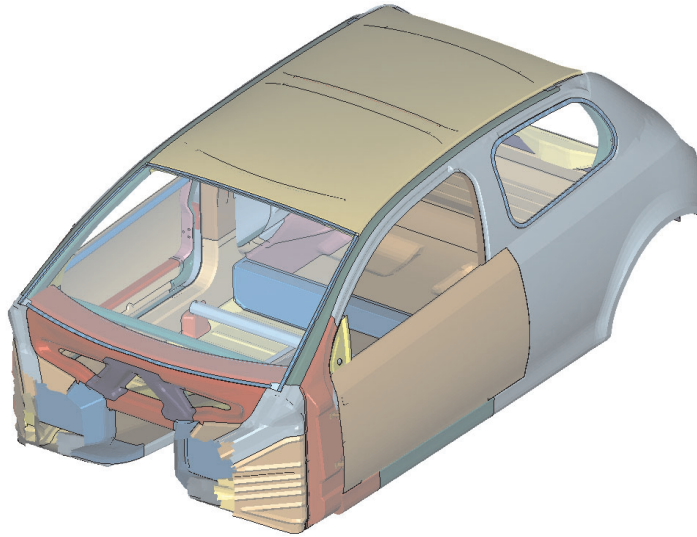


Figure 10.3.4-3 C-Class US-SINCAP undeformed shape

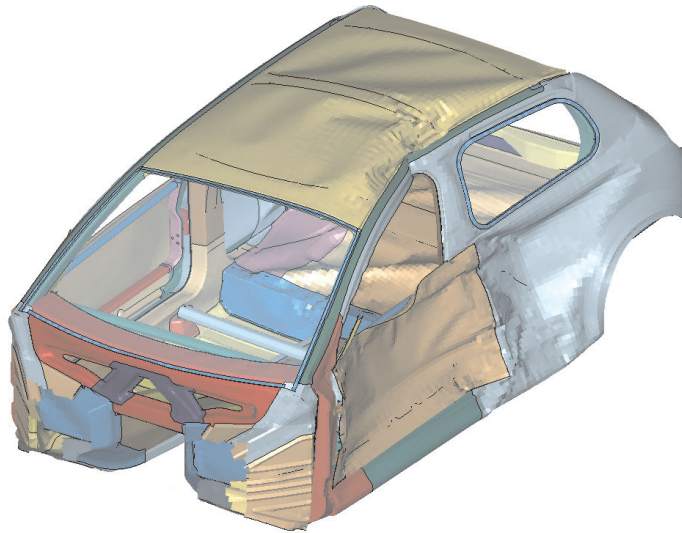


Figure 10.3.4-4 C-Class US-SINCAP deformed shape

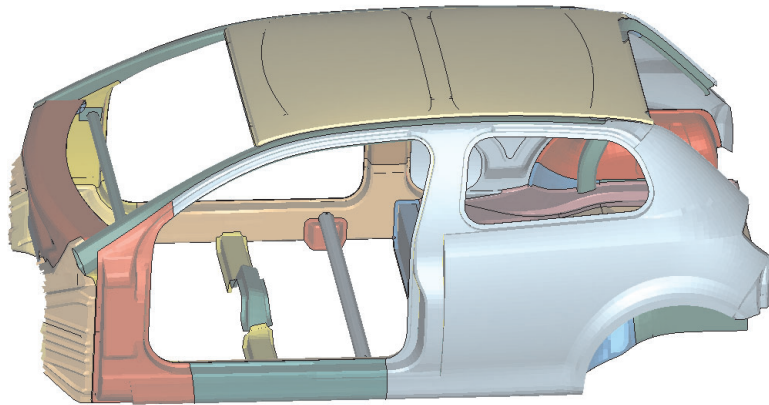


Figure 10.3.4-5 C-Class US-SINCAP undeformed shape

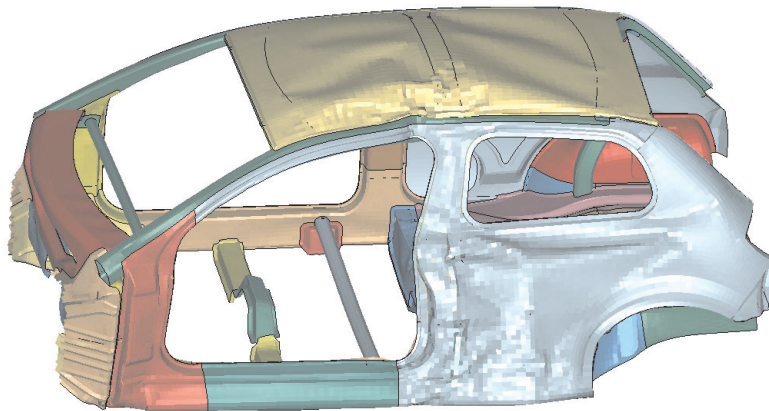


Figure 10.3.4-6 C-Class US-SINCAP deformed shape

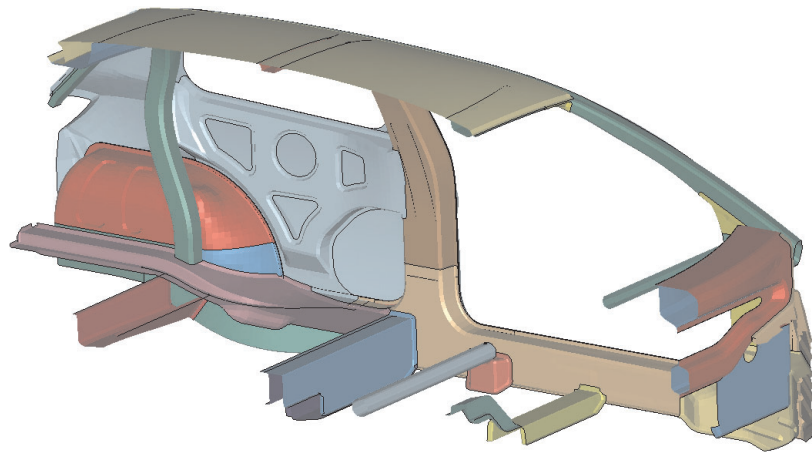


Figure 10.3.4-7 C-Class US-SINCAP undeformed shape

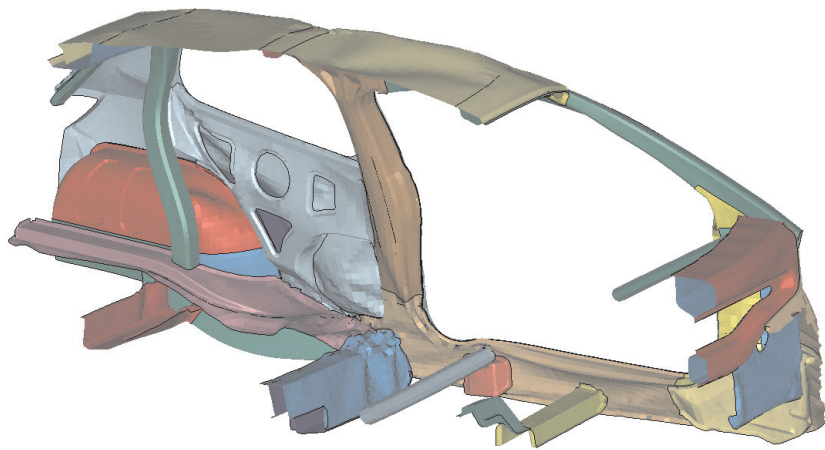


Figure 10.3.4-8 C-Class US-SINCAP deformed shape

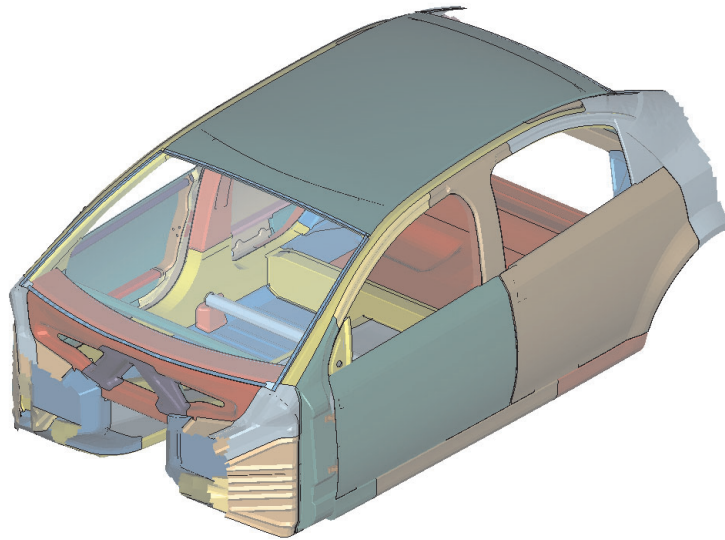


Figure 10.3.4-9 PNGV-Class US-SINCAP undeformed shape

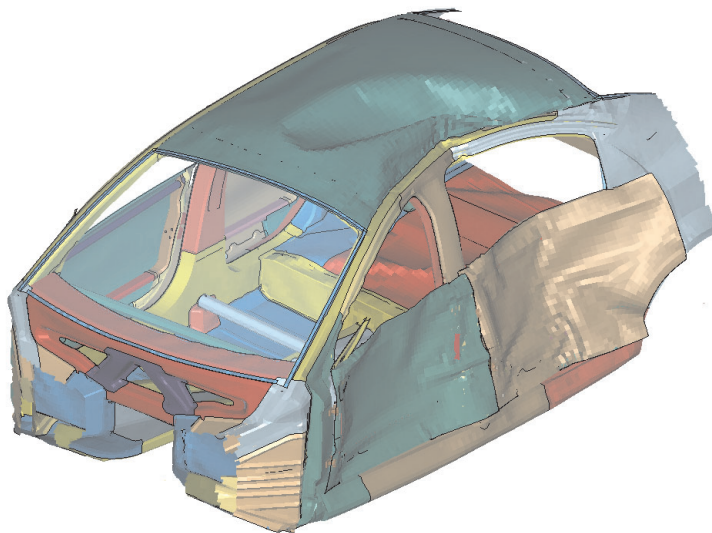


Figure 10.3.4-10 PNGV-Class US-SINCAP deformed shape

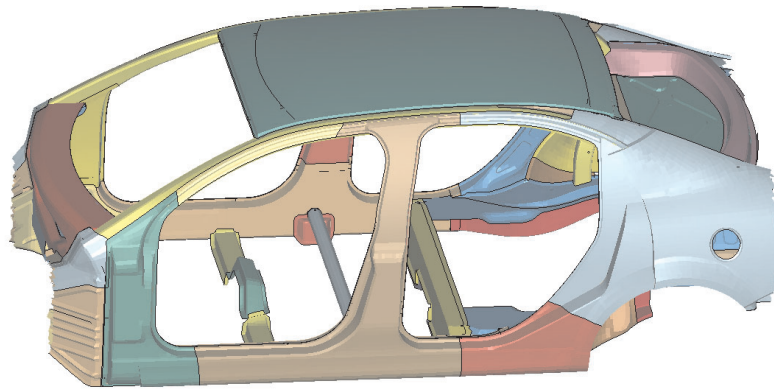


Figure 10.3.4-11 PNGV-Class US-SINCAP undeformed shape

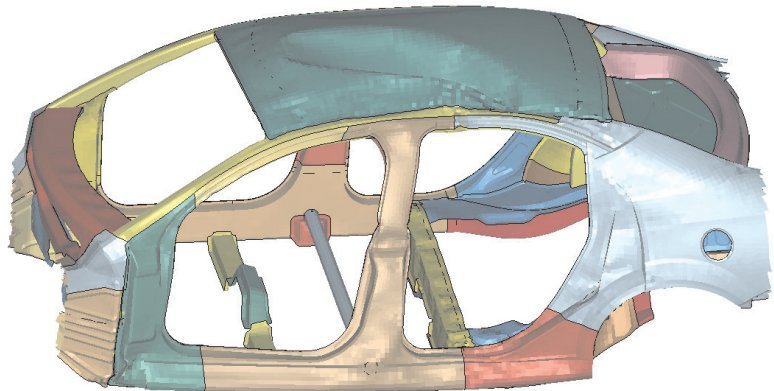


Figure 10.3.4-12 PNGV-Class US-SINCAP deformed shape

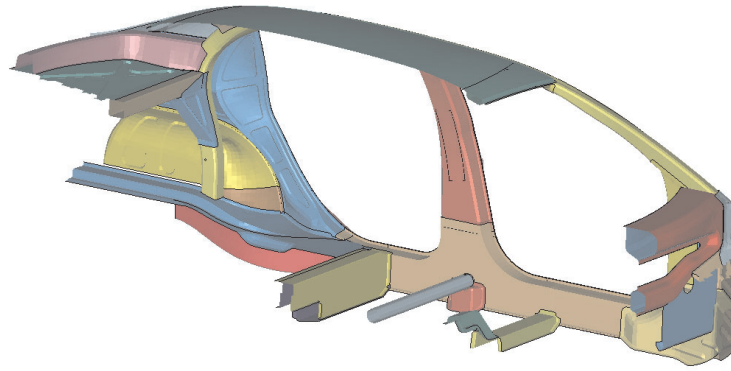


Figure 10.3.4-13 PNGV-Class US-SINCAP undeformed shape

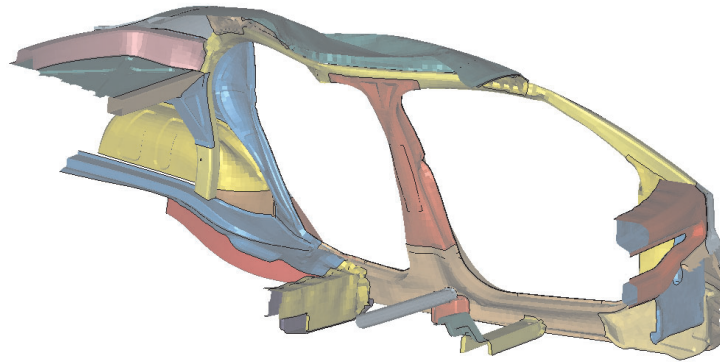


Figure 10.3.4-14 PNGV-Class US-SINCAP deformed shape

The intrusion velocity of the B-pillar in the region of the thorax is an important parameter for occupant injury. Figures 10.3.4-15 and 10.3.4-16 show the B-pillar intrusion velocities of the C-Class and PNGV-Class vehicles.

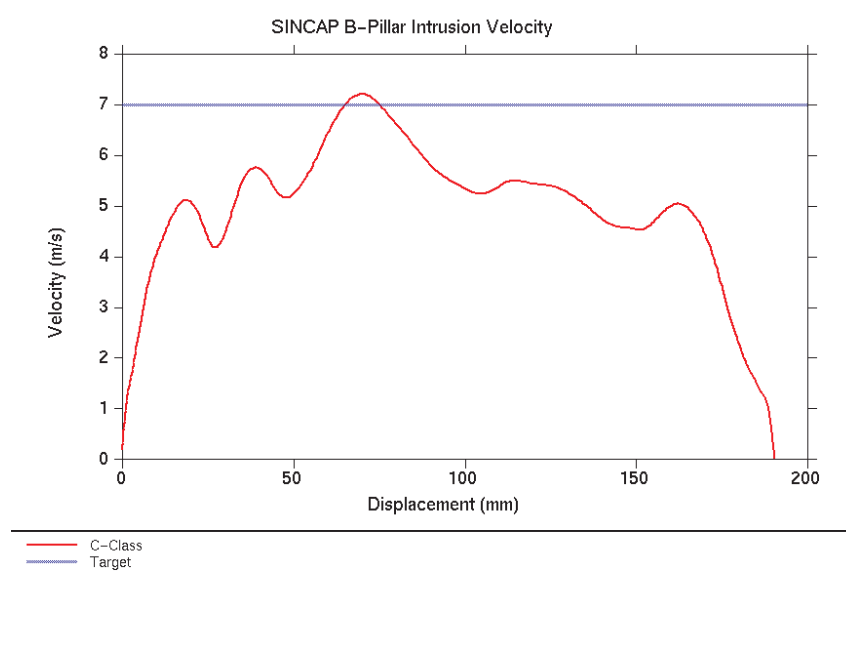


Figure 10.3.4-15 C-Class US-NCAP B-Pillar intrusion velocity at waist

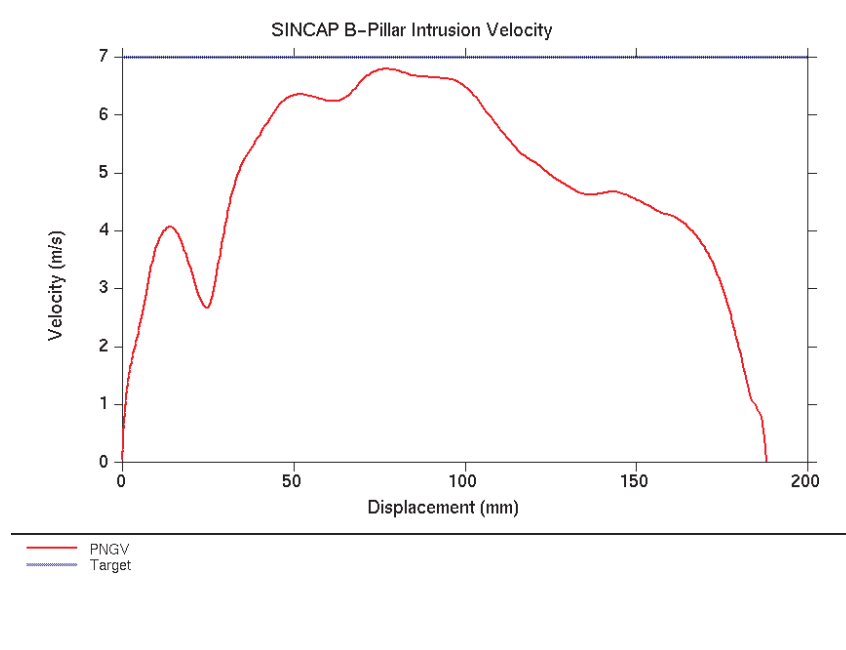


Figure 10.3.4-16 PNGV-Class US-SINCAP B-Pillar intrusion velocity at waist

The results presented are the average intrusion velocities of two points on the B-pillar located at the mid-height. Figures 10.3.4-17 and 10.3.4-18 show the measurement point locations on the C-Class and PNGV-Class vehicle models. Selecting this mid-height location for measuring the intrusion velocities enables comparison with the real test data presented later in this report.

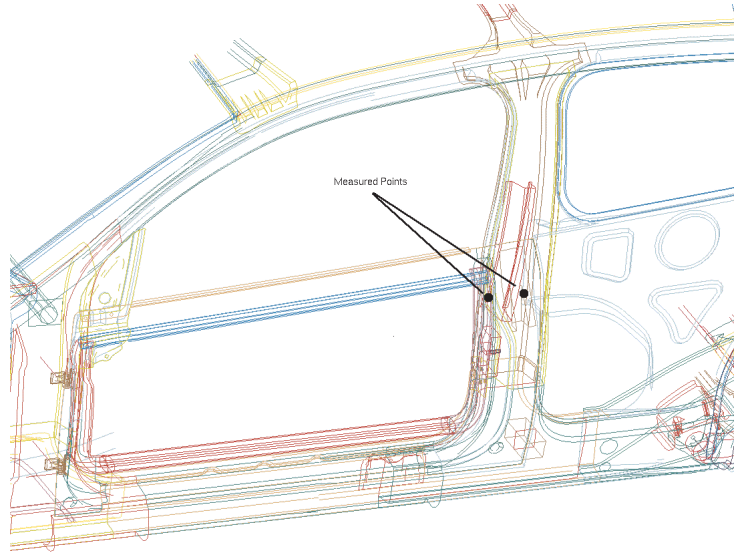


Figure 10.3.4-17 C-Class US-SINCAP B-Pillar intrusion measurement point locations

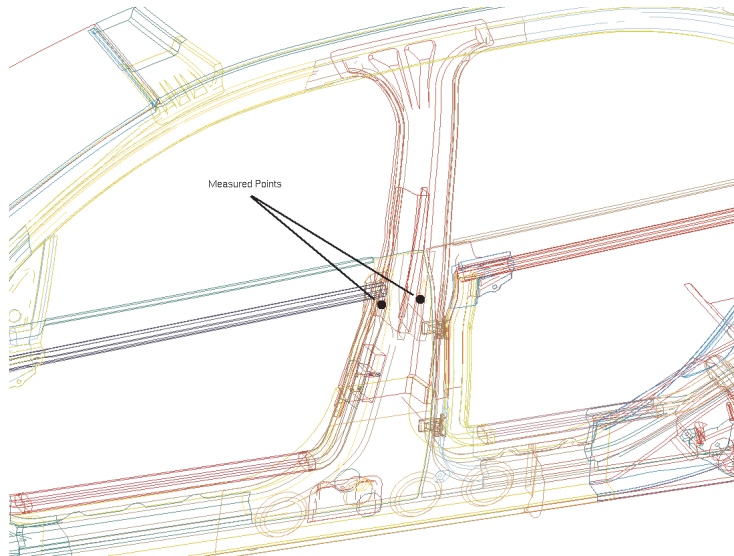


Figure 10.3.4-18 PNGV-Class US-SINCAP B-Pillar intrusion measurement point locations

Figures 10.3.4-19 and 10.3.4-20 give an overview of the energy distribution for US-SINCAP crash event. Four components, which absorb the highest levels of energy in the structure are presented.

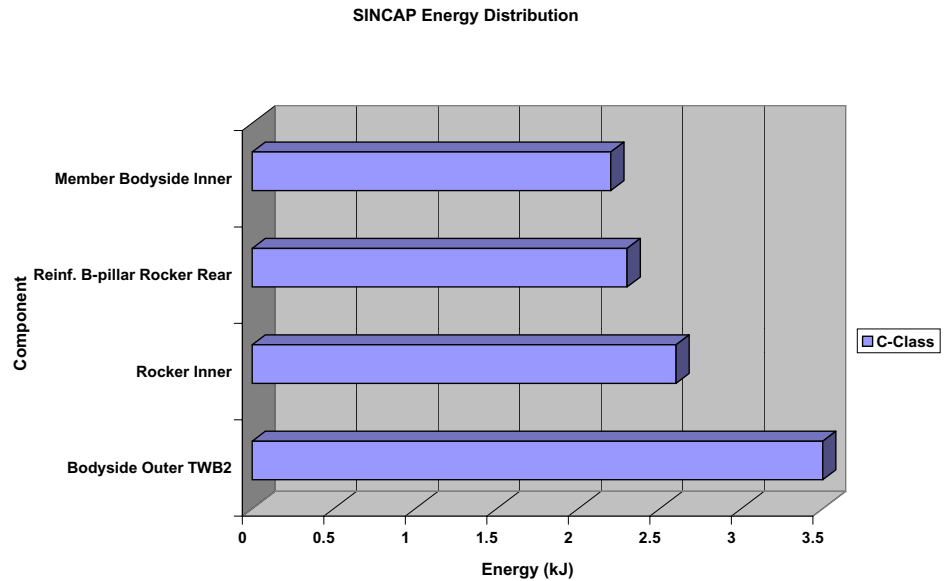


Figure 10.3.4-19 C-Class US-SINCAP energy distribution

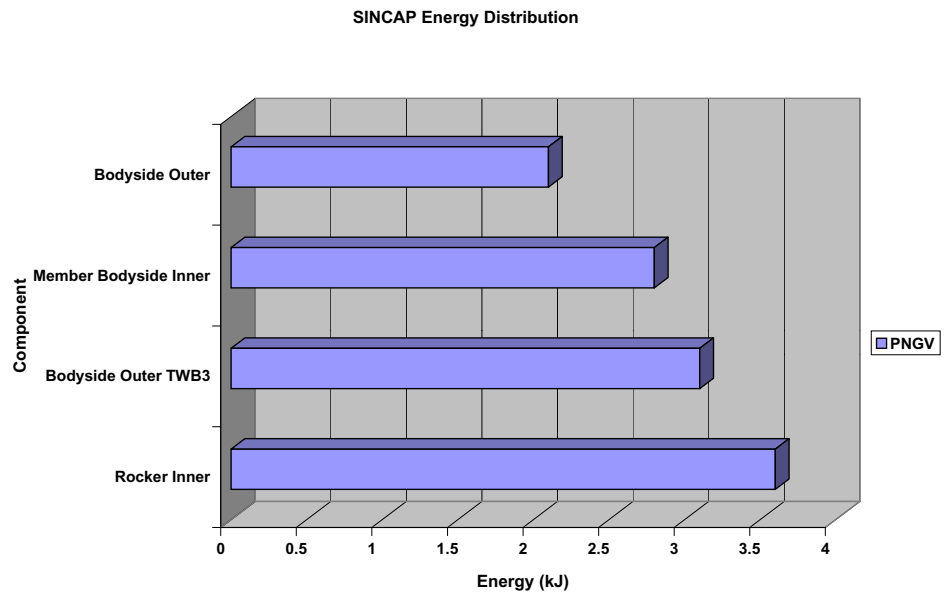


Figure 10.3.4-20 PNGV-Class US-SINCAP energy distribution

The proportion of the total vehicle internal energy absorbed by the doors in the US-SINCAP event is 12% for the C-Class and 17% for the PNGV-Class. The Figures 10.3.4-21 and 10.3.4-22 show the distribution of energy within the door structures for the C-Class and PNGV-Class vehicles respectively.

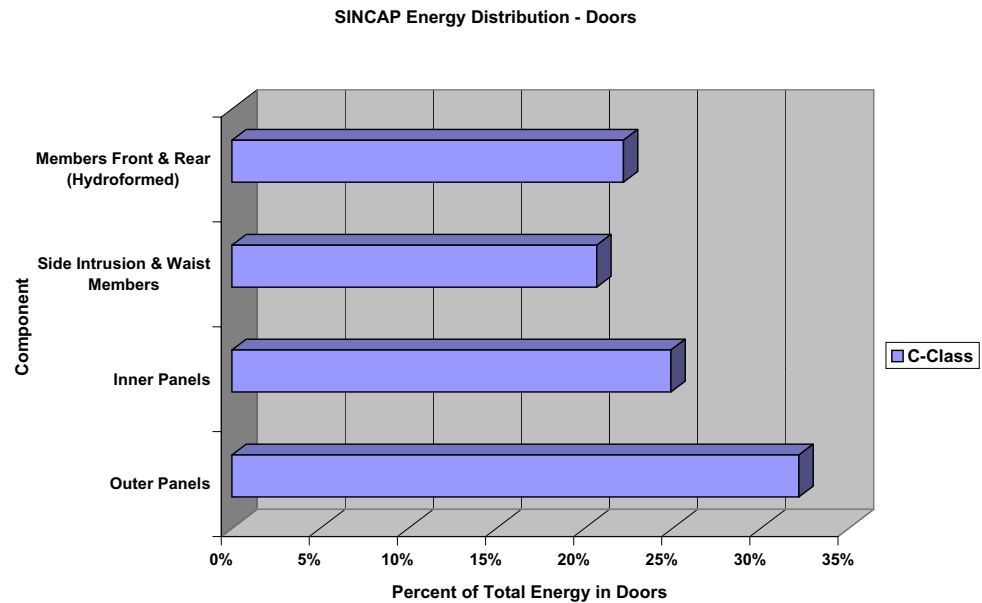


Figure 10.3.4-21 C-Class US-SINCAP energy distribution - doors

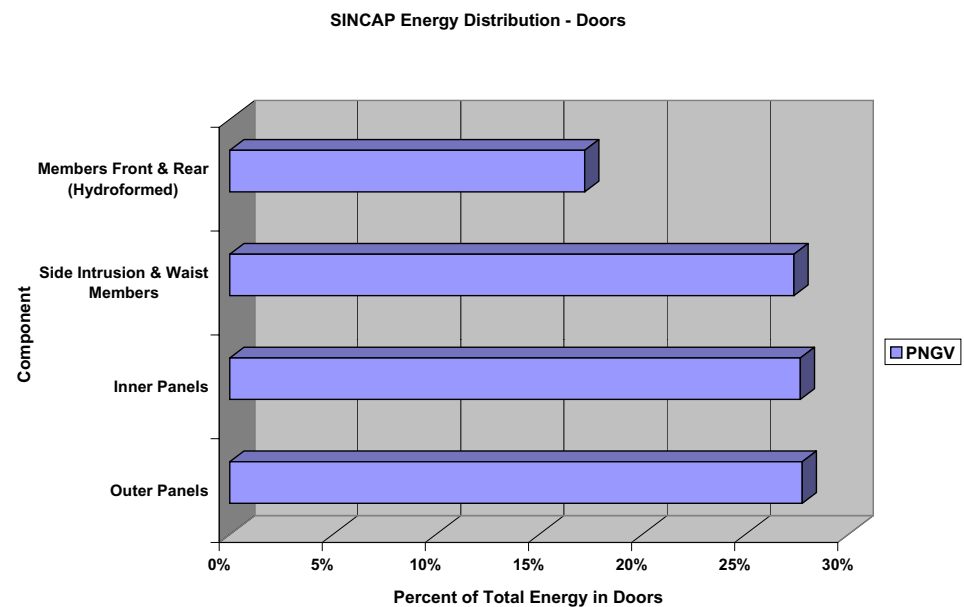


Figure 10.3.4-22 PNGV-Class US-SINCAP energy distribution - doors

Table 10.3.4-1 summarizes the results for this event.

Table 10.3.4-1 US-SINCAP results

SINCAP	C-Class	PNGV-Class	Target
B-Pillar Intrusion Velocity (m/sec)	7.2	6.8	7
Maximum Intrusion at waist (mm)	190	185	n/a

The C-Class vehicle does not meet the intrusion velocity target, but the results that were achieved are adequate to demonstrate a good level of structural performance at the concept design stage. Section 10.4 Star Rating Assessment presents a comparison of these results with production vehicles and demonstrates that the ULSAB-AVC concept has achieved a high level of crashworthiness.

The following table 10.3.4-2 explains the timing of events during the side impact crash.

Table 10.3.4-2 US-SINCAP crash events summary

Time (msec)		US-SINCAP Timing of Major Events
C-Class	PNGV-Class	
12	12	Front door side impact beam contacts B-pillar
14	14	Kick-up crossmember begins to crush
-	16	Load taken on seat tube extension
20	24	Roof begins to deform
26	30	B-pillar bends at waist, but remains stable
51	52	Maximum intrusion reached

10.3.5. Side Pole Impact

The side pole impact considered for ULSAB-AVC is based on the test specified in the US regulation FMVSS 201 and that adopted for the Euro-NCAP test program. The vehicle is propelled sideways at a speed of 20 mph (32 km/h) into a fixed, rigid pole of 10 inches (254 mm) diameter which is aligned with the center of the driver's head. The impact speed chosen for the ULSAB-AVC project is 10% higher than the speed specified in FMVSS 201 and Euro-NCAP. The test configuration is shown in Figures 10.3.5-1 and 10.3.5-2 for the C-Class and PNGV-Class vehicles.

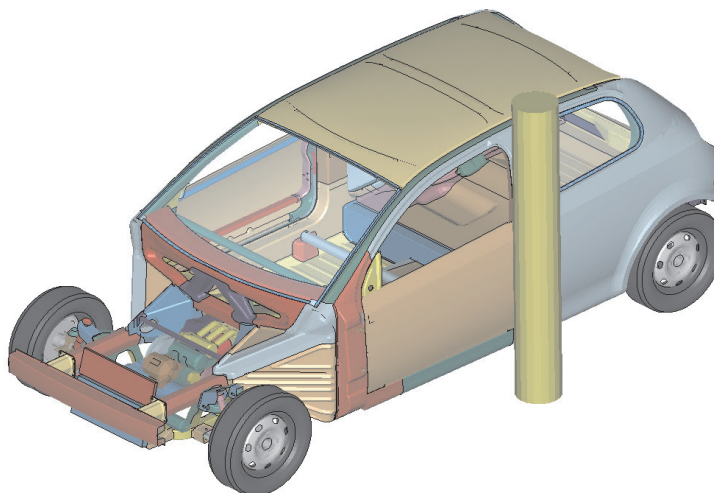


Figure 10.3.5-1 C-Class Side Pole Impact configuration

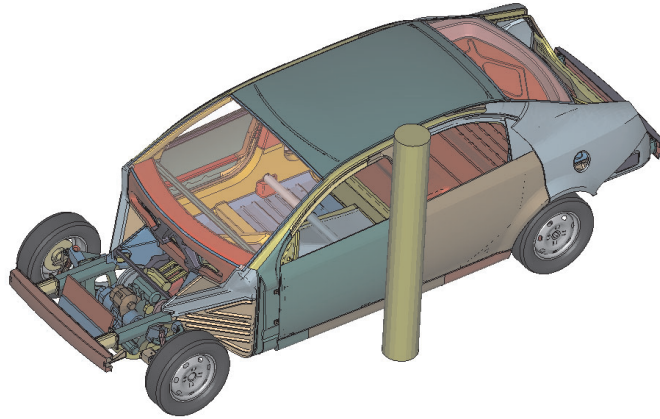


Figure 10.3.5-2 PNGV-Class Side Pole Impact configuration

Minimizing occupant injury in this test is dependent on the integrity of the body structure as well as the secondary restraint systems such as side head airbags. Because the scope of analysis did not include side impact dummies, injury assessment could not be made. The focus was on good structural performance measured by the intrusion velocity of the pole at the time when impact with the driver's head would occur, and overall deformation of the structure.

The side pole impact undeformed (time = 0 msec) and deformed shapes (time = 80 ms) for the C-Class and PNGV-Class vehicles are shown in Figures 10.3.5-3 to 10.

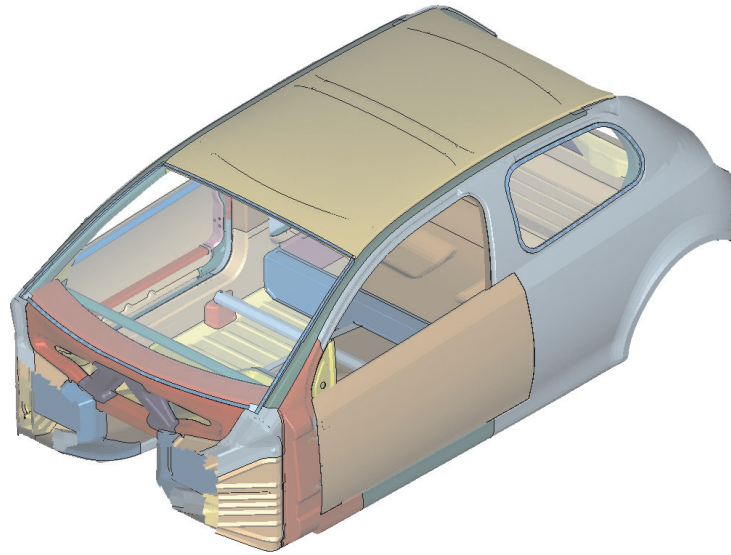


Figure 10.3.5-3 C-Class Side Pole Impact undeformed shape

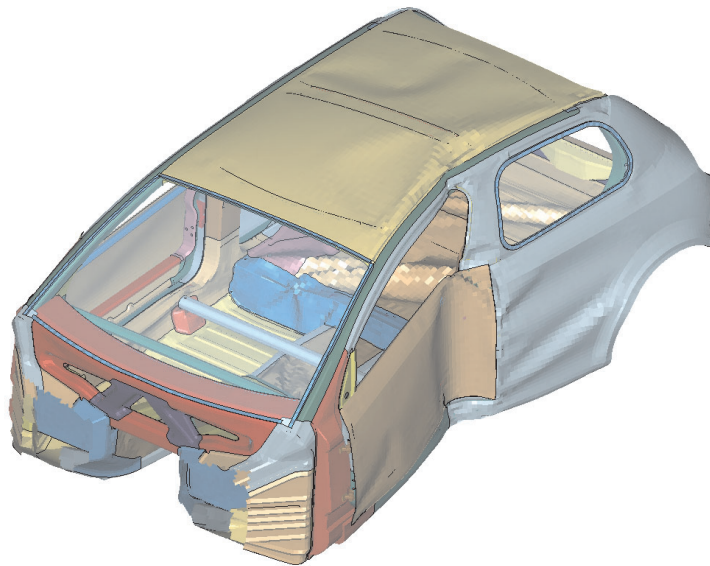


Figure 10.3.5-4 C-Class Side Pole Impact deformed shape

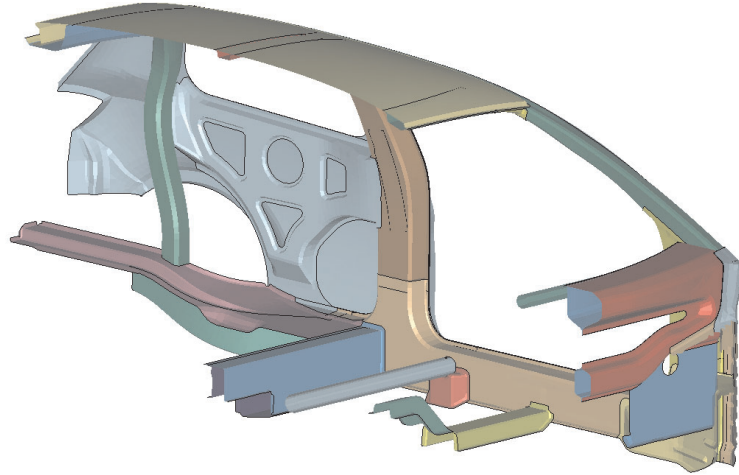


Figure 10.3.5-5 C-Class Side Pole Impact undeformed shape

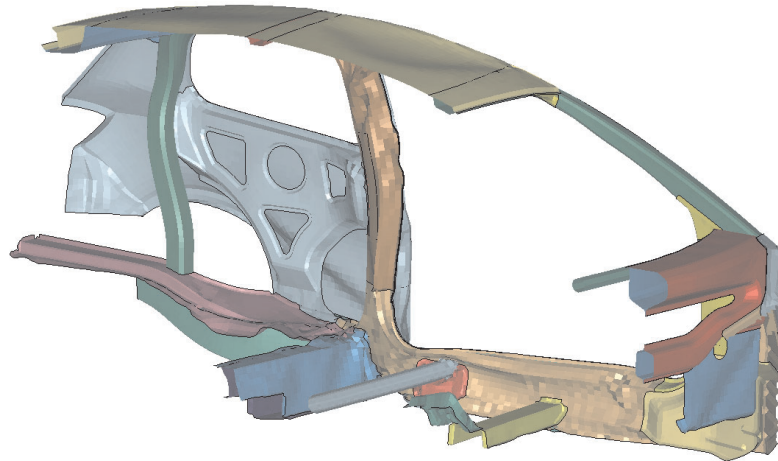


Figure 10.3.5-6 C-Class Side Pole Impact deformed shape

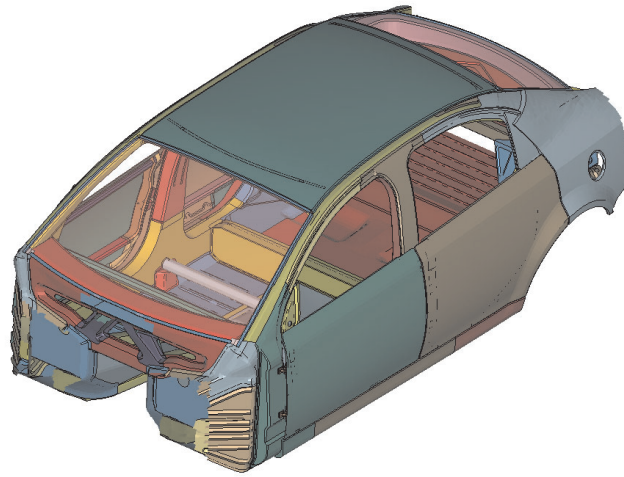


Figure 10.3.5-7 PNGV-Class Side Pole Impact undeformed shape

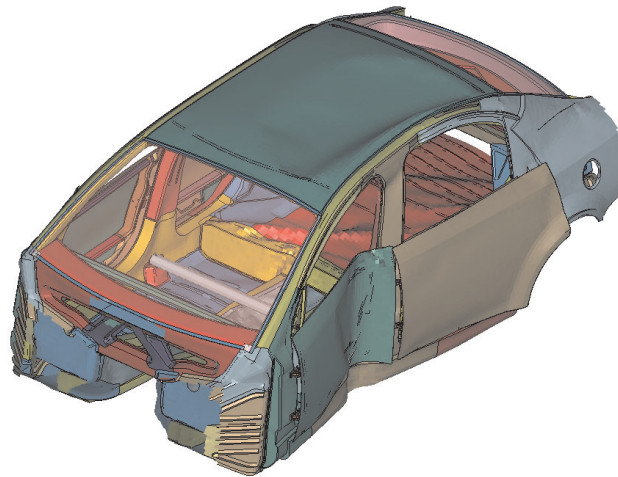


Figure 10.3.5-8 PNGV-Class Side Pole Impact deformed shape

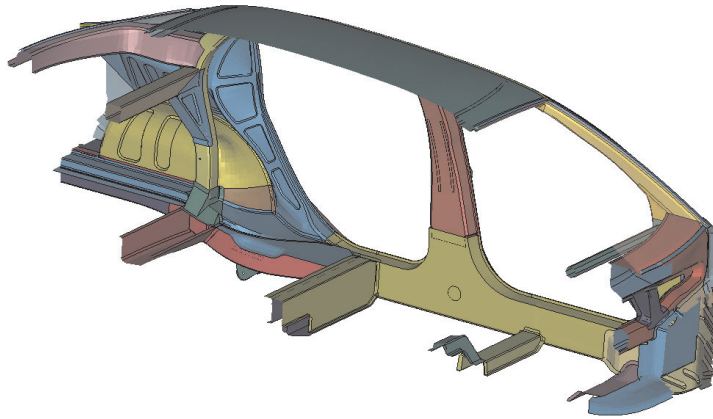


Figure 10.3.5-9 PNGV-Class Side Pole Impact undeformed shape

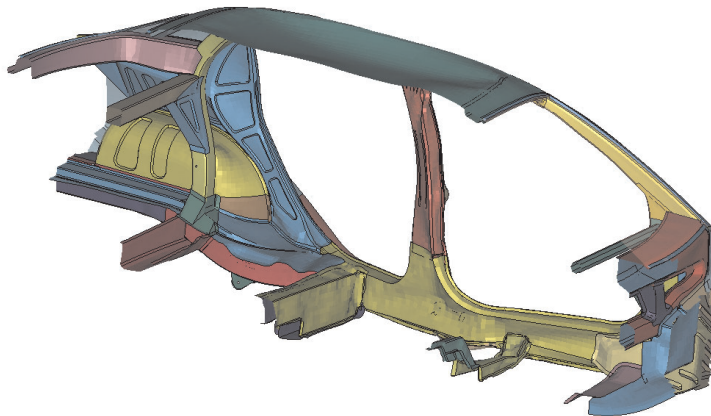


Figure 10.3.5-10 PNGV-Class Side Pole Impact deformed shape

Figures 10.3.5-11 and 10.3.5-12 give an overview of the energy distribution for the Side Pole crash event. Four components, which absorb the highest levels of energy in the structure are presented. The fixed seating concept contributed to the good performance in this crash event. The Crossmember Front Seat, Crossmember Seat Support and Extension Member Seat are shown in these figures as significant components for energy absorption.

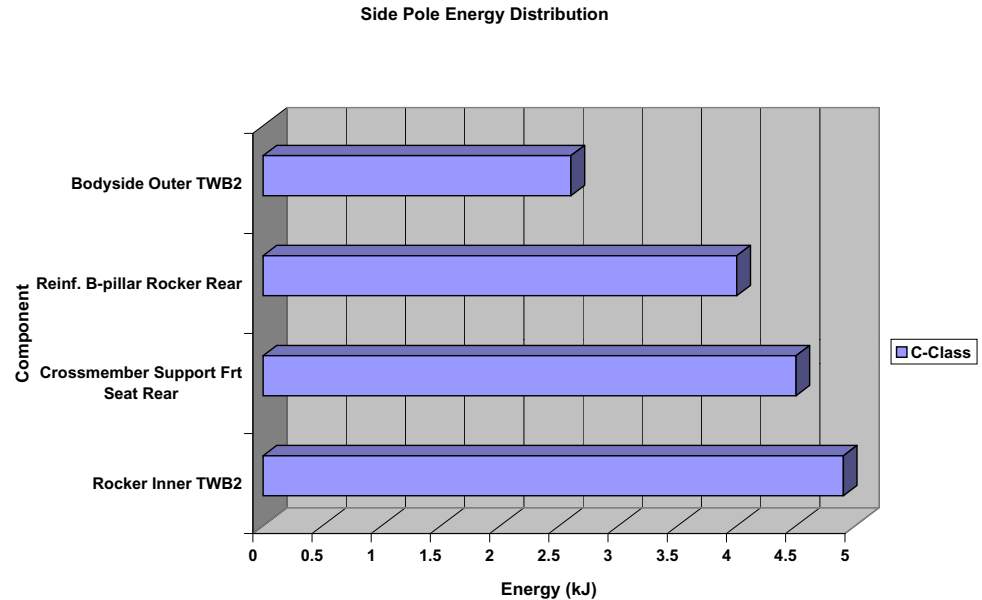


Figure 10.3.5-11 C-Class Side Pole energy distribution

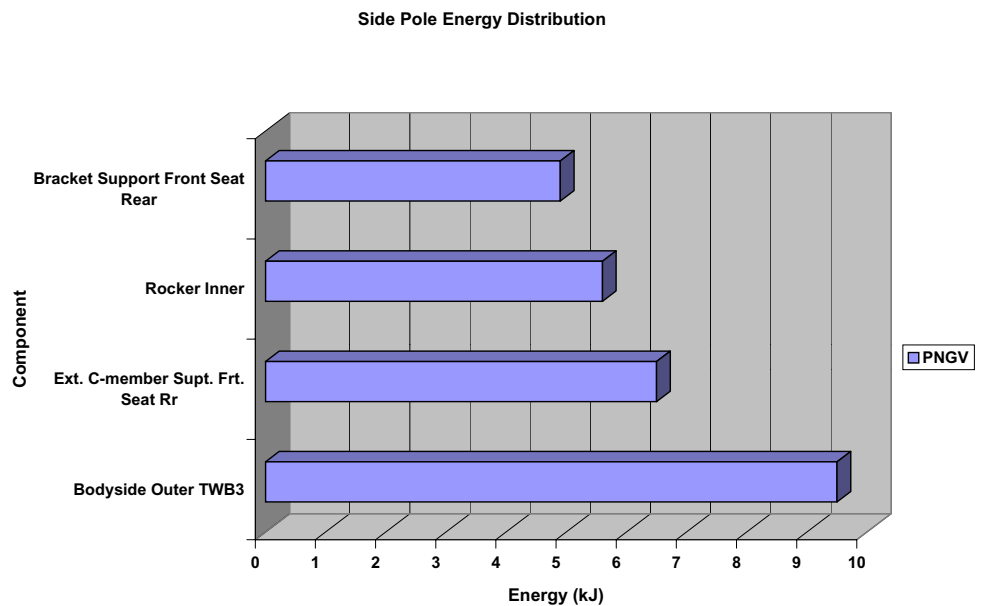


Figure 10.3.5-12 PNGV-Class Side pole energy distribution

The proportion of the total vehicle internal energy absorbed by the doors in the Side Pole event is 5% for the C-Class and 4% for the PNGV-Class. The Figures 10.3.4-21 and 10.3.4-22 show the distribution of energy within the door structures for the C-Class and PNGV-Class vehicles respectively.

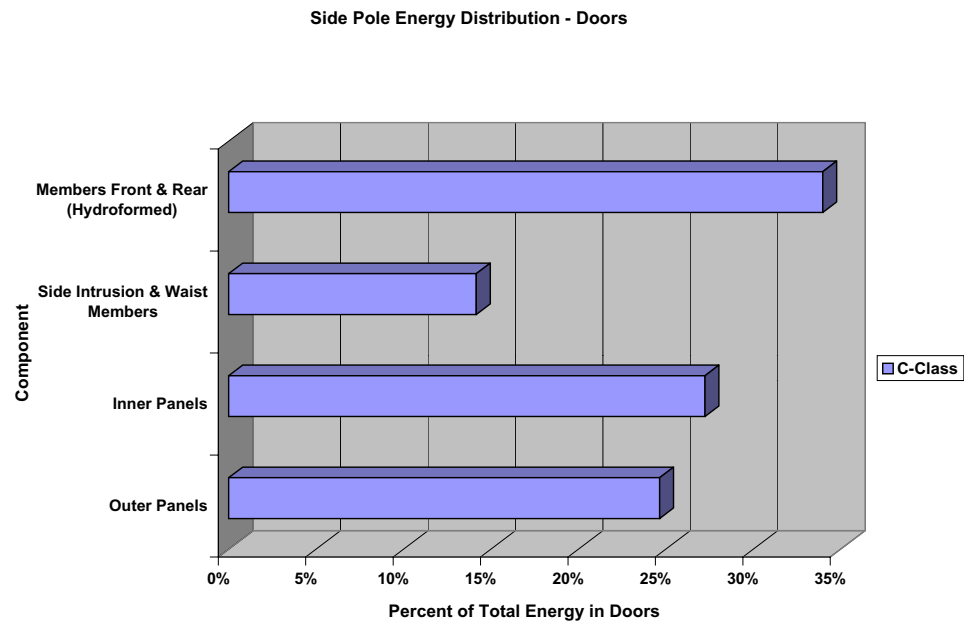


Figure 10.3.5-13 C-Class Side Pole energy distribution - doors

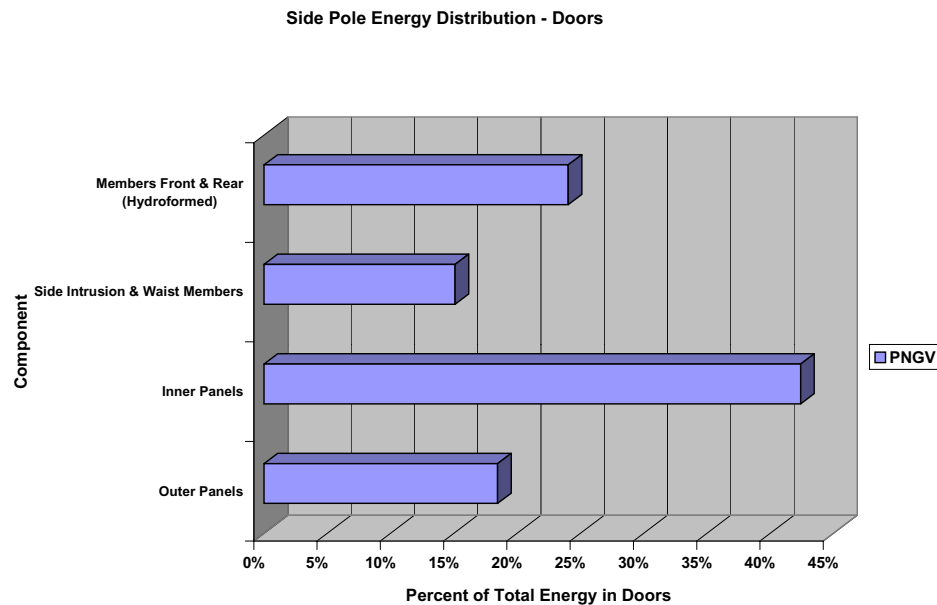


Figure 10.3.5-14 PNGV-Class Side Pole energy distribution - doors

Table 10.3.5-1 summarizes the results for this event. Figures 10.3.5-11 and 10.3.5-12 show the pole intrusion velocities of the C-Class and PNGV-Class vehicles.

Table 10.3.5-1 Side Pole Impact intrusion velocity summary

Side Pole	C-Class	PNGV-Class	Target
Pole Intrusion Velocity at point when pole strikes occupant (m/sec)	7.8	5.3	< 8
Maximum Intrusion (mm)	345	300	< 500

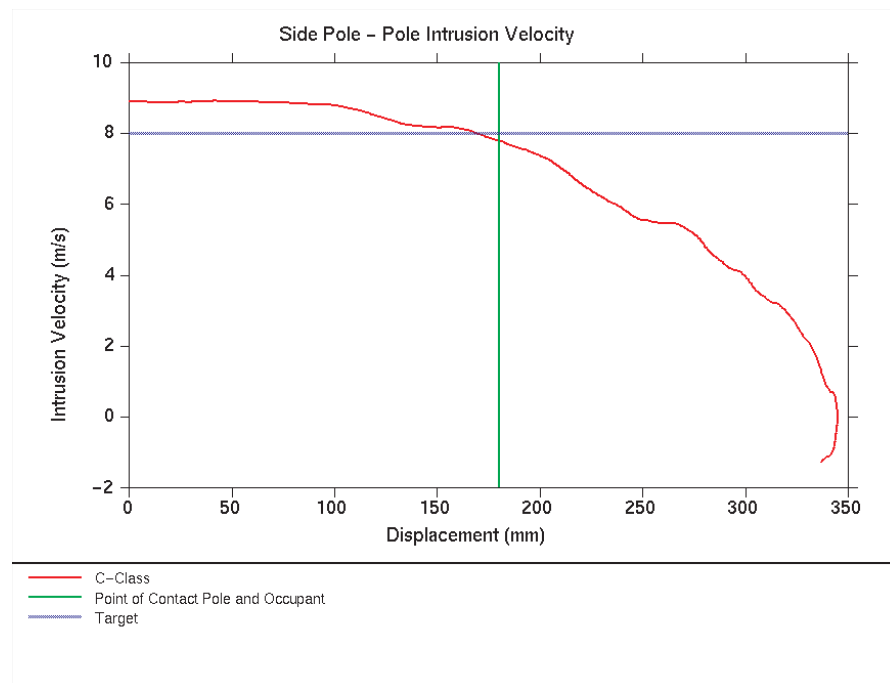


Figure 10.3.5-11 C-Class Side Pole Impact intrusion velocity

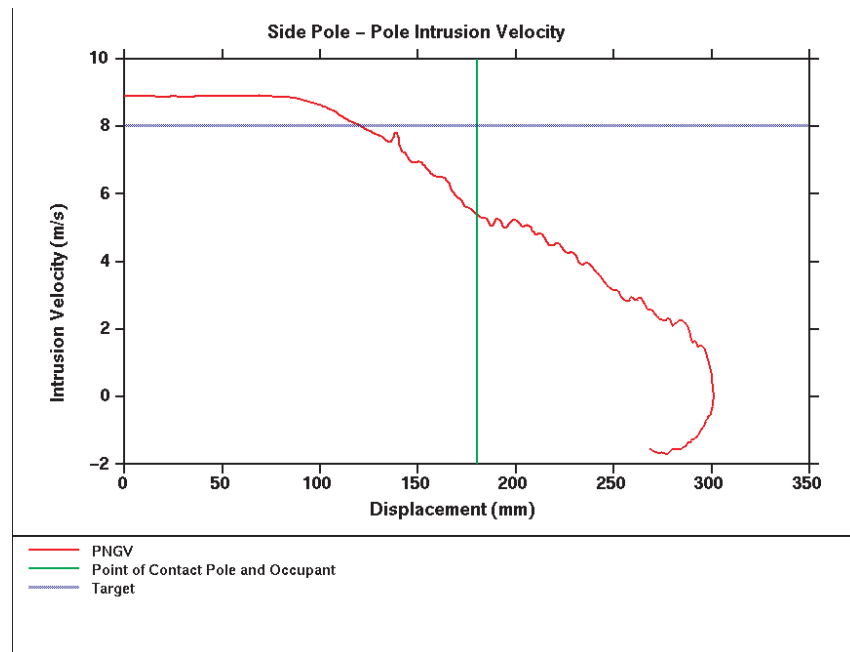


Figure 10.3.5-12 PNGV-Class Side Pole Impact intrusion velocity

10.3.6. Roof Crush/Rollover

The conditions for the roof crush analysis are based on US Federal Standard FMVSS 216. The requirement is designed to protect the occupants in the event of a rollover accident. The test specifies a rigid planar loading device to load the front corner of the roof structure at a given angle and sets a target for the load which must be sustained within a displacement of 127 mm (5 inches). For the ULSAB-AVC program, the target load has been increased from the 1.5 times the vehicle curb mass (as specified in FMVSS 216) to 2.5 times the vehicle curb mass, which equates to 27.0 kN based on the PNGV-Class diesel variant. The target load was increased to take into account anticipated future requirements associated with vehicle rollover tests.

In FMVSS 216 the complete body-in-white is assembled and clamped at the lower edge of the rocker. The rigid loading device applies the load in a quasi-static manner to the structure. The loading arrangement is shown in Figures 10.3.6-1 and 10.3.6-2.

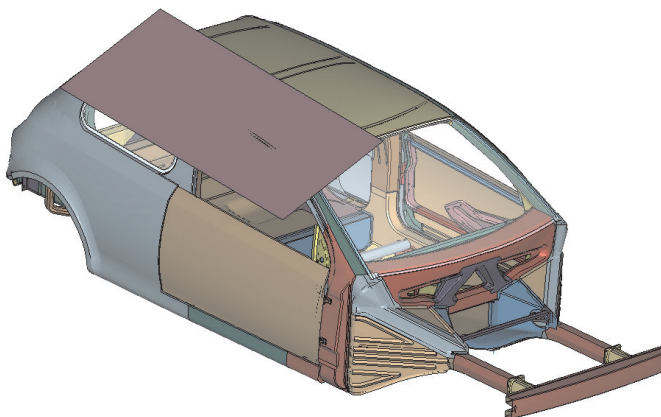


Figure 10.3.6-1 C-Class Roof Crush/Rollover loading arrangement

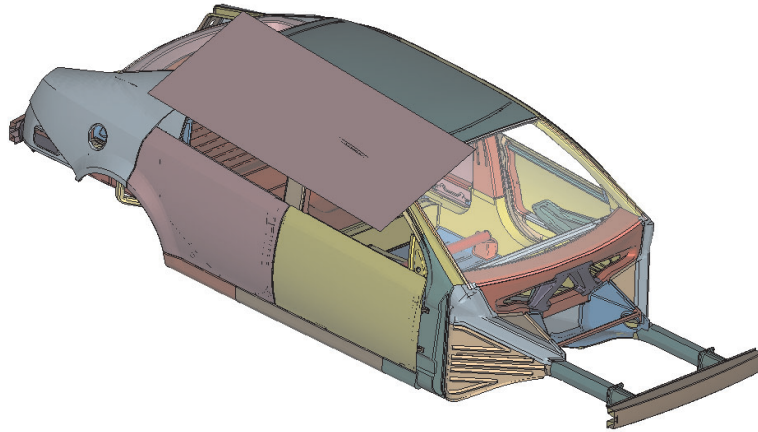


Figure 10.3.6-2 PNGV-Class Roof Crush/Rollover loading arrangement

Figures 10.3.6-3 and 10.3.6-5 show the undeformed shape of the C-Class and PNGV-Class FE-models used for the roof crush simulation. The shapes of the structures after the limit of 127 mm deformation are shown in Figures 10.3.6-4 and 10.3.6-6.

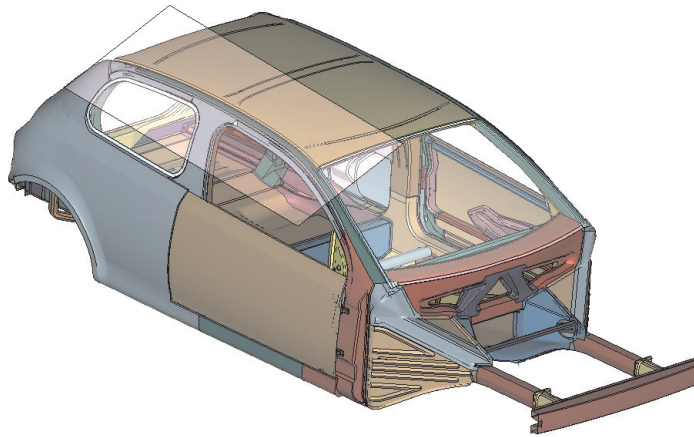


Figure 10.3.6-3 C-Class Roof Crush / Rollover undeformed shape

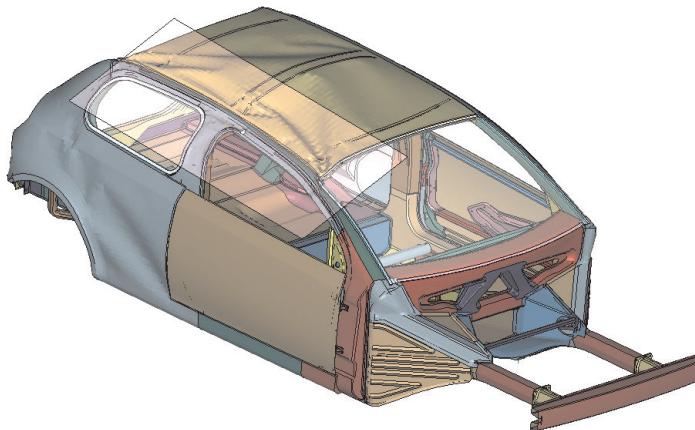


Figure 10.3.6-4 C-Class Roof Crush / Rollover deformed shape at 127 mm displacement

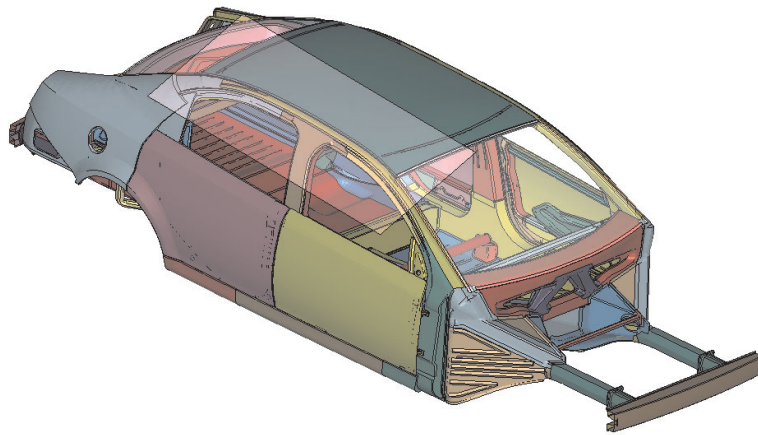


Figure 10.3.6-5 PNGV-Class Roof Crush / Rollover undeformed shape

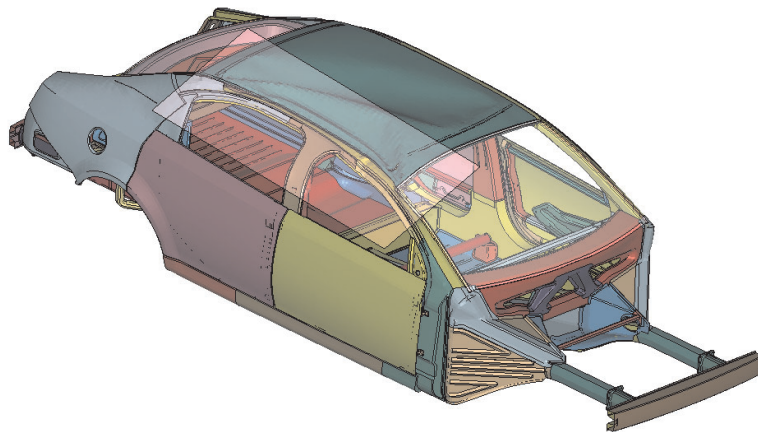


Figure 10.3.6-6 PNGV-Class Roof Crush / Rollover deformed shape at 127 mm displacement

The force versus displacement curves for each vehicle are shown in Figures 10.3.6-7 and 10.3.6-8. Results for each vehicle are summarized in Table 10.3.6-1.

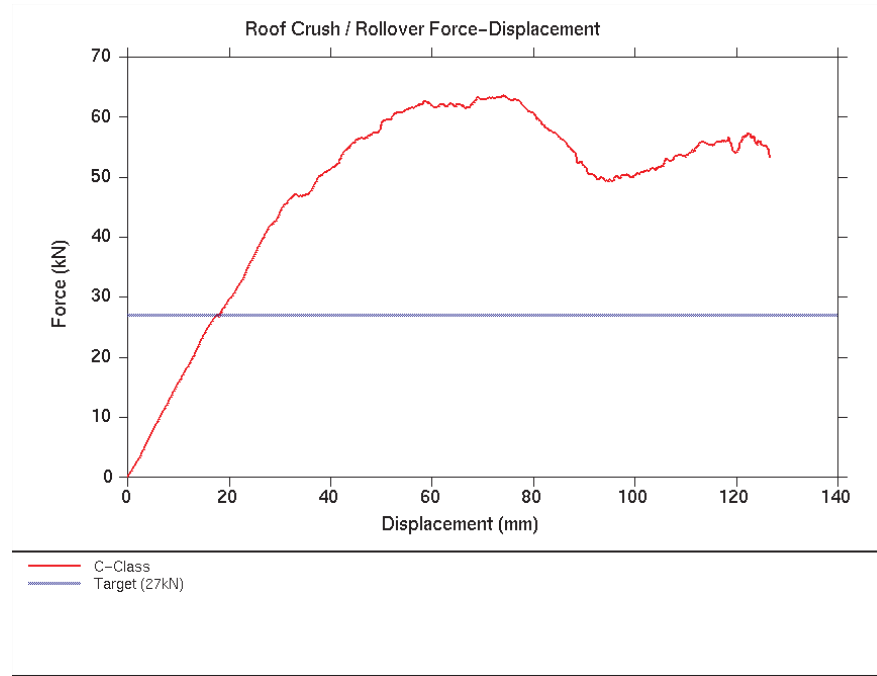


Figure 10.3.6-7 C-Class Roof Crush / Rollover force-displacement results

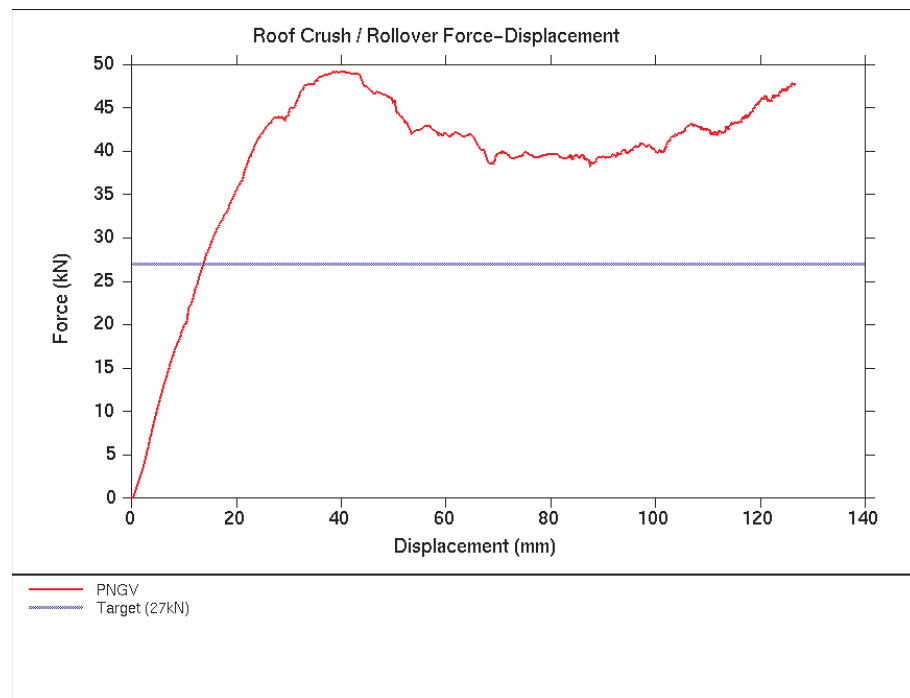


Figure 10.3.6-8 PNGV-Class Roof Crush / Rollover force-displacement results

The analysis shows that the roof structures meet the peak load requirements and the deformation mode is steady and predictable.

Table 10.3.6-1 Roof Crush/Rollover results summary

Roof Crush	C-Class	PNGV-Class	Target
Peak Force (kN)	64	49	> 27
Displacement to achieve 27 kN (mm)	20	20	< 127

10.3.7 Low Speed Impact

The PNGV-Class vehicle was subjected to a 15 km/h impact into a rigid barrier to investigate the reparability of the front end structure. The objective of the design was to limit the deformation to the bumper beam and bumper brackets (which is a bolt-on system) and sustain no permanent deformation in the main structure.

Figure 10.3.7-1 shows the undeformed structure and Figure 10.3.7-2 shows the deformed structure at the end of the impact with contours of plastic strain. The results show the permanent deformation to be contained within the bumper system. The minor local strain predicted in the bumper attachment bracket at the end of the rail could be eliminated with detailed design of this bracket.

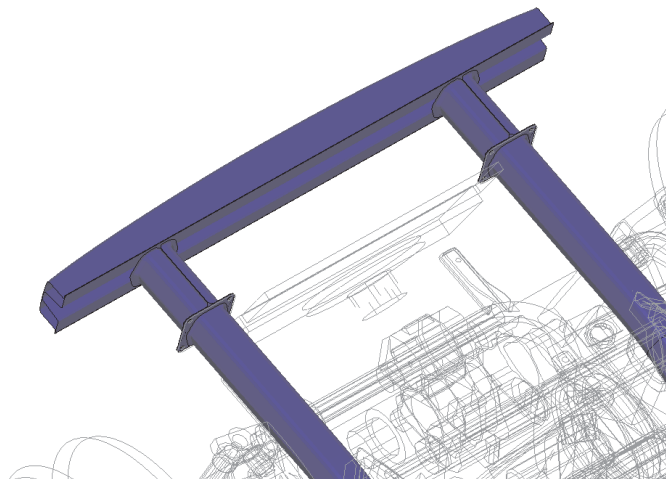


Figure 10.3.7-1 PNGV-Class Low Speed Impact undeformed shape

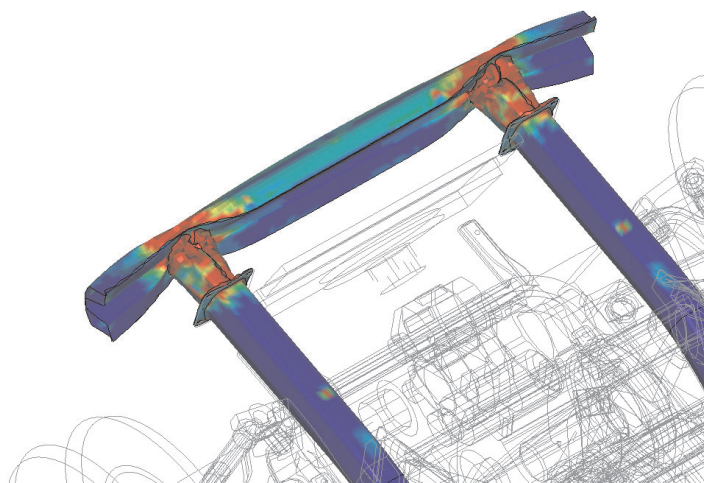


Figure 10.3.7-2 PNGV-Class Low Speed Impact deformed shape

10.4 Star Rating Assessment

The Star Rating system is a means of presenting the occupant injury results of the NCAP crash tests, which can be easily understood by consumers. Different Star Rating Systems are used for the NCAP tests in the United States and Europe. In the United States, separate Star Ratings (up to five stars) are awarded to vehicles for the US-NCAP Front Impact test and the SINCAP Side Impact test. In Europe, the Euro-NCAP Star Rating (up to five stars) is a combined rating for vehicles based on performance in the Offset Front Impact, European Side Impact, and Side Pole Impact tests.

As no occupant injury predictions have been included in the ULSAB-AVC simulations, it is not possible to directly predict the Star Rating of the C-Class and PNGV-Class ULSAB-AVC concept designs. However, the potential of the ULSAB-AVC concept to achieve a given Star Rating has been assessed by comparing the predicted structural performance of the ULSAB-AVC vehicles with that of current vehicles. The purpose of ULSAB-AVC is not to develop occupant restraint systems, but to develop a concept structure which would provide a good basis for further development in a detailed design phase which would achieve a high level of crashworthiness with state-of-the-art restraint systems.

The following sections summarize the assessment of Star Rating potential for ULSAB-AVC.

10.4.1 US-NCAP

The Star Rating for the US-NCAP 35mph frontal impact is based on the occupant injury parameters of Head Injury Criterion (HIC) and Chest Acceleration for the driver and passenger occupants.

For comparison with the C-Class and PNGV-Class ULSAB-AVC concept structures, a number of current vehicles were selected from the Compact and Mid-Size weight classes which achieved Four-Star or Five-Star driver performance. It is not the purpose or intention of this report to provide comparisons of the performance of current vehicles on the market. For this reason the comparison vehicles will not be identified. The data for the comparison vehicles was obtained from the NHTSA and is publicly available.

The comparison vehicles are summarized in Table 10.4.1-1.

Table 10.4.1-1 Comparison vehicle summary

US-NCAP Comparison Vehicles	
Four-star	Five-star
A	D
B	E
C	F
	G

The displacement, velocity and acceleration curves from the comparison vehicles are presented along with the C-Class and PNGV results in Figures 10.4.1-1 to 12. These figures show that the results of the two ULSAB-AVC variants reflect closely the structural performance of the comparison vehicles.

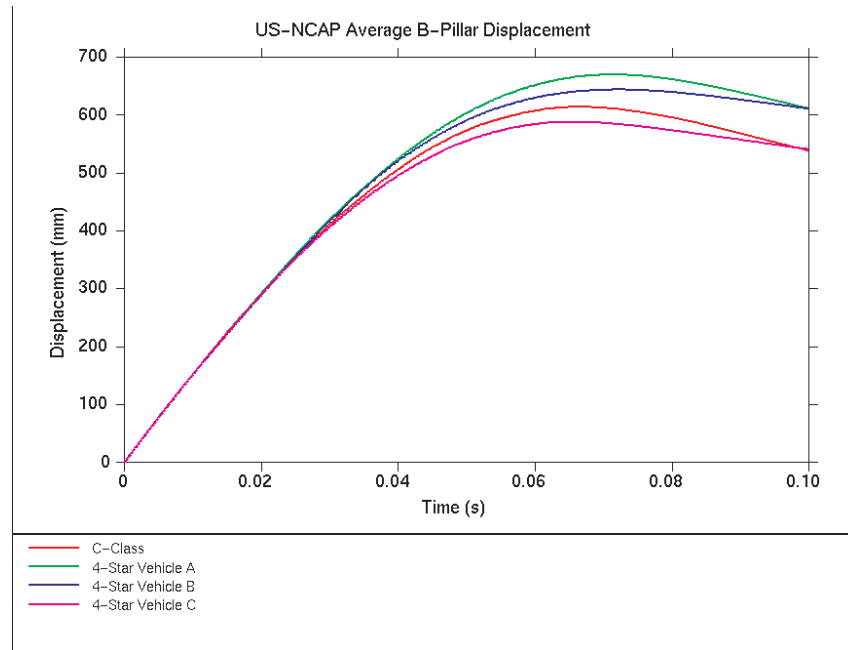


Figure 10.4.1-1 C-Class comparison of B-Pillar displacement results with 4-star vehicles

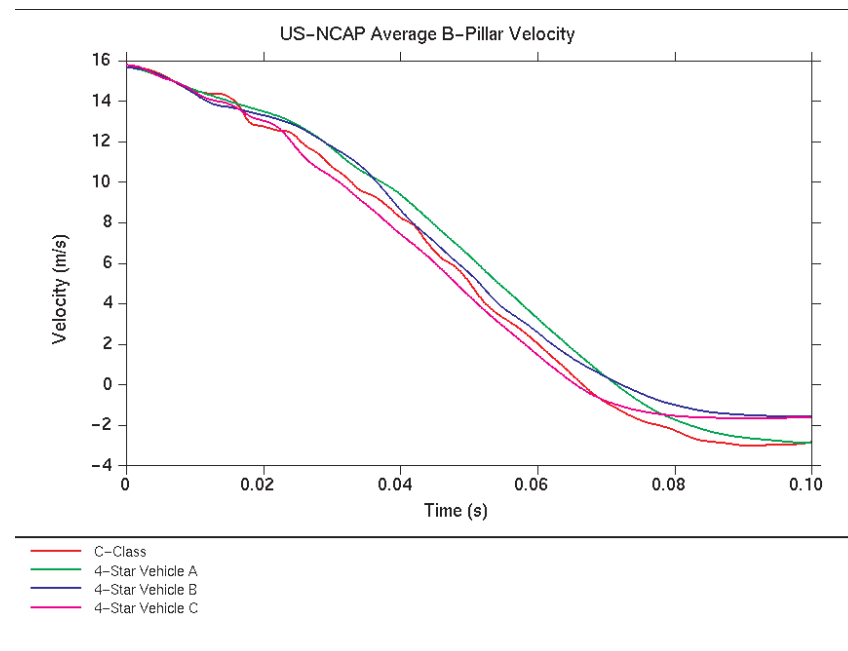


Figure 10.4.1-2 C-Class comparison of B-Pillar velocity results with 4-star vehicles

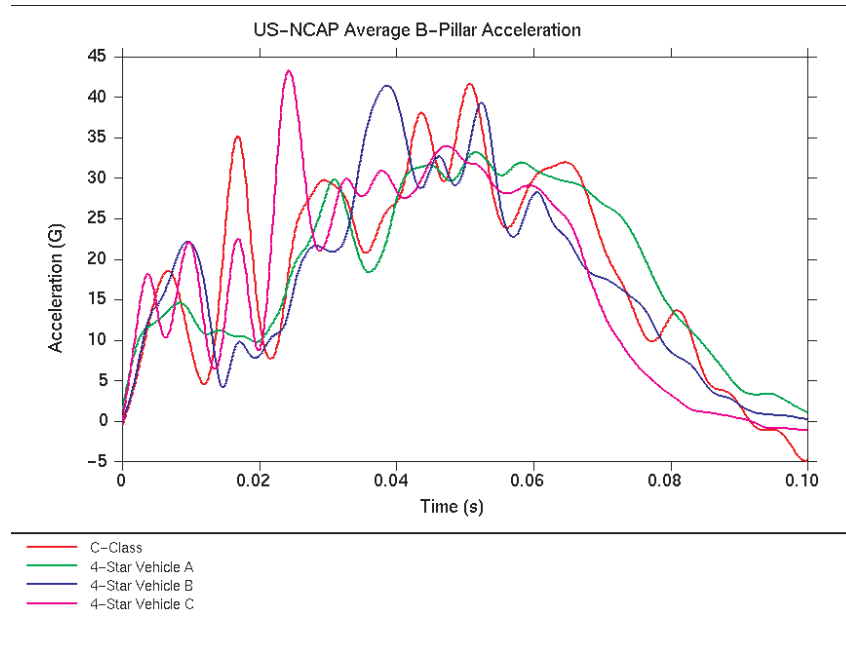


Figure 10.4.1-3 C-Class comparison of B-Pillar acceleration results with 4-star vehicles

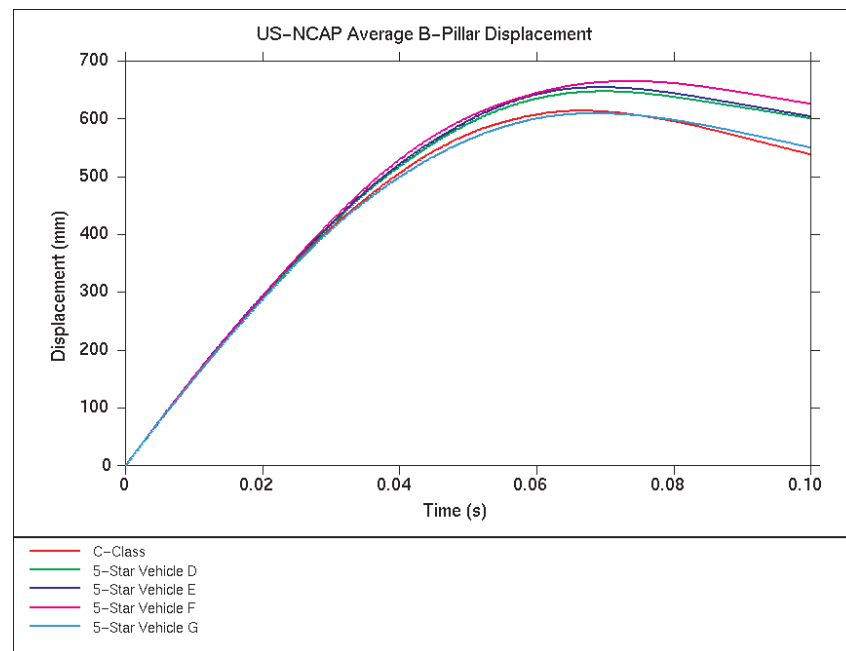


Figure 10.4.1-4 C-Class comparison of B-Pillar displacement results with 5-star vehicles

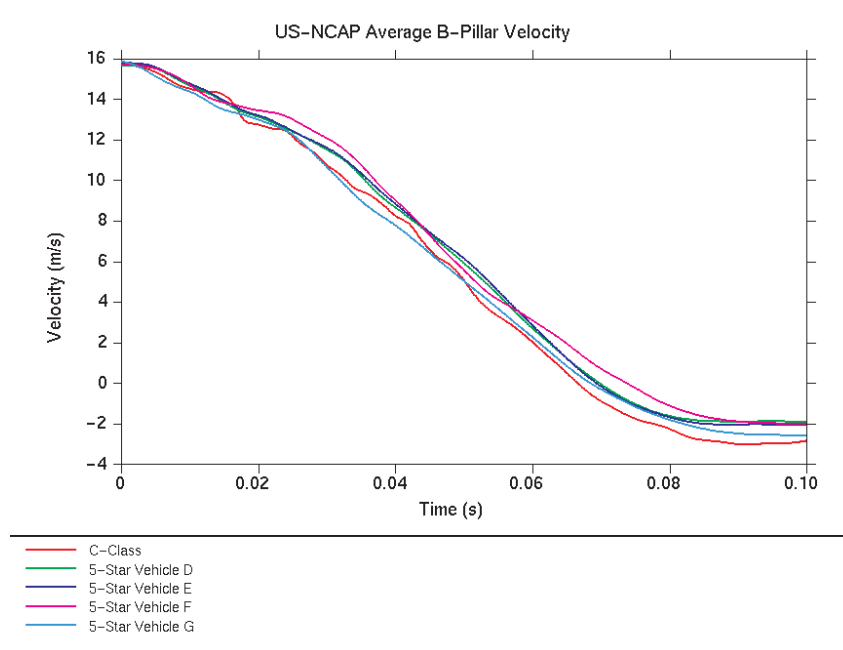


Figure 10.4.1-5 C-Class comparison of B-Pillar velocity results with 5-star vehicles

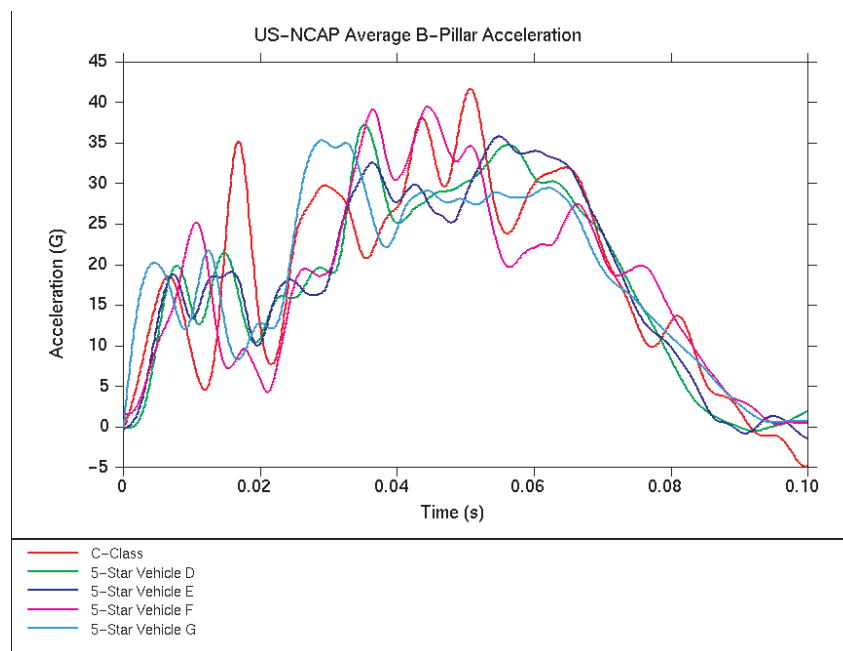


Figure 10.4.1-6 C-Class comparison of B-Pillar acceleration results with 5-star vehicles

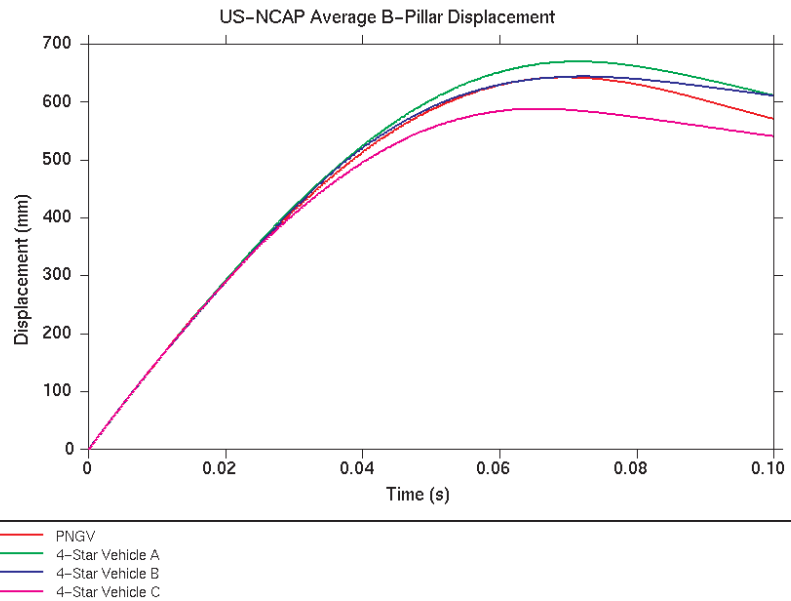


Figure 10.4.1-7 PNGV-Class comparison of B-Pillar displacement results with 4-star vehicles

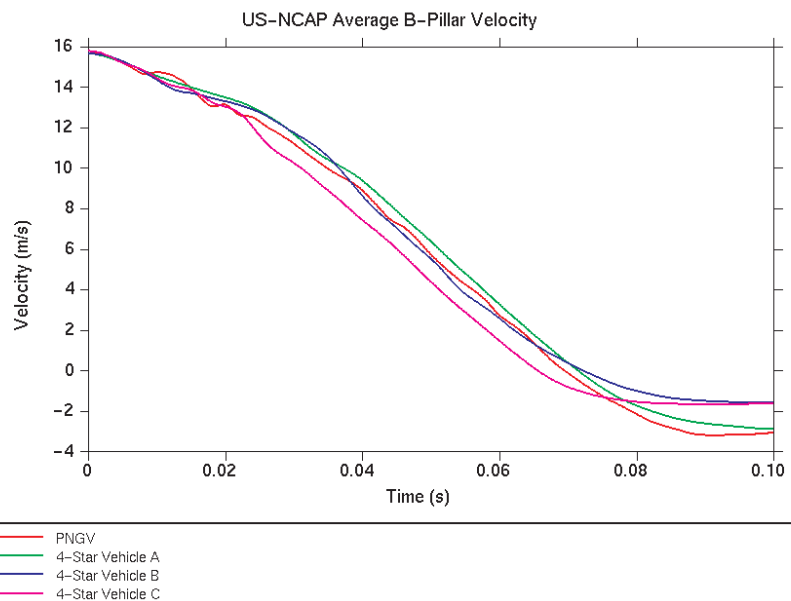


Figure 10.4.1-8 PNGV-Class comparison of B-Pillar velocity results with 4-star vehicles

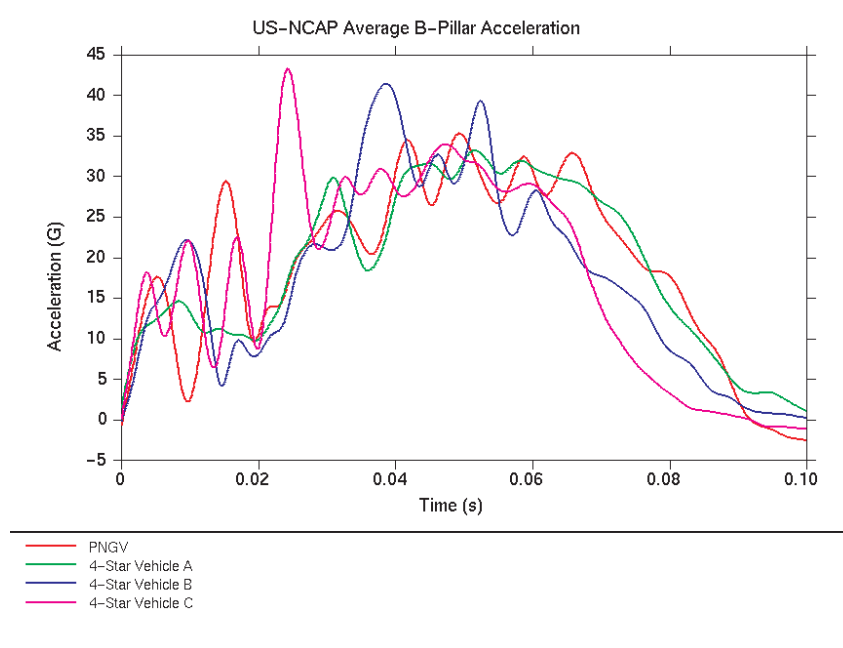


Figure 10.4.1-9 PNGV-Class comparison of B-Pillar acceleration results with 4-star vehicles

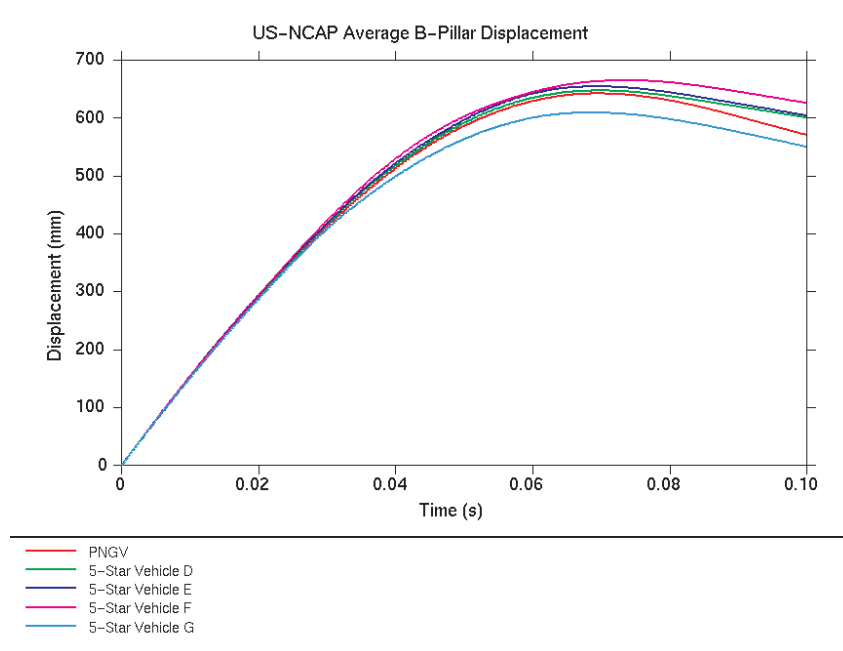


Figure 10.4.1-10 PNGV-Class comparison of B-Pillar displacement results with 5-star vehicles

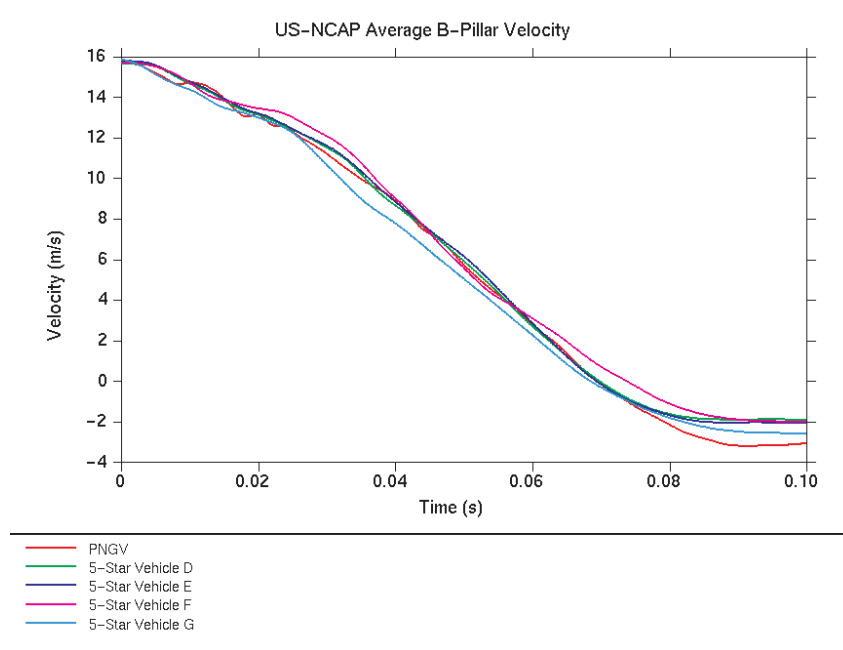


Figure 10.4.1-11 PNGV-Class comparison of B-Pillar velocity results with 5-star vehicles

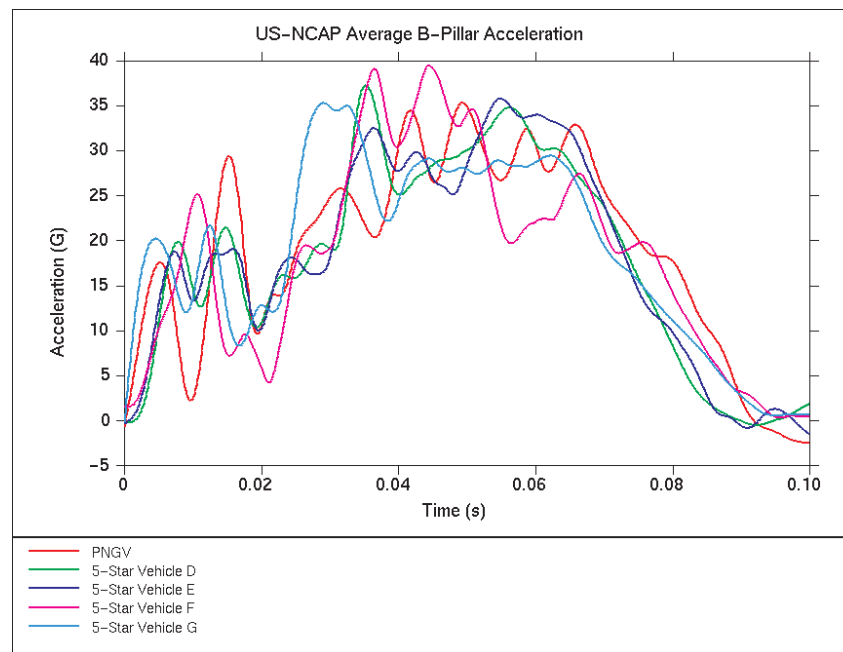


Figure 10.4.1-12 PNGV-Class comparison of B-Pillar acceleration results with 5-star vehicles

In order to present the results in a simplified form, a number of parameters have been chosen to characterize the structural performance of the vehicles for this test. These parameters are:

- Dynamic crush distance
- Time to zero velocity (i.e. time of maximum dynamic crush)
- Average B-pillar acceleration in the time window 40-70 msec.
- Peak B-pillar acceleration in the time window 40-70 msec.

The results of the parameter comparison are shown in Figures 10.4.1-13 to 16.

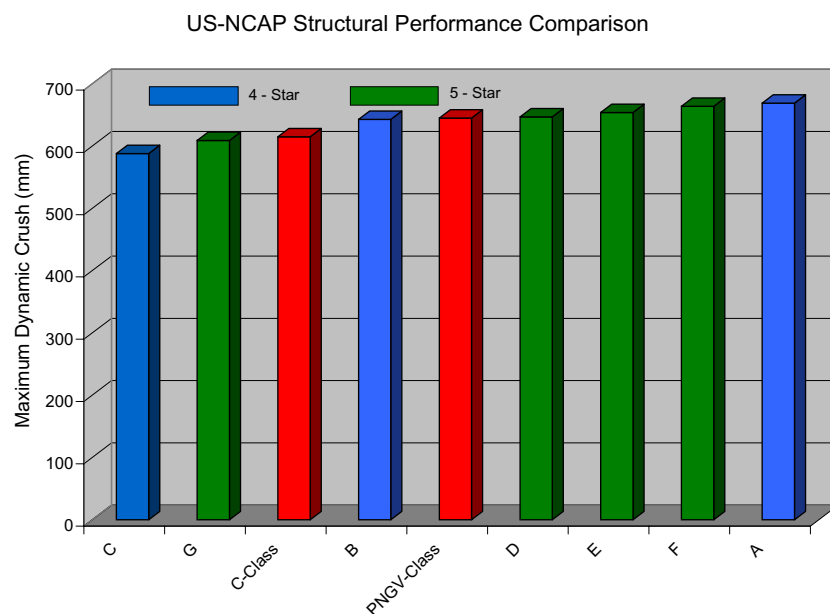


Figure 10.4.1-13 Dynamic crush parameter comparison

US NCAP Structural Performance Comparison

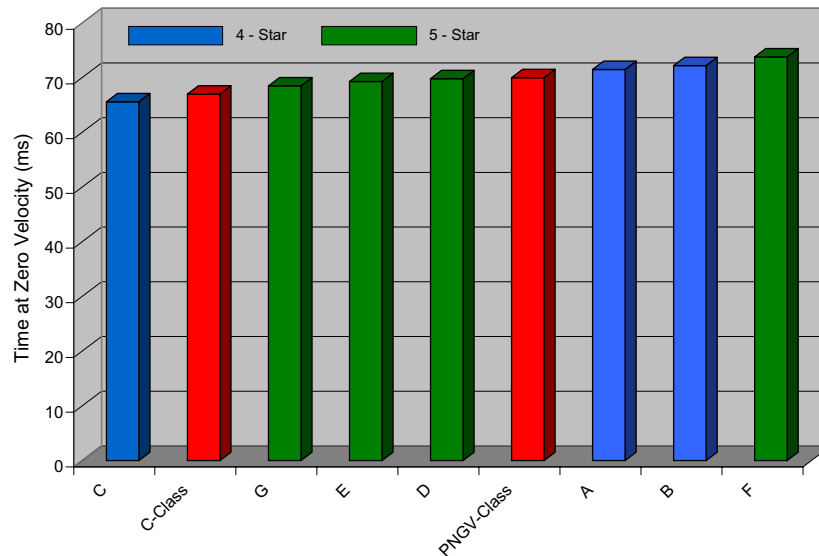


Figure 10.4.1-14 Time to zero velocity parameter comparison

US NCAP Structural Performance Comparison

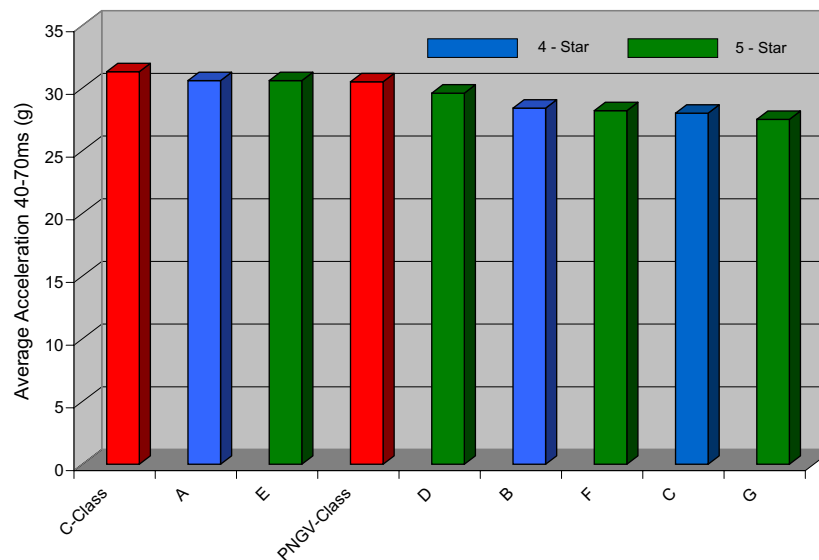


Figure 10.4.1-15 Average B-pillar acceleration 40-70 msec. parameter comparison

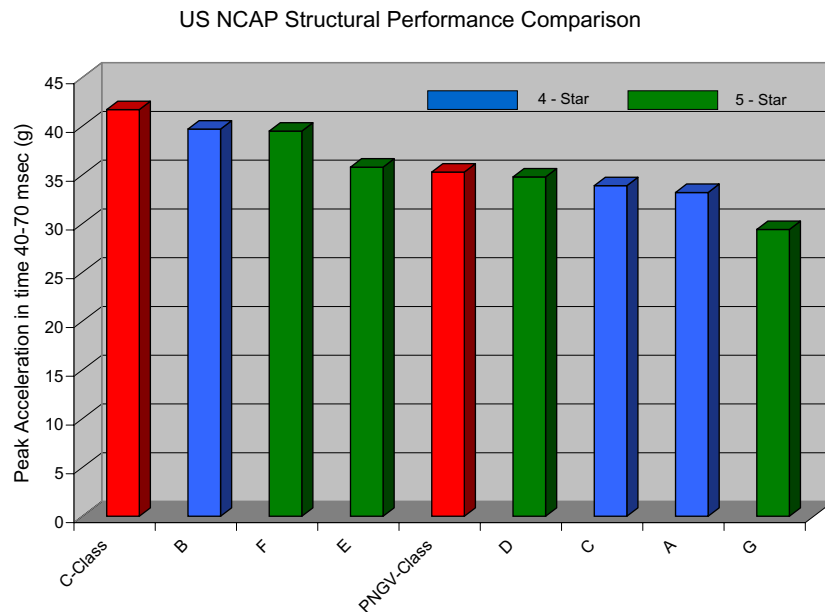


Figure 10.4.1-16 Peak B-pillar acceleration 40-70 msec. parameter comparison

The structural performance of the ULSAB-AVC PNGV-Class vehicle is assessed to be a good basis for Five-Star performance in the US-NCAP test. The ULSAB-AVC C-Class design demonstrates a slightly 'harder' response in the US-NCAP test. The C-Class is assessed to provide a basis for Four-Star or Five-Star performance for the US-NCAP test.

Actual performance in the US-NCAP frontal impact is not dependent on structural response alone, but many factors, including occupant position, and the design of the seats, restraint system, instrument panel, and steering column. The assessed Star Rating potential assumes the further development of the detailed vehicle design will include development of an occupant restraint system, which would fully utilize the potential predicted by the structural performance.

10.4.2 US-SINCAP

The Star Rating for the US Side Impact NCAP test is based on the measured occupant injury parameter Thoracic Trauma Index (TTI) for the front and rear seat occupants.

For comparison with the C-Class and PNGV-Class ULSAB-AVC concept structures, two current vehicles were selected from the Compact and Mid-Size weight classes which achieved Five-Star performance. As in the US-NCAP comparison, the comparison vehicles will not be identified. The data for the comparison vehicles was obtained from the NHTSA and is publicly available. The comparison vehicles are summarized in Table 10.4.2-1:

Table 10.4.2-1 US-SINCAP comparison vehicles

SINCAP Comparison Vehicles	
Five Star	
	H
	J

Comparisons of the B-pillar intrusion velocity graphs are shown in Figures 10.4.2-1 and 10.4.2-2 for the PNGV-Class and C-Class vehicles. Both the C-Class and PNGV-Class structures demonstrate intrusion velocity characteristics similar to the two comparison vehicles. Peak intrusion velocities for the ULSAB-AVC designs are less than the comparison vehicles as is the maximum intrusion. The C-Class and PNGV-Class structural performance is assessed to be a good basis for Five-Star performance in the US-SINCAP test.

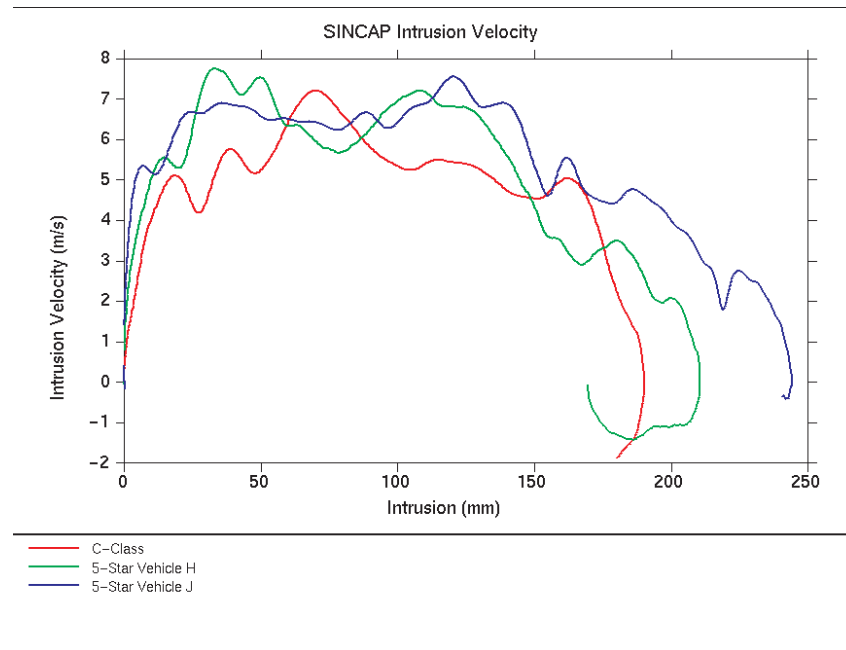


Figure 10.4.2-1 C-Class comparison of B-Pillar intrusion velocity results with 5-star vehicles

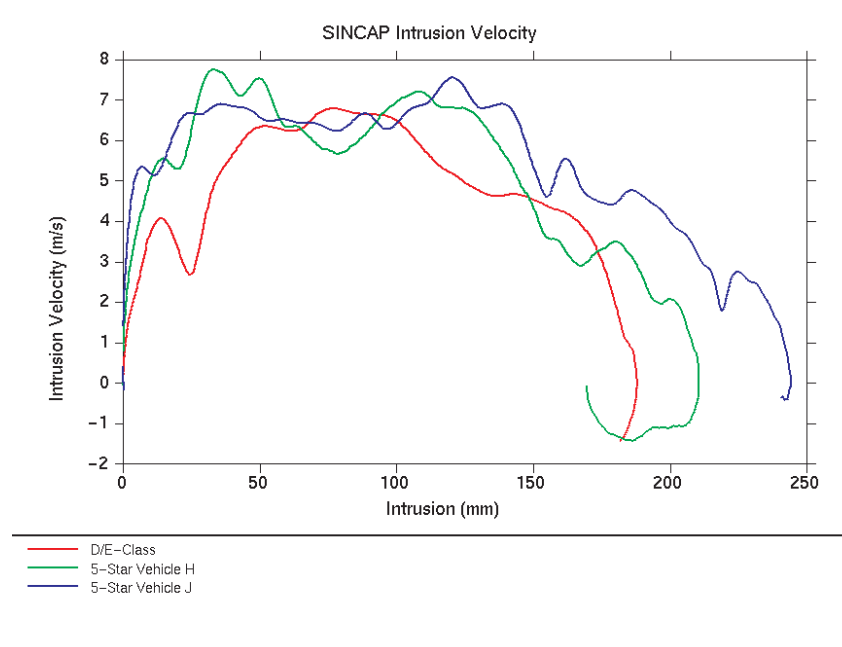


Figure 10.4.2-2 PNGV-Class comparison of B-Pillar intrusion velocity results with 5-star vehicles

10.4.3 Euro-NCAP

The Euro-NCAP Star Rating is a combined rating based on the occupant injury parameters and vehicle structural performance measured in the following tests:

- Offset Deformable Barrier Front Impact
- European Side Impact
- Side Pole Impact

The maximum Star Rating for the Euro-NCAP tests is Five-Stars.

Euro-NCAP test reports and detailed results are not as freely available to the public as the NHTSA database. Therefore, it was not possible to conduct a detailed comparison of the structural performance of the ULSAB-AVC concept design with current vehicles. However, an assessment of the general structural performance of the ULSAB-AVC designs is described below.

For the frontal offset impact, the performance of both the C-Class and PNGV-Class structures is good and has the characteristic of a stable occupant compartment where the predicted residual footwell intrusion levels are below 150 mm. The footwell intrusion parameter is being measured in the Euro-NCAP tests and is important for minimizing occupant lower leg injury, but at the present time does not directly influence the Star Rating. A-pillar displacement and steering column movement are also low, which demonstrate a stable basis for the deployment of a steering wheel airbag.

No analysis of the European Side Impact was undertaken in the ULSAB-AVC program. The US-SINCAP test was selected for analysis on the basis of the heavier barrier (1370 kg compared to the European side impact barrier of 950 kg), and the more severe structural requirement. Good performance in the US-SINCAP test does not necessarily guarantee good performance in the European Side Impact test due to the different test configurations and crash test dummies specified for each test. However, the structural behavior predicted for the ULSAB-AVC C-Class and PNGV-Class vehicles where the B-pillar remains stable without collapse of the section at the waist, is a desirable structural characteristic to aid in achieving low occupant injury levels in the European Side Impact test.

The ULSAB-AVC C-Class and PNGV-Class vehicles demonstrated good performance in the Side Pole Impact which was undertaken at a speed 10% higher than the impact speed specified in the Euro-NCAP test. The strong side structure of ULSAB-AVC would allow the impact to be sensed and a side head airbag to be deployed in sufficient time to enable the loads on the occupant to be minimized.

Considering the overall performance of the ULSAB-AVC C-Class and PNGV-Class concept vehicles, the structures are considered to provide a good basis to achieve Five-Star performance in the Euro-NCAP tests.

10.5. Institute for Highway Safety (IIHS) Assessment

The Insurance Institute for Highway Safety (IIHS) is an independent, non-profit, research and communications organization in the USA funded by auto insurers and dedicated to reducing highway crash deaths, injuries and property losses. The IIHS undertakes crashworthiness evaluations of new passenger vehicles and has adopted the 40 mph, 40% offset front impact test with the deformable barrier as a basis for these evaluations. The results are published, and an overall evaluation is provided for a vehicle: Good, Acceptable, Marginal and Poor. The overall evaluation is a combined rating from the performance of the vehicle in the areas of:

- Structure/Safety Cage
- Injury Measures
- Restraints/Dummy Kinematics

The Euro-NCAP frontal offset test considered in the ULSAB-AVC program is the same test used in the IIHS crashworthiness evaluations. The ULSAB-AVC C-Class and PNGV-Class concept designs have been evaluated using the IIHS guidelines for structure/safety cage part of the assessment and the results are presented in this section. An overall evaluation for the ULSAB-AVC concepts can not be made because the restraint system design and occupant simulation was not included in the concept design project.

Figures 10.5-1 and 10.5-2 present the structure evaluation for the C-Class and PNGV-Class vehicles respectively. The IIHS structural assessment measures the deformation at points on the brake pedal, and instrument panel, in addition to points on the body structure (footwell or toe pan and door aperture). The measurement points which are not on the body structure (brake pedal, left and right instrument panel) have been excluded from the diagram, as these components were not explicitly modeled.

Both of the ULSAB-AVC vehicles lie within the 'Good' range for structural performance, which demonstrates the structural concept is a good basis for the further development of the design in a detailed design phase.

This result is further confirmation of the high level of crashworthiness achieved for these concept mass-efficient steel body structures.

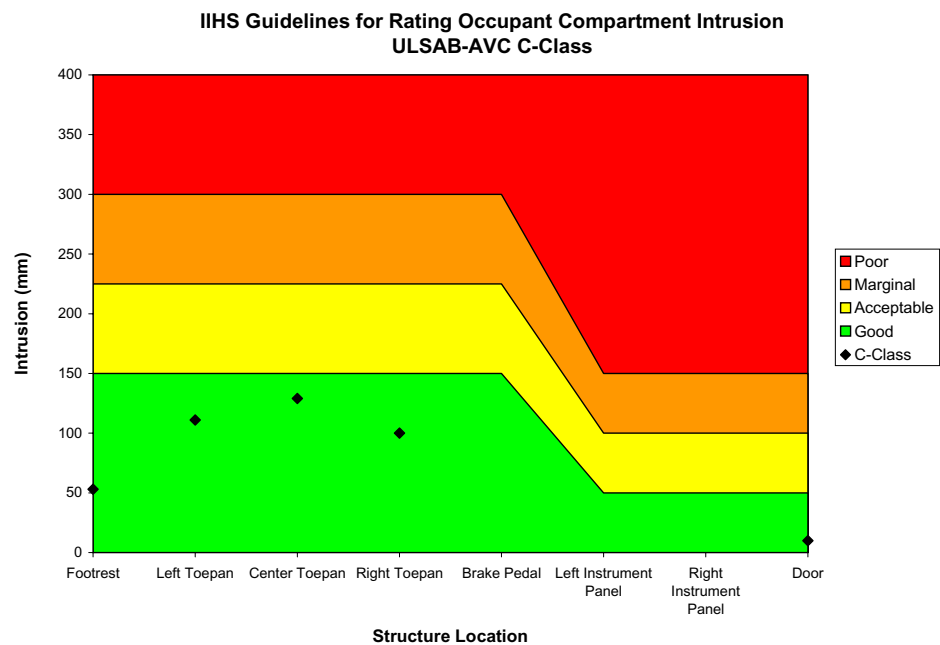


Figure 10.5-1 C-Class IIHS structure evaluation

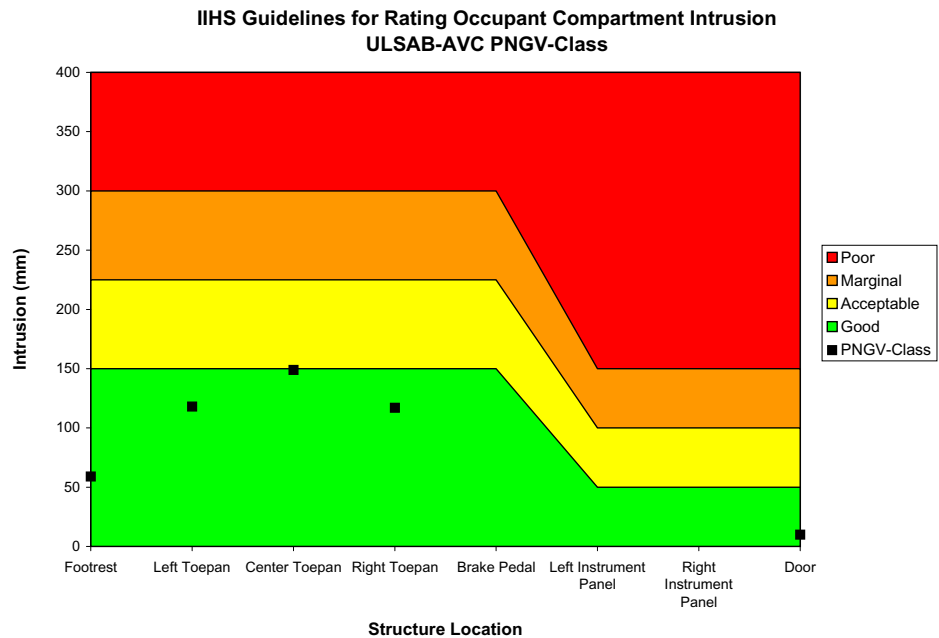


Figure 10.5-2 PNGV-Class IIHS structure evaluation

10.6. CAE Analysis Summary

The CAE analysis results have predicted good structural performance for the ULSAB-AVC C-Class and PNGV-Class concept structures both in the structural stiffness load cases and crashworthiness events. The concept structures are also mass efficient.

A good compromise has been achieved between the US-NCAP front impact event and the Euro-NCAP offset frontal impact. The final structures demonstrate crash pulses which are comparable to Four-Star and Five-Star US-NCAP vehicles at the same time having stable occupant compartments and reasonable levels of footwell intrusion for the Euro-NCAP offset frontal impact.

The C-Class and PNGV-Class concepts demonstrate good structural characteristics for the US-SINCAP and Side Pole Impact events. Low levels of intrusion velocity have been achieved for the US-SINCAP. These results are comparable to Five-Star SINCAP vehicles.

The rear crash performance for both ULSAB-AVC designs show good results for fuel system integrity and deformation in the rear seat area.

10

CAE Analysis Results

PORSCHE
Engineering Services, Inc.

The ULSAB-AVC structures also demonstrate good performance for the Roof Crush / Rollover condition.

The goal of ULSAB-AVC was to maintain the high standards of state of the art crash requirements without compromising the ULSAB-AVC program goal to achieve a mass efficient vehicle. The CAE analysis results demonstrate that this goal has been achieved with the C-Class and the PNGV-Class concept designs.

The ULSAB-AVC structures provide an excellent basis for further development in a detailed design phase. CAE would also be required during a detail design phase as a tool to monitor structural performance and aid design decisions.